Aus dem CharitéCentrum
für Frauen-, Kinder- und Jugendmedizin mit Perinatalzentrum und Humangenetik
Klinik für Neonatologie
Direktor: Prof. Dr. Christoph Bührer

Habilitationsschrift

The Protective Role of PPARγ in Pulmonary Arterial Hypertension

zur Erlangung der Venia legendi
für das Fach Kinder- und Jugendmedizin

vorgelegt dem Fakultätsrat der Medizinischen Fakultät
Charité Universitätsmedizin Berlin

von

Dr. med. Georg Hansmann

Eingereicht: Januar 2009
Dekanin: Prof. Dr. Annette Grüters-Kieslich

1. Gutachter: Prof. Dr. Sven Dittrich, Erlangen

2. Gutachter: Prof. Dr. Dietmar Schranz, Gießen

Datum des öffentlich-wissenschaftlichen Vortrags: 25. Januar 2010

Wir müssen es riskieren, anfechtbare Dinge zu sagen, wenn dadurch lebenswichtige Fragen aufgerührt werden.

We need to take risks and raise controversial questions if by doing so we touch issues central to life.

Dietrich Bonhoeffer
1906-1945

Table of Contents

Abbreviations

ApoE	apolipoprotein E
BMP	bone morphogenetic protein
BMP-RII	bone morphogenetic protein receptor II
EGF	epidermal growth factor
EGFR	epidermal growth factor receptor
ET-1	endothelin-1
HDL-C.	high density lipoprotein cholesterol (plasma)
HOMA-IR	homeostatic model assessment for insulin resistance
HOMA-IR =	fasting glucose [mmol/l] x fasting insulin [μU/ml] ÷ 22.5
IR	insulin resistance
LDL-C.	low density lipoprotein cholesterol (plasma)
LRP	LDL receptor related protein
LVH	left ventricular hypertrophy
6MWD	6-minute walk distance
MS	metabolic syndrome
PAH	pulmonary arterial hypertension
PAP	pulmonary artery pressure
PDGF-BB	platelet-dervived growth factor B homodimer (BB)
PDGFR-β	platelet-dervived growth factor beta
PH	pulmonary hypertension
PPARγ	peroxisome proliferator-activated receptor gamma
PVR	pulmonary vascular resistance
RVH	right ventricular hypertrophy
RVSP	right ventricular systolic pressure
SPPARM	selective PPAR modulators
TG	triglycerides (plasma)
TG/HDL-C.	triglyceride-to-HDL-cholesterol ratio (plasma)
TR	tricuspid regurgitation
TZD	thiazolidinedione (i.e., pioglitazone, rosiglitazone)
VLDL-C.	very low density lipoprotein cholesterol

1. Introduction

Pulmonary arterial hypertension (PAH) is characterized by progressive obliteration of pulmonary arterioles leading to increased pulmonary vascular resistance (PVR), right heart failure, and death in ≈40-60% of PAH patients 5 years after diagnosis[1]. Recent US epidemiologic data report an increase in hospitalizations and mortality from PAH due to increased physician awareness and better diagnostic approaches[2]. Although PAH is a rare disease, with an estimated prevalence of 30-50 cases per million[3], the PAH in certain at-risk groups is substantially higher. For example, the prevalence is 0.5% in HIV-infected patients[4], ≈16% in systemic sclerosis[5], and as high as 20-40% in patients with sickle cell disease[6, 7].

1.1 Clinical Classification of Pulmonary Hypertension (Venice 2003, Dana Point 2008)

In 2003, during the *Third World Symposium on pulmonary hypertension (PH) held in Venice, Italy*, it was decided to maintain the general architecture and philosophy of the Evian classification (1999). However, some modifications have been made, mainly to abandon the term "primary pulmonary hypertension" and to replace it with "idiopathic pulmonary hypertension"; to reclassify pulmonary veno-occlusive disease and pulmonary capillary hemangiomatosis; to update risk factors and associated conditions for pulmonary arterial hypertension and to propose guidelines in order to improve the classification of congenital systemic-to-pulmonary shunts[8].

Clinical Classification of Pulmonary Hypertension (Venice, 2003)[8, 9]

Category 1. Pulmonary arterial hypertension (PAH)
1.1. Idiopathic (IPAH)
1.2. Familial (FPAH)
1.3. Associated with (APAH):
1.3.1. Collagen vascular disease
1.3.2. Congenital systemic-to-pulmonary shunts #
1.3.3. Portal hypertension
1.3.4. HIV infection
1.3.5. Drugs and toxins
1.3.6. Other (thyroid disorders, glycogen storage disease, Gaucher disease, hereditary hemorrhagic telangiectasia, hemoglobinopathies, myeloproliferative disorders, splenectomy)
1.4. Associated with significant venous or capillary involvement
1.4.1. Pulmonary veno-occlusive disease (PVOD)
1.4.2. Pulmonary capillary hemangiomatosis (PCH)
1.5. Persistent pulmonary hypertension of the newborn

Category 2. Pulmonary hypertension with left heart disease
2.1. Left-sided atrial or ventricular heart disease
2.2. Left-sided valvular heart disease

Category 3. Pulmonary hypertension associated with lung diseases and/or hypoxemia
3.1. Chronic obstructive pulmonary disease
3.2. Interstitial lung disease
3.3. Sleep-disordered breathing
3.4. Alveolar hypoventilation disorders
3.5. Chronic exposure to high altitude
3.6. Developmental abnormalities

Category 4. Pulmonary hypertension due to chronic thrombotic and/or embolic disease
4.1. Thromboembolic obstruction of proximal pulmonary arteries
4.2. Thromboembolic obstruction of distal pulmonary arteries
4.3. Non-thrombotic pulmonary embolism (tumor, parasites, foreign material)

Category 5. Miscellaneous
Sarcoidosis, histiocytosis X, lymphangiomatosis, compression of pulmonary vessels (adenopathy, tumor, fibrosing mediastinitis)

[#] For the classification of congenital systemic-to-pulmonary shunts see Simonneau et al. [8].

In 2008, experts at the *Fourth World Symposium on Pulmonary Hypertension (PH) held in Dana Point, California*, made only small modifications to the published PH classification, but developed new treatment algorithms for PAH[10] (see **1.2**). The revised Clinical Classification of Pulmonary Hypertension (Dana Point, 2008) is expected to be published in 2009.

1.2 Definition, Diagnosis and Current Treatment of Pulmonary Arterial Hypertension

Definition of PAH (Gaine et al. Lancet, 1998)[11]:

1) Increased mean pulmonary arterial pressure (mPAP), i.e. mPAP > 25mmHg at rest, or mPAP > 30 mmHg during exercise, and

2) Normal pulmonary capillary wedge pressure (PCWP < 15mmHg), and

3) Associated adverse changes in the pulmonary vasculature (arteriopathy), and at the level of the right ventricle (e.g., RV hypertrophy).

Other definitions incorporated high pulmonary vascular resistance (PVR > 3 Wood units) as diagnostic criterion for PAH.

Current diagnostic approaches include cardiac catheterization, echocardiography and cardiac magnetic resonance imaging (MRI) ± angiography[12, 13], particularly focusing on the detrimental RV mass, volume and function including RV pressure volume loops[14, 15]. Further diagnostic techniques such as [^{18}F]fluorodeoxyglucose positron emission tomography (PET)[16] are under development.

By the end of 2008, there are 7 approved drugs for the *treatment of PAH* worldwide, all of which are considered to be pulmonary vasodilators: Endothelin-1 (ET-1) receptor antagonists (ERA),

phosphodiesterase-5 (PDE-5) inhibitors, and prostacyclins (i.e., PGI_2 analogues)[17, 18]. Fifteen published randomized clinical trials have demonstrated their (moderate) effectiveness, mainly based on a short-term improvement in exercise tolerance, as measured by a 6-minute-walk test. Hemodynamically, the drugs tend to raise cardiac output with little effect on pulmonary artery pressure (PAP). Yet, there has never been a single randomized clinical trial for PAH that lasted beyond 16 weeks that has demonstrated sustained clinical benefit or any reduction in mortality[19]. The improvement in 6-minute walk distance (30-40m) resembles about 3 steps a minute and has not been shown to equate with improved survival. In light of the reports that a 54-m improvement is the smallest change that adult patients can relate to actually feeling better[20] and a 90-m improvement in 6-minute walk distance (6MWD) is achievable with exercise training alone[21], H.A. Ghofrani et al. [19] recently wondered whether the drug therapies for PAH have had any impact on the disease at all.

The treatment algorithm that has recently been developed in Dana Point (2008), California, will contain a number of important innovations for patients with pulmonary *arterial* hypertension (PAH), but also for those with other forms of PH. In PAH patients, a targeted therapy with ERA or PDE5 inhibitors is now recommended for patients in functional class II. Combination therapy (ERA and/or PDE-5 inhibitors and/or prostanoids) is proposed if the clinical response to monotherapy is not adequate[10]. It is more and more recognized that early, targeted PAH therapy is probably the most promising way to treat this fatal disease in children[22] and adults[23]. Whether the approved drugs for PAH may be applied to patients with non-category 1 (i.e., non-PAH) pulmonary hypertension, underlies an ongoing debate[24].

1.3 Pathobiology of Pulmonary Arterial Hypertension

The pathobiology of PAH is complex and multifactorial (reviewed in[11, 17, 25-29]), and none of the current therapies has been shown to be universally effective or able to reverse advanced pulmonary vascular disease (characterized by plexiformic vascular lesions)[1, 17, 19].

1.3.1 PDGF-BB- and EGF-Signaling in Pulmonary Arterial Hypertension

A hallmark of PAH is enhanced platelet-derived growth factor B (PDGF-BB homodimer)[30] and epidermal growth factor (EGF) signaling[31, 32]. Both PDGF-BB, through its receptor, PDGFR-β, and EGF via the EGF receptor (EGFR), activate mitogen-activated protein kinases (MAPK) in vascular smooth muscle cells (SMC). Activated MAPK induce growth-promoting genes (e.g., cyclin D1) and subsequently SMC proliferation, migration and survival – all key features of pulmonary vascular remodeling (**Figure 1a**).

Imatinib (STI571), a compound used to treat chronic myeloid leukemia, blocks the tyrosine kinase activity of PDGFR-β and other proteins (e.g., ABL, Bcr-Abl, c-KIT), but hardly affects the EGFR (i.e., also a receptor tyrosine kinase, RTK). Interestingly, oral treatment with imatinib lowered pulmonary vascular resistance in cases of endstage PAH and led to remarkable clinical improvement[33, 34]. A multicenter, blinded, randomized, placebo-controlled trial on imatinib as add-on therapy for severe PAH has just been completed in 2008 (PI: Ghofrani HA; EU: EudraCT-no. 2005-005569-12; US: IND no. 76,778; final results pending). Since none of the current PAH therapies have been demonstrated to be uniformly effective, it can be expected that some patients may not respond to additional PDGFR-β blockade by imatinib. Those non-responders might have ongoing mitogenic stimulation through the EGFR-MAPK axis that is not affected by imatinib (**Figure 1**). Hence, a drug target downstream of PDGFR-β and EGFR that - when activated - inhibits MAPK activity and multiple other growth-promoting pathways, may be of additional and even greater benefit than receptor tyrosine kinase blockers, and able to arrest or reverse advanced clinical PAH (**Figure 1b**).

Figure 1

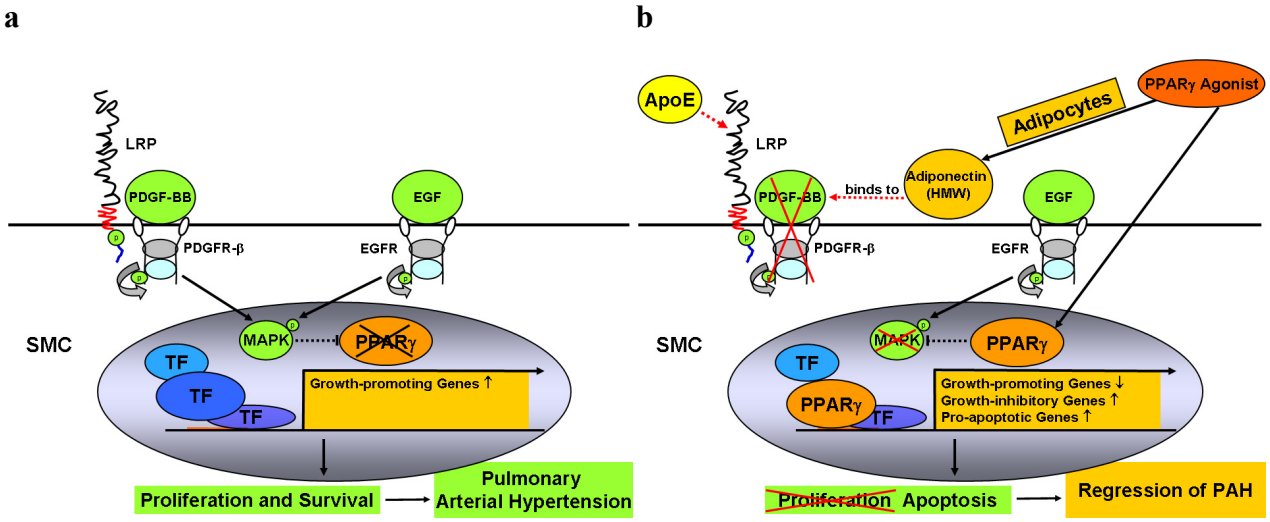

Figure 1 Model

a, Heightened PDGF-BB- and EGF-signaling leading to SMC proliferation and survival is a key clinical feature of PAH. Deficiency of both apoE and LRP enhances mitogenic PDGF-BB-MAPK-signaling that turns on the cell cycle machinery (e.g., cyclin D1) and other growth-promoting genes.

b, PPARγ activation induces growth-inhibitory and pro-apoptotic genes in SMC, and inhibits cell cycle promoting genes such as telomerase, cyclin D1 and retinoblastoma protein. Moreover, PPARγ induces phosphatases that can directly inactivate MAPK (e.g., pERK) downstream of PDFR-β and EGFR. Besides gene regulation in SMC, PPARγ agonists induce the anti-mitogenic adipocytokine apiponectin that sequesters the ligand PDGF-BB ("vasocrine signaling from fat cells"). By blocking important survival pathways downstream of activated PDGFR-β, e.g., phosphatidylinositol 3-kinase (PI3K), PPARγ agonists may also lead to apoptosis of SMC. Therefore, PPARγ agonists have the potential to reverse SMC proliferation and vascular remodeling in PAH patients.

Abbreviations: apoE, apolipoprotein E; EGF, epidermal growth factor; LRP, low density lipoprotein (LDL) receptor related protein; MAPK, mitogen-activated protein kinase; PDGF-BB, platelet-derived growth factor BB; PPARγ, peroxisome proliferator-activated receptor gamma; SMC, smooth muscle cell(s); TF, transcription factor

1.3.2 Bone Morphogenetic Protein Receptor II (BMP-RII) Dysfunction in PAH

Loss-of-function-mutations in the bone morphogenetic protein receptor II (BMP-RII) gene are common in familial PAH (FPAH; 50-60%)[35-37], idiopathic PAH (IPAH; 10-20%), and PAH associated with other conditions (APAH; 6-9%) such as congenital heart defects or anorexic drug use (fenfluramine derivates)[38, 39]. Moreover, independent of a mutation, patients with IPAH/FPAH (formerly called "primary PH"), and even those with APAH (also called "secondary PAH") in the absence of a known mutation, have reduced pulmonary expression of BMP-RII[40]. The inheritance pattern of (mutant) BMP-RII in FPAH is that of a dominant gene with low penetrance, in that only ≈20% of affected family members develop the disease[37]. Thus, there are likely additional genetic and environmental (e.g., metabolic) modifiers , so-called "second hits" [41], that contribute to the impaired anti-mitogenic function of BMP-RII, and the development of PAH. This suggests it might be possible to rescue the adverse sequelae of BMP-RII dysfunction by manipulating its downstream effectors and environmental modifiers to advantage.

1.4 Peroxisome Proliferator-Activated Receptor Gamma (PPARγ): A Vasoprotective, Insulin-Sensitizing Transcription Factor

Peroxisome proliferator-activated receptors (PPARs: α, β/δ, γ) are ligand-activated transcription factors belonging to the nuclear receptor superfamily. PPARγ plays a major role in adipogenesis and glucose metabolism[42, 43], and its deficiency in fat and skeletal muscle cells leads to insulin resistance (IR)[42, 44]. Upon ligand activation, PPARγ heterodimerizes with the retinoid X receptor (RXR) and regulates multiple target genes[45, 46], e.g., the glucose tranporter GLUT4[47], adiponectin[48], interleukin 6 (IL-6)[49], monocyte chemoattractant protein 1 (MCP-1[50, 51], also known as CCL2[52]), ET-1[53, 54] and the endogenous endothelial NO synthase (eNOS) inhibitor asymmetric dimethylarginine (ADMA)[55, 56]. PPARs can also interact with signaling molecules to regulate gene expression independent of DNA-binding[46]. For example, PPARγ impairs phosphorylation (i.e., activation) of extracellular-regulated kinase (ERK)[57, 58], a MAP kinase downstream of PDGF receptor beta that is implicated in SMC proliferation and migration[45] (see also **1.3.1**). The antidiabetic drugs rosiglitazone and pioglitazone, both PPARγ ligands of the thiazolidinedione (TZD) class, inhibit PDGF-BB-induced SMC proliferation and migration in culture and in animal models of systemic cardiovascular disease[45, 59, 60], and therefore have therapeutic potential beyond insulin resistance.

1.5 PPARγ - A Drug Target Downstream of Bone Morphogenetic Protein Receptor II ?

It was unknown whether the transcription factor PPARγ acts downstream of BMP-RII; if this was the case, it can be expected that BMP-RII dysfunction would lead to decreased endogenous PPARγ activity. Previously, BMP-2 has been shown to stimulate adipogenic differentiation of mesenchymal precursor cells in synergy with the PPARγ agonist rosiglitazone, but BMP-2 alone (500ng/ml) had no effect on adipocyte differentiation[61]. Apolipoprotein E (apoE) was found to be upregulated by BMP-2 in a murine mesenchymal progenitor cell line (C3H10T1/2)[62], however, prior to publication of my studies, apoE had not been demonstrated to be expressed in *vascular smooth muscle cells* at all.

There is supporting evidence that links PPARγ with transcription of apoE. A functional peroxisome-proliferator-activated-receptor response element (PPRE) specific for PPARγ had been identified in the apoE gene control region (apoE/apoCI intergenic region) by studies on a glioblastoma-astrocytoma cell line (U-87 MG). A conditional disruption of the PPARγ gene (PPARG) in mice results in decreased apoE expression in macrophages[63], and PPARγ activation leads to apoE mRNA expression and protein secretion in an adipocyte cell line[64]. Moreover, the anti-mitogenic and pro-apoptotic effects of PPARγ in *systemic* cardiovascular disease are well established[43, 45, 59, 65]. Interestingly, mRNA expression of all three BMP-2, PPARγ and apoE is decreased in lung tissues from PAH patients[40, 66, 67]. Our own published work presented here is - to the best of our knowledge - the first evidence of an antiproliferative BMP-2/PPARγ/apoE axis in primary cells[68], and the first demonstration of the vasoprotective effects of PPARγ and apoE in *pulmonary* vascular disease.

1.6 The Link Between Insulin Resistance and Pulmonary Arterial Hypertension

Over the past two decades, we have seen a remarkable increase in the number of children, adolescents[69] and adults[70] with the metabolic syndrome (MS) at high risk for *systemic* cardiovascular disease[71]. However, it was unknown whether the key features of the metabolic syndrome[70-77] - obesity, dyslipidemia and insulin resistance (IR) - are associated with clinical pulmonary arterial hypertension. Recent findings, however, support such an association. Patients with idiopathic PAH have reduced pulmonary mRNA expression of PPARγ[66], a ligand-activated nuclear receptor and transcription factor that regulates adipogenesis and glucose metabolism[42-44]. They also have reduced pulmonary mRNA expression of apoE[67], a protective factor known to reduce circulating oxidized low-density lipoprotein (oxLDL) and atherogenesis in the vessel wall[78]. Deficiency of both PPARγ and apoE has been linked to insulin resistance and the "metabolic

syndrome" [43, 78]. Moreover, elevation of several circulating factors (i.e., ET-1[53, 79, 80], IL-6[49, 81], etc.[82]; see **1.4**) that are normally repressed by PPARγ is not only associated with IR but also implicated in the pathobiology of PAH. Adiponectin (see **Figure 1b**), a PPARγ target that is exclusively expressed in adipocytes, reverses insulin resistance[83], and is independently linked with a reduced risk of type 2 diabetes in apparently healthy individuals[84].

Low adiponectin and high CRP and IL-6 levels are associated with an increased risk for insulin resistance, metabolic syndrome, systemic and possibly also pulmonary vascular disease in humans[82, 85]. Yudkin and colleagues[86] previously proposed that detrimental adipocytokines such as TNF-α and IL-6 (both elevated in IR states), are secreted from perivascular fat cells ("vasocrine signaling"), and inhibit the eNOS-pathway of insulin signaling, leaving unopposed vasoconstriction mediated by endothelin-1 (ET-1), a key player in PAH[79]. ET-1 inhibits adiponectin secretion[87] and insulin sensitivity in healthy human subjects[88]. Chronic ET-1 receptor blockade (that is approved for PAH therapy) may normalize these abnormalities, and restore vasoreactivity in IR states[89]. Increased pulmonary ET-1 expression[79] and plasma elevation of the eNOS inhibitor ADMA[90] were observed in PAH patients, and heightened ADMA levels negatively correlated with hemodynamic performance and human survival rates[90], underlining the clinical relevance of these findings.

Intriguingly, PAH patients who underwent a 15-week exercise program had a remarkable and significant improvement in 6-minute-walk distance (91±61m) when compared to control PAH patients (-15±54m)[21]. Although many factors and mechanism could explain the benefits of exercise in these PAH patients, it is plausible that such gain of function is associated with improved insulin and lipid profiles.

In the studies presented here, we first studied PPARγ and apoE as potential downstream effectors of the BMP receptor II, and their antiproliferative effects in the pulmonary circulation *in vitro* and *in vivo* (**see 2.1**). We next investigated whether insulin resistance that occurs in apoE knock out mice fed a high fat diet, may be linked to PAH, and whether the latter can be reversed by PPARγ activation (**see 2.2**). Finally, the prevalence of insulin resistance in a cohort of 81 women with PAH *vs.* a matched control population was determined, and a possible association with poorer outcome at 6-months follow up was explored (**see 2.3**).

2. Results and Discussion

2.1 A Novel Antiproliferative BMP-2/PPARγ/ApoE Axis In Vascular Smooth Muscle Cells And Its Vasoprotective Role In Pulmonary Hypertension

Bone morphogenetic protein 2 (BMP-2) is a negative regulator of smooth muscle cell (SMC) growth, but the mechanism by which it counteracts proliferation induced by growth factors (i.e., PDGF-BB, EGF) associated with PAH[30, 32] remains to be characterized. Loss-of-function-mutations in the BMP-RII gene are common in PAH (see introduction, **1.3.2**) [35-39], and even in the absence of a mutation, PAH patients frequently have reduced pulmonary expression of BMP-RII[40]. This suggests it might be possible to rescue the adverse sequelae of reduced expression and anti-mitogenic signaling of BMP-RII by manipulating its downstream effectors to advantage.

Two potential downstream effectors of BMP-RII signaling are the transcription factor PPARγ and its putative target, apoE[91]. Interestingly, mRNA expression of both factors, in addition to BMP-2, is decreased in lung tissues from PAH patients [40, 66, 67]. There is supporting evidence in cell lines and macrophages that links PPARγ with transcription of apoE (see introduction **1.4, 1.5**). ApoE inhibits PDGF-BB-mediated SMC proliferation and migration [92, 93] by binding to LDL receptor related protein (LRP) and internalizing the PDGFR-β [94, 95]. Heightened arterial PDGF-BB-/MAPK signaling is not only evident in apoE deficient mice [96], but is also a key clinical feature of pulmonary vascular disease in humans[30, 33, 97].

We hypothesized that both PPARγ and apoE act downstream of BMP-2/BMP-RII in primary cells (i.e., human and murine PASMC), and prevent SMC proliferation in response to PDGF-BB (**Figure 2**). For long term gene silencing of human BMP-RII, I first constructed a pLentivirus 6 with an integrated small hairpin (sh) oligonucleotide directed against the mRNA of human BMP-RII (shRNAi). We confirmed, by RT-qPCR, an 85% stable knock down of BMP-RII mRNA in shBMP-RIIi *vs.* shLacZi (control) transfected human (H) PASMC (see J Clin Invest, 2008, Supplementary Figure 1). I established western immunoblotting on cell fractions (nuclear matrix, nuclear extract, cytoplasmic extract) in human PASMC to investigate phosphorylation, intracellular expression and shuttling of MAP kinases and transcription factors, and applied a new multiplex transcription factor (TF) assay to the nuclear extracts. To explore the vasoprotective role of PPARγ in preventing the development of PAH in an intact animal, we created a transgenic mouse with targeted deletion of PPARγ in arterial SMC (*SM22α Cre PPARγ$^{flox/flox}$; abbrev. SMC PPARγ -/-*), and determined hemodynamics by RV catheterization (RVSP, RV dp/dt max. and min.), echocardiography, and systemic blood pressure (tail cuff method). We also assessed RV hypertrophy (mass ratio RV/LV+septum), and peripheral PA muscularization by histology

(MOVAT staining, immunohistochemistry using antibodies directed against alpha smooth muscle actin (αSM-actin) and proliferating cell nuclear antigen (PCNA). In addition, we studied murine and human PASMC deficient in either PPARγ or apoE under several experimental conditions.

Figure 2

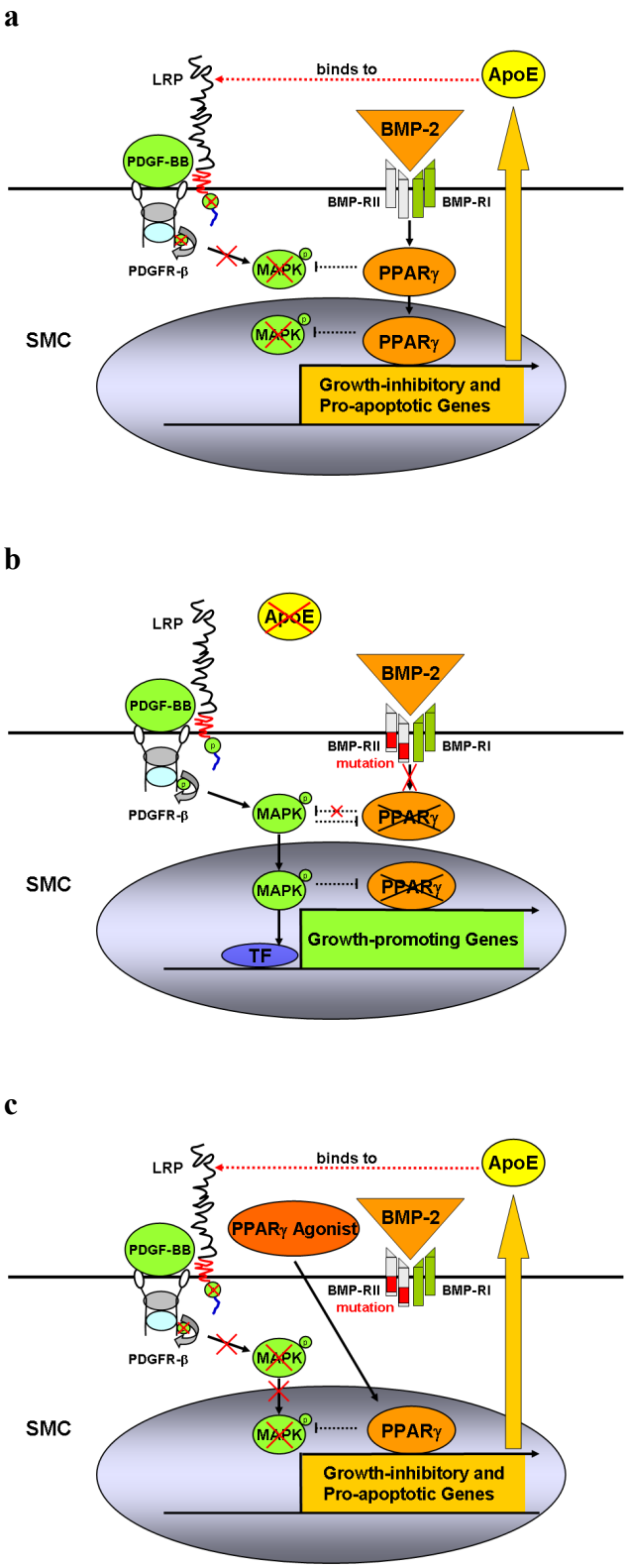

Figure 2, Model: A novel antiproliferative BMP-2/ApoE/PPARγ-axis protects against pulmonary arterial hypertension. This schema incorporates the findings described in our paper and the literature to date as discussed.

a, BMP-2 Inhibits SMC Proliferation via PPARγ and ApoE. ApoE impairs PDGF-BB-MAPK signaling by binding to LDL receptor related protein (LRP), thereby initiating endocytosis and degradation of the LRP–PDGFR-β–PDGF-B complex. PPARγ induces LRP and other growth-inhibitory/pro-apoptotic genes in SMC, and inhibits cell cycle and other growth promoting genes such as telomerase, cyclin D1 and retinoblastoma protein. Moreover, PPARγ induces phosphatases that can directly inactivate pERK, i.e. a MAPK.

b, BMP-RII Dysfunction Promotes SMC Proliferation and Survival in PAH. Heightened PDGF-BB-signaling leading to SMC proliferation is a key clinical feature of PAH. Deficiency of both apoE and LRP enhance mitogenic PDGF-BB-MAPK-signaling. Loss-of-function mutations in the BMP-RII gene will decrease endogenous PPARγ activity, leading to unopposed MAPK-signaling, SMC proliferation and survival, and ultimately development of pulmonary arterial hypertension.

c, PPARγ Agonists Can Rescue BMP-RII Dysfunction and Reverse PAH. PPARγ agonists such as rosiglitazone or pioglitazone might reverse SMC proliferation and vascular remodeling in PAH patients with or without BMP-RII dysfunction via induction of apoE and other growth-inhibitory/pro-apoptotic genes (as indicated), and through repression of growth-promoting genes (not shown).

Abbreviations: apoE, apolipoprotein E; BMP-2, bone morphogenetic protein 2; BMP-RII, BMP receptor II; EGF, epidermal growth factor; LRP, low density lipoprotein (LDL) receptor related protein; MAPK, mitogen-activated protein kinase (e.g., extracellular regulated kinase, ERK); PDGF-BB, platelet-derived growth factor BB; PPARγ, peroxisome proliferator-activated receptor gamma; SMC, smooth muscle cell(s); TF, transcription factor. From: Hansmann G et al., J Clin Invest 2008; 118:1846–185.

BMP-2 Mediated Inhibition of Human PASMC Proliferation Requires BMP-RII, PPARγ and ApoE. Recombinant BMP-2 (10ng/ml) inhibited PDGF-BB-induced proliferation in LacZi control but not in shBMR-RIIi HPASMC as determined by cell counts and a biochemical MTT assay. We also confirmed that siBMP-RII abolished BMP-2-induced phosphorylation of Smad 1/5/8, a pathway known to be downstream of BMP-RII (see J Clin Invest, 2008; Supplementary Figure 4)

Opposing Effects of PDGF-BB and BMP-2 on pERK and PPARγ Activation in Human PASMC. We next determined whether BMP-2 and PDGF-BB might have opposing effects on the subcellular localization of pERK and PPARγ that would explain their functional antagonism in PASMC. PPARγ has been shown to activate phosphatases and prevent ERK phosphorylation in vascular SMC [57, 58]. In addition, PPARγ activation can directly inhibit PDGF-BB-mediated pERK activity [98] by blocking its nuclear translocation[99]. Conversely, PDGF-BB-/PDGFR-β-mediated phosphorylation of ERK has been shown to lead to phosphorylation and thereby inactivation of PPARγ at its N-terminal [100] (**Figure 2b**).

PDGF-BB stimulated a 3-5 fold increase of pERK1/2 in nuclear extracts, and a 4-fold rise of pERK1 in cytoplasmic extracts of HPASMC. BMP-2, however, led to a rapid decrease in pERK 1/2 in nuclear extracts, and significantly reduced pERK2 in cytoplasmic extracts. PDGF-BB rapidly and transiently decreased nuclear protein levels and DNA-binding of PPARγ. This decrease in PPARγ-DNA-binding temporally coincided with the rapid appearance of pERK1/2 in the nucleus upon PDGF-BB stimulation. There was no significant change in PPARγ levels in cytoplasmic extracts. In contrast to PDGF-BB, BMP-2 induced a rapid and marked increase in PPARγ-DNA-binding associated with elevated levels of PPARγ protein in nuclear extracts (two key experiments). The latter could represent stabilization of PPARγ, but since PPARγ tended to be concomitantly lower in cytoplasmic extracts, transient nuclear shuttling of PPARγ is also likely. Of note, BMP-2 mediated PPARγ activation in HPASMC occurred earlier than phosphorylation of Smad1/5/8 (see Supplementary Figure 4). Therefore pSmad1/5/8 does not appear to mediate DNA-binding of PPARγ upon BMP-2 stimulation.

BMP-2 and a PPARγ Agonist Inhibit PDGF-BB-Signaling in Human PASMC. We next determined whether BMP-2 and PPARγ activation inhibit PDGF-BB-Induced MAPK pathways (i.e., pERK1/2). BMP-2 inhibited PDGF-BB-induced nuclear and cytoplasmic ERK phosphorylation. BMP-2 also prevented PDGF-BB-mediated inhibition of PPARγ DNA-binding. In fact an increase in PPARγ DNA-binding was observed with BMP-2 despite concomitant PDGF-BB stimulation. Moreover, 24h preincubation with the PPARγ agonist rosiglitazone significantly reduced and delayed PDGF-BB-induced ERK phosphorylation in total cell lysates. Hence, BMP-2 and the

PPARγ agonist rosiglitazone act as functional antagonists of PDGF-BB-signaling by inhibiting ERK1/2 phosphorylation (**Figure 2**).

The PPARγ Agonist Rosiglitazone Blocks PDGF-BB-Induced Proliferation of BMP-RII Mutant HPASMC. We next investigated whether PPARγ activation could inhibit PDGF-BB-induced proliferation of human (H) PASMC with a loss-of-function mutation in the BMP-RII gene. Therefore we isolated PASMC from the explanted lung of a patient with FPAH known to harbor a frameshift mutation in BMP-RII. As expected, BMP-2 inhibited PDGF-BB-induced proliferation in control but not BMP-RII mutant HPASMC. However, the PPARγ agonist rosiglitazone blocked PDGF-BB-induced proliferation both in control and BMP-RII mutant cells so that cell numbers were similar to unstimulated controls. Thus, PPARγ agonists have the potential to 'rescue' the growth-inhibitory effect of BMP-2 in PASMC with BMP-RII dysfunction (**Figure 2c**).

BMP-2 and Rosiglitazone Induce ApoE Expression and Secretion in Human PASMC. Since the growth-inhibitory effect of BMP-2 is absent in apoE deficient PASMC, we hypothesized that apoE might be a transcriptional target of BMP-2-activated PPARγ in SMC. We could show for the first time that apoE protein is expressed in vascular smooth muscle cells. Intriguingly, both BMP-2 and rosiglitazone induced apoE protein expression and secretion in HPASMC. The BMP-2-mediated upregulation of apoE protein was reduced by half in PASMC harvested from SMC PPARγ -/- mice. This suggests the induction of apoE expression by BMP-2 is to a great extent PPARγ-dependent (**Figure 2**).

Finally, we show that mice with deletion of PPARγ in SMC (SM22α Cre PPARγ $^{flox/flox}$ mice; abbreviated SMC PPARγ -/-) spontaneously develop PAH as indicated by elevated RVSP (29.0 vs. 21.5mmHg, $p<0.001$), RVH (RV/LV+S 0.46 vs. 0.26, $p<0.0001$), and enhanced peripheral PA muscularization at the alveolar wall level. We found the muscular thickening in the small pulmonary arteries of SMC PPARγ -/- mice to be associated with stronger expression of αSM-actin (a SMC marker) and growth-promotive PCNA in the muscle layer of the arterial wall. Systemic blood pressure, RV function and LV function, and cardiac output were not significantly different when comparing the two groups. LV enddiastolic inner diameter, LV enddiastolic posterior wall thickness and end-diastolic interventricular septum thickness as measures of LV dilatation and hypertrophy (LVH) were not different between the two genotypes. Thus, LV dysfunction does not account for the PAH in SMC PPARγ -/-mice. SMC PPARγ -/- mice had similar hematocrit and glucose values but slightly higher white blood cell (WBC) counts than controls.

Why does deletion of PPARγ in arterial smooth muscle cells lead to spontaneous development of PAH in mice? Activated PPARγ can induce multiple other growth-inhibitory and pro-apoptotic gene products, and repress growth-promoting factors in vascular cells (see **2.4** for details). We discovered a novel antipoliferative BMP-2/PPARγ/apoE axis in vascular smooth muscle cells that blocks PDGF-BB-induced signaling (i.e., PDGF-Rβ, pERK) and SMC proliferation, as described above. Others have shown that PPARγ activation blocks PDGF gene expression [101] and induces the expression of LRP [102], the receptor necessary for apoE-mediated suppression of PDGF-BB signaling[94, 95] (**Figure 2**). Moreover, activated PPARγ stabilizes the cyclin-dependent kinase inhibitor $p27^{KIP1}$ [103], and inhibits telomerase activity[104], retinoblastoma protein phosphorylation[103], and ultimately G1→S phase transition, cell cycle progression and vascular SMC proliferation[103]. By blocking important survival pathways downstream of activated PDGFR-β, i.e., phosphoinositiol-3-kinase (PI3K) [105], PPARγ agonists also lead to apoptosis of proliferating vascular cells[45, 106]. In addition, it is known that PPARγ ligands impair production of matrix metalloproteinases[107] that can be activated by elastase[108]. Dr. Rabinovitch's group has shown that inhibition of this proteolytic cascade not only prevents but also reverses advanced fatal PAH in rats[109].

Previous studies have shown beneficial effects of BMP-2 [110], PPARγ activation [45] and apoE [92, 93] in preventing systemic vascular pathology, but our observations are the first indication that all three factors are linked. More recently a connection between PPARγ and apoE has been made in patients with Alzheimer's disease in that the improvement of cognitive function with rosiglitazone is not apparent in patients who carry the APOE epsilon 4 allele [111]. Hence, the novel axis we describe here may be relevant in addressing mechanisms that underlie many different pathologic processes.

In summary, our study[68] revealed a novel PPARγ-apoE axis downstream of BMP-2 signaling in human pulmonary artery smooth muscle cells. Failure to activate PPARγ in response to BMP-2 when BMP-RII is dysfunctional could place a patient at risk for the development or progression of PAH. We suggest that PPARγ agonists can rescue BMP-RII dysfunction and reverse SMC proliferation and vascular remodeling in PAH patients, and may be efficient, antiproliferative agents even in those patients without BMP-RII dysfunction.

Cited own reference, reproduced with permission from the American Society for Clinical Investigation:

Hansmann G, de Jesus Perez VA, Alastalo TP, Alvira CM, Guignabert C, Bekkers J, Schellong S, Urashima T, Wang L, Morrell NW, Rabinovitch M (2008). An antiproliferative BMP-2/ PPARγ/ApoE-axis in human and murine SMCs and and its role in pulmonary hypertension. **Journal of Clinical Investigation** 118:1846-1857 *epub April 1, 2008*

Research article

An antiproliferative BMP-2/PPARγ/apoE axis in human and murine SMCs and its role in pulmonary hypertension

Georg Hansmann,[1,2] Vinicio A. de Jesus Perez,[1] Tero-Pekka Alastalo,[1] Cristina M. Alvira,[1] Christophe Guignabert,[1] Janine M. Bekker,[1] Stefan Schellong,[1] Takashi Urashima,[1] Lingli Wang,[1] Nicholas W. Morrell,[3] and Marlene Rabinovitch[1]

[1]Department of Pediatrics, Stanford University School of Medicine, Stanford, California, USA. [2]Department of Pediatrics, UCSF, San Francisco, California, USA. [3]Department of Medicine, University of Cambridge, Cambridge, United Kingdom.

Loss-of-function mutations in bone morphogenetic protein receptor II (BMP-RII) are linked to pulmonary arterial hypertension (PAH); the ligand for BMP-RII, BMP-2, is a negative regulator of SMC growth. Here, we report an interplay between PPARγ and its transcriptional target apoE downstream of BMP-2 signaling. BMP-2/BMP-RII signaling prevented PDGF-BB–induced proliferation of human and murine pulmonary artery SMCs (PASMCs) by decreasing nuclear phospho-ERK and inducing DNA binding of PPARγ that is independent of Smad1/5/8 phosphorylation. Both BMP-2 and a PPARγ agonist stimulated production and secretion of apoE by SMCs. Using a variety of methods, including short hairpin RNAi in human PASMCs, PAH patient–derived BMP-RII mutant PASMCs, a PPARγ antagonist, and PASMCs isolated from PPARγ- and apoE-deficient mice, we demonstrated that the antiproliferative effect of BMP-2 was BMP-RII, PPARγ, and apoE dependent. Furthermore, we created mice with targeted deletion of PPARγ in SMCs and showed that they spontaneously developed PAH, as indicated by elevated RV systolic pressure, RV hypertrophy, and increased muscularization of the distal pulmonary arteries. Thus, PPARγ-mediated events could protect against PAH, and PPARγ agonists may reverse PAH in patients with or without BMP-RII dysfunction.

Introduction

Bone morphogenetic protein 2 (BMP-2) is a negative regulator of SMC growth, but the mechanism by which it counteracts proliferation induced by growth factors (i.e., PDGF-BB, EGF) associated with pulmonary arterial hypertension (PAH) (1, 2) remains to be characterized. Loss-of-function-mutations in the BMP receptor II (BMP-RII) gene occur in 50%–60% of patients with familial PAH (FPAH) (3–5), 10%–20% of patients with idiopathic PAH (IPAH), and 6%–9% of patients with secondary forms of PAH associated with anorexic drug use (fenfluramine derivates) or congenital heart defects (APAH) (6, 7). However, independent of a mutation, patients with IPAH/FPAH (formerly called "primary PH"), and even those with APAH (formerly called "secondary" PAH), albeit to a lesser extent, have reduced pulmonary expression of BMP-RII (8). Thus, there are likely environmental modifiers and additional genetic factors that contribute to the decreased expression and function of BMP-RII in association with the development of PAH. This would suggest that it might be possible to rescue the adverse sequelae of reduced expression and antimitogenic signaling of BMP-RII by manipulating its downstream effectors to advantage.

Two potential downstream effectors of BMP-RII signaling are the transcription factor PPARγ and its putative target apoE (9). Interestingly, mRNA expression of both factors, in addition to BMP-2, is decreased in lung tissues from PAH patients (8, 10, 11). PPARs are ligand-activated transcription factors belonging to the nuclear receptor superfamily. Upon ligand activation, PPARs heterodimerize with the retinoid X receptor (RXR) and bind to PPAR response elements (PPREs) in regulatory promoter regions of their target genes (12, 13). PPARs can also interact with signaling molecules to regulate gene expression independent of DNA binding (13). For example, PPARγ impairs phosphorylation (i.e., activation) of ERK (14, 15), a MAPK downstream of PDGF-BB/PDGFR-β signaling implicated in SMC proliferation and migration (12).

There is supporting evidence that links PPARγ with transcription of apoE. A functional PPARγ response element is present in the apoE promotor (9), conditional disruption of the PPARγ gene (*Pparg*) in mice results in decreased apoE expression in macrophages (16), and PPARγ activation leads to apoE mRNA expression and protein secretion in an adipocyte cell line (17). apoE inhibits PDGF-BB–mediated SMC proliferation and migration (18, 19) by binding to LDL receptor–related protein (LRP) and internalizing the PDGFR-β (20, 21). Heightened arterial PDGF-BB/MAPK signaling is not only evident in apoE$^{-/-}$ mice (22), but is also a key clinical feature of pulmonary vascular disease underlying PAH (2, 23, 24).

We have recently shown that insulin-resistant apoE-deficient (apoE$^{-/-}$) mice on a high-fat diet develop PAH. However, the fact that a PPARγ agonist reversed PAH in this model (25) suggests that PPARγ targets independent of apoE are also important in suppressing pulmonary vascular remodeling. The antidiabetic drugs rosiglitazone and pioglitazone, both PPARγ ligands of the thiazolidinedione (TZD) class, inhibit PDGF-BB–induced SMC proliferation and migration in culture and in animal models of systemic cardiovascular disease (reviewed in ref. 12). Because of these and additional antiinflammatory and proapoptotic effects of PPARγ activation (reviewed in ref. 12), PPARγ agonists may be useful in the future treatment of PAH.

Nonstandard abbreviations used: BMP-2, bone morphogenetic protein 2; BMP-RII, BMP receptor II; FPAH, familial PAH; HPASMC, human PASMC; PAH, pulmonary arterial hypertension; PASMC, pulmonary artery SMC; RVSP, RV systolic pressure.

Conflict of interest: The authors have declared that no conflict of interest exists.

Citation for this article: *J. Clin. Invest.* **118**:1846–1857 (2008). doi:10.1172/JCI32503.

Here, we report for the first time to our knowledge that both PPARγ and apoE act downstream of BMP-2/BMP-RII in primary cells (human and murine pulmonary artery SMCs [PASMCs]) and prevent SMC proliferation in response to PDGF-BB. BMP-2–mediated PPARγ activation occurs earlier than Smad1/5/8 phosphorylation and therefore appears to be independent of this established signaling axis downstream of BMP-RII. BMP-2 induces a decrease in nuclear phospho-ERK, and rapid nuclear shuttling and DNA binding of PPARγ, whereas PDGF-BB has the opposite effects. Both BMP-2 and the PPARγ agonist rosiglitazone stimulate production and secretion of apoE in PASMCs. Using short hairpin RNAi in human PASMCs (HPASMCs), PASMCs from a patient with FPAH and a mutation in BMP-RII (W9X), a PPARγ antagonist, and PASMCs lacking PPARγ or apoE, we demonstrate that the antiproliferative effect of BMP-2 is BMP-RII, PPARγ, and apoE dependent. Consistent with these data, we show that mice with deletion of PPARγ in SMCs (*SM22α Cre PPARγ$^{flox/flox}$* mice) spontaneously develop PAH. Taken together, our results reveal a novel PPARγ/apoE axis downstream of BMP-2 signaling that could explain the antiproliferative effect of BMP-RII activation in HPASMCs. Our data also suggest that PPARγ agonists might reverse SMC proliferation and vascular remodeling in PAH patients with or without BMP-RII dysfunction.

Results

Additional results are provided in the supplemental material (available online with this article; doi:10.1172/JCI32503DS1).

BMP-2–mediated inhibition of HPASMC proliferation requires BMP-RII, PPARγ, and apoE. For long-term gene silencing of human BMP-RII, we constructed a pLentivirus 6 with an integrated short hairpin oligonucleotide directed against the mRNA of human BMP-RII (shRNAi). We confirmed, by quantitative RT-PCR, an 85% stable knockdown of BMP-RII mRNA in shBMP-RIIi versus shLacZi (control) transfected HPASMCs (Supplemental Figure 1). Recombinant BMP-2 (10 ng/ml) inhibited PDGF-BB–induced proliferation in LacZi control but not in shBMR-RIIi HPASMCs as judged by cell counts (Figure 1). Results of MTT proliferation assays shown in Supplemental Figure 2 are consistent with cell counts. We reproduced the growth-inhibitory effect of BMP-2, with the same low concentration (10 ng/ml) of BMP-4 and -7, although BMP-7 appeared to have a weaker effect than BMP-2 and -4. Furthermore, with siBMP-RII (knockdown), there was less growth inhibition in response to BMP-2, -4, and -7 (Supplemental Figure 3). We also confirmed that siBMP-RII abolished BMP-2–induced phosphorylation of Smad1/5/8 (Supplemental Figure 4).

We then showed that the BMP-2–mediated inhibition of PDGF-BB–induced HPASMC proliferation requires not only BMP-RII, but also PPARγ. First, the antimitogenic effect of BMP-2 could be reproduced by the PPARγ agonist rosiglitazone (1 μM) (Figure 1B). Second, the antiproliferative effect of BMP-2 was lost in the presence of the irreversible PPARγ antagonist GW9662 (Figure 1C). Finally, BMP-2–mediated inhibition of PDGF-BB–induced cell proliferation was not observed in murine PASMCs with deletion of PPARγ but was found in PASMCs from littermate controls (Figure 1D). To address whether the effect of PPARγ could be mediated by induction of apoE, we first established that a physiological dose of recombinant apoE (10 μM) completely blocked PDGF-BB–induced proliferation of HPASMCs (Figure 1E). Moreover, the growth-inhibitory effect of BMP-2 on PDGF-BB–induced cell proliferation was lost in PASMCs from apoE$^{-/-}$ mice (Figure 1F). Taken together, these data support the presence of a novel antiproliferative axis downstream of BMP-2 that requires BMP-RII signaling, PPARγ activation, and production of apoE, a lipoprotein not previously known to be synthesized by SMC. Documentation of apoE production and secretion in HPASMCs in response to BMP-2 and rosiglitazone is described below.

Opposing effects of PDGF-BB and BMP-2 on phospho-ERK and PPARγ activation in HPASMCs. We next determined whether BMP-2 and PDGF-BB might have opposing effects on the subcellular localization of phospho-ERK and PPARγ that would explain their functional antagonism in PASMCs. PPARγ has been shown to activate phosphatases and prevent ERK phosphorylation in vascular SMCs (14, 15). In addition, PPARγ activation can directly inhibit PDGF-BB–mediated phospho-ERK activity (26) by blocking its nuclear translocation (27). Conversely, PDGF-BB/PDGFR-β–mediated phosphorylation of ERK leads to phosphorylation and thereby inactivation of PPARγ at its N terminus (28).

PDGF-BB stimulated a 3- to 5-fold increase in phospho-ERK1/2 in nuclear extracts and a 4-fold rise in phospho-ERK1 in cytoplasmic extracts (Figure 2A). BMP-2, however, led to a rapid decrease in phospho-ERK1/2 in nuclear extracts (Figure 2B) and significantly reduced phospho-ERK2 in cytoplasmic extracts (Figure 2B). PDGF-BB rapidly and transiently decreased nuclear protein levels and DNA binding of PPARγ. This decrease in PPARγ DNA binding (Figure 2C, upper panel) temporally coincided with the rapid appearance of phospho-ERK1/2 in the nucleus upon PDGF-BB stimulation (maximum at 5–10 min; Figure 2A). There was no significant change in PPARγ levels in cytoplasmic extracts (Figure 2C). In contrast to PDGF-BB, BMP-2 induced a rapid and marked increase in PPARγ DNA binding (Figure 2D) associated with elevated levels of PPARγ protein in nuclear extracts. This could represent stabilization of PPARγ, but since PPARγ tended to be concomitantly lower in cytoplasmic extracts, transient nuclear shuttling of PPARγ is also likely (Figure 2D). Of note, BMP-2–mediated PPARγ activation in HPASMCs (Figure 2, B and D) occurred earlier than phosphorylation of Smad1/5/8 (Supplemental Figure 4). Therefore, phospho-Smad1/5/8 does not appear to mediate DNA binding of PPARγ.

Interestingly, when we prepared total cell lysates containing the cytoplasmic membrane fraction, we found that BMP-2 induces rapid ERK1/2 phosphorylation (Supplemental Figure 5A). This fraction is absent in nuclear and cytoplasmic extract preparations due to high spin steps. We showed by immunohistochemistry that concomitant with the rapid decrease in phospho-ERK1/2 in the nucleus (shown by Western immunoblot in Figure 2B), BMP-2 led to strong phospho-ERK1/2 staining at the cytoplasmic membrane (Supplemental Figure 5B). It has been previously demonstrated in other cell types that phospho-ERK binds to cytoplasmic membrane proteins such as the receptor for advanced glycation end products (29).

BMP-2 and a PPARγ agonist inhibit PDGF-BB signaling in HPASMCs. We next determined whether BMP-2 and PPARγ activation inhibit PDGF-BB–induced MAPK pathways (i.e., phospho-ERK1/2). BMP-2 inhibited PDGF-BB–induced nuclear and cytoplasmic ERK phosphorylation (Figure 3A). BMP-2 also prevented PDGF-BB–mediated inhibition of PPARγ DNA binding. In fact an increase in PPARγ DNA binding was observed with BMP-2 despite concomitant PDGF-BB stimulation (Figure 3B). Moreover, 24-hour preincubation with the PPARγ agonist rosiglitazone significantly reduced and delayed PDGF-BB–induced ERK phosphorylation in total cell lysates (Figure 3C). Hence, BMP-2 and the PPARγ agonist rosiglitazone act as functional antagonists of PDGF-BB signaling by inhibiting ERK1/2 phosphorylation.

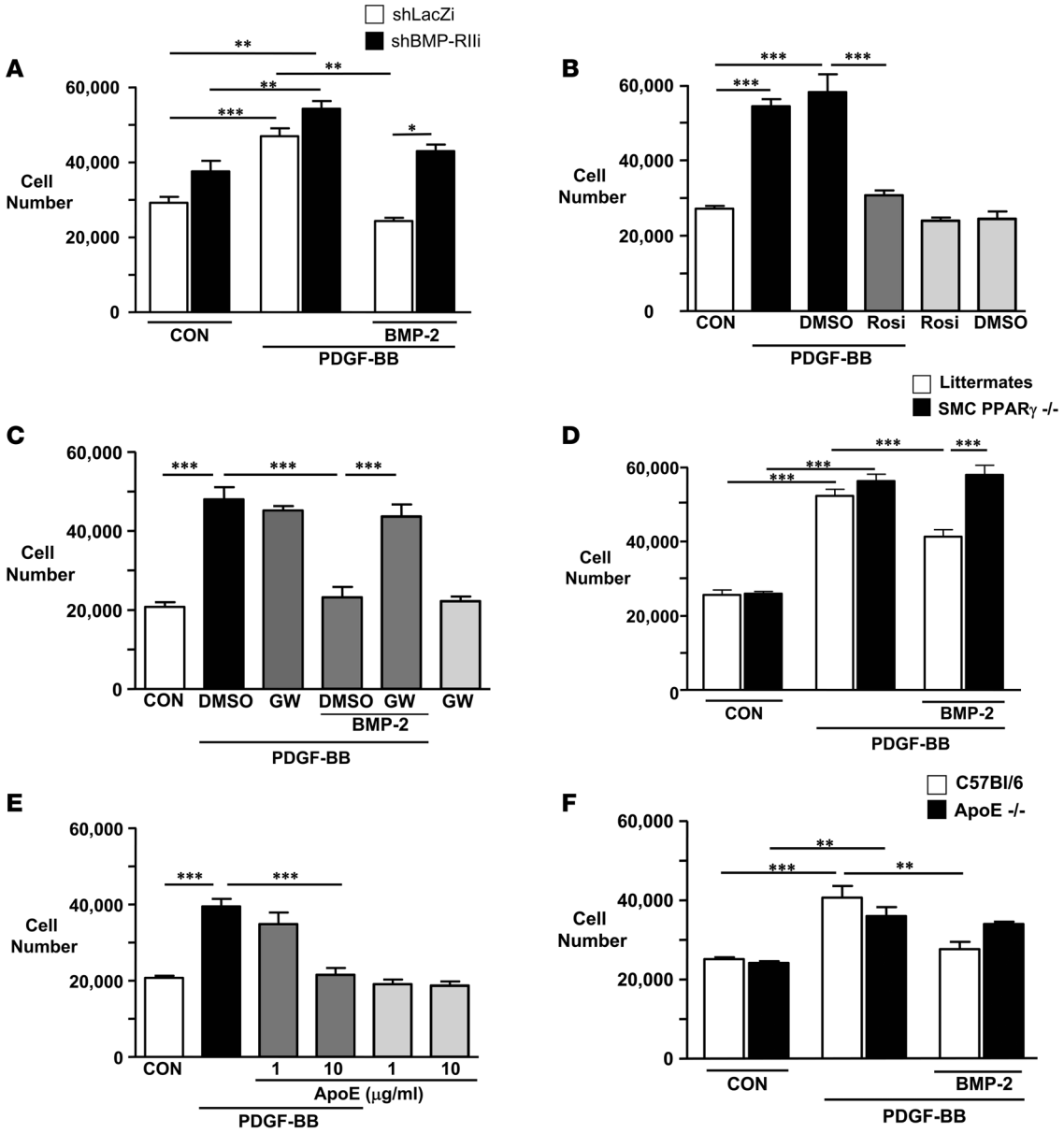

Figure 1

Antiproliferative effects of BMP-2 (**A**, **C**, **D**, and **F**), the PPARγ agonist rosiglitazone (Rosi; **B**), and apoE (**E**) on PDGF-BB–induced proliferation of human (**A**, **B**, **C**, and **E**) and murine (**D** and **F**) PASMCs. PASMCs were seeded at 2.5×10^4 cells per well of a 24-well plate in 500 μl of growth medium and allowed to adhere overnight. The cells were washed with PBS prior to the addition of starvation media (0.1% FBS) and incubated for 24 hours (murine PASMCs) or 48 hours (HPASMCs) and then stimulated with PDGF-BB (20 ng/ml) for 72 hours. BMP-2 (10 ng/ml), rosiglitazone (1 μM), and recombinant human apoE (1–10 μM) were added to quiescent cells 30 minutes prior to PDGF-BB stimulation. The PPARγ antagonist GW9662 (GW; 1 μM) was added 24 hours prior to the addition of BMP-2. Cells were finally washed twice with PBS, trypsinized, and counted in a hemacytometer (4 counts per well). Cell numbers in controls at time points 0 (CON) and 72 hours were not significantly different. **A**: shLacZi, HPASMCs transfected with short hairpin LacZi pLentivirus 6 (control); shBMP-RIIi, HPASMCs transfected with short hairpin pLentivirus 6 BMP-RIIi (i.e., BMP-RII–deficient PASMCs). **D**: Littermates, littermate control PASMCs; SMC PPARγ$^{-/-}$, PASMCs isolated from *SM22α Cre PPARγ$^{flox/flox}$* mice. **F**: C57BL/6, control murine PASMCs; apoE$^{-/-}$, PASMCs isolated from apoE-deficient mice. Bars represent mean ± SEM ($n = 3$ in **A**, **D**, and **F**; $n = 4$ in **B** and **C**; $n = 6$ in **E**; $n = 12$ in controls of **A**). $^*P < 0.05$; $^{**}P < 0.01$; $^{***}P < 0.001$ as indicated; ANOVA with Bonferroni's multiple comparison test.

Rosiglitazone blocks PDGF-BB–induced proliferation of BMP-RII mutant HPASMCs. We next investigated whether PPARγ activation could inhibit PDGF-BB–induced proliferation of HPASMCs with a loss-of-function mutation in the BMP-RII. Therefore, we isolated PASMCs from the explanted lung of a patient with FPAH known to harbor a frameshift mutation in BMP-RII. BMP-2 inhibited PDGF-BB–induced proliferation in WT but not BMP-RII mutant HPASMCs (Figure 4). In contrast, the PPARγ agonist rosiglitazone blocked PDGF-BB–induced proliferation in both WT and BMP-RII mutant cells so that cell numbers were similar to those in unstim-

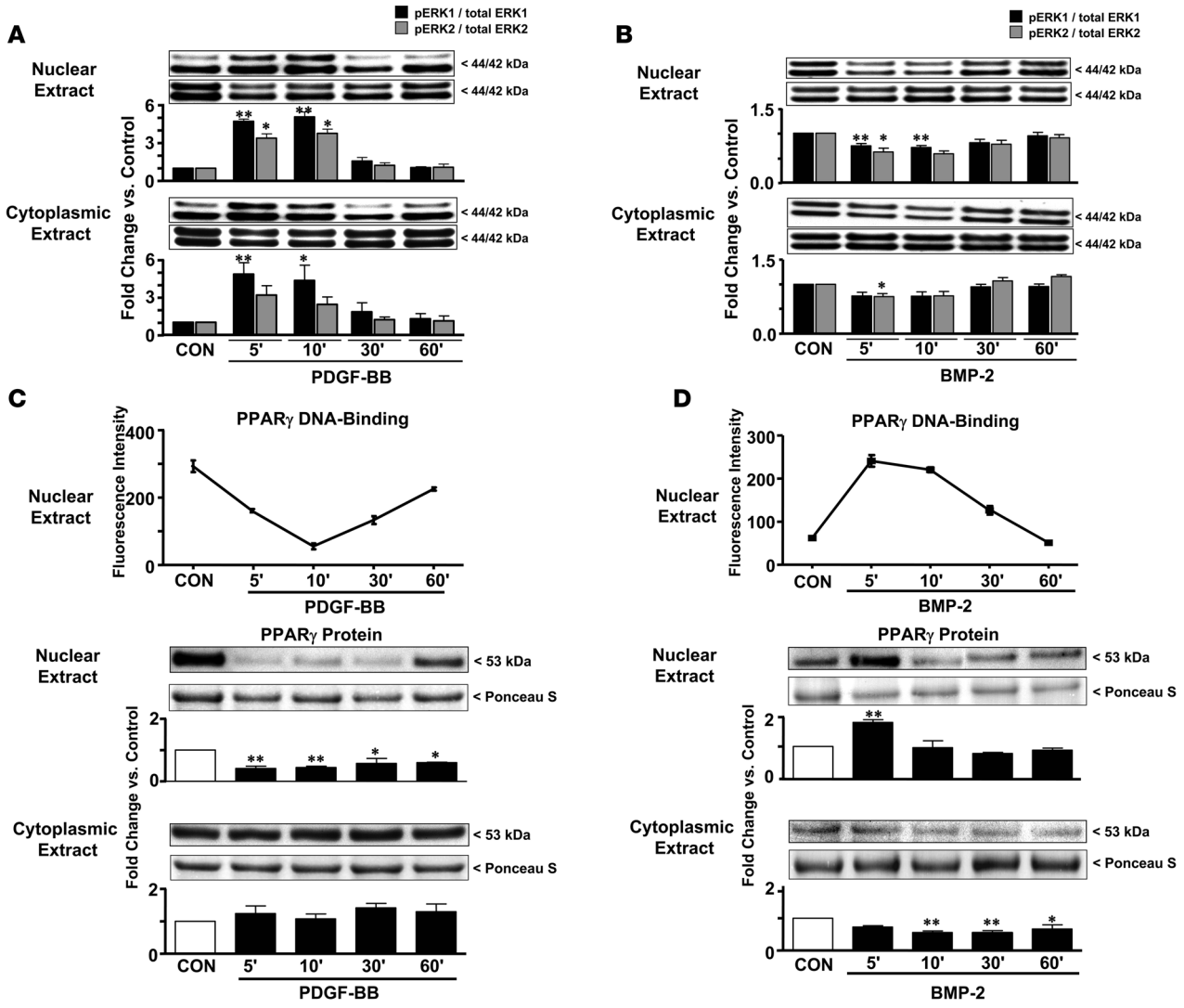

Figure 2

PDGF-BB (**A** and **C**) and BMP-2 (**B** and **D**) have opposing effects in HPASMCs on protein levels of phospho-ERK/total ERK (**A** and **B**), PPARγ DNA binding in nuclear extracts (upper panels in **C** and **D**), and PPARγ protein in nuclear and cytoplasmic extracts (lower panels in **C** and **D**). Cells were stimulated with PDGF-BB (20 ng/ml) or BMP-2 (10 ng/ml) as described in the legend for Figure 1. In separate experiments, we determined that neither of the solvents (DMSO, sterile water; both 1:10,000) influenced the results. Western immunoblotting and PPARγ DNA binding assays are described in Methods. For the PPARγ DNA binding assay, bars represent median ± SEM of triplicate measurements of 1 representative experiment of 2 (**C**) and 3 (**D**) independent experiments with similar results. For protein levels in cell fractions, bars represent mean ± SEM (n = 3–4). $^*P < 0.05$; $^{**}P < 0.01$ versus control; ANOVA with Dunnett's post-hoc test.

ulated controls (Figure 4). BMP-2 and rosiglitazone, in the (low) concentrations used, had no significant effect on the basal cell proliferation rate (Figure 4). Thus, PPARγ agonists have the potential to rescue the growth-inhibitory effect of BMP-2 in PASMCs with BMP-RII dysfunction.

BMP-2 and rosiglitazone induce apoE expression and secretion in HPASMCs. Since the growth-inhibitory effect of BMP-2 is absent in apoE-deficient PASMCs (Figure 1F), we hypothesized that apoE might be a transcriptional target of BMP-2–activated PPARγ in SMCs. Indeed, both BMP-2 and rosiglitazone induced apoE protein expression (cell lysates) and secretion (supernatant) in HPASMCs (Figure 5A). Moreover, the BMP-2–mediated upregulation of apoE protein was reduced by half in PASMCs harvested from *SM22α Cre PPARγ$^{flox/flox}$* mice (Figure 5B). This suggests that the induction of apoE expression by BMP-2 is to a great extent PPARγ dependent.

Creation of mice with targeted deletion of PPARγ in arterial SMCs (SM22α Cre PPARγ$^{flox/flox}$). To explore the vasoprotective role of PPARγ in preventing the development of PAH in an intact animal, we investigated a transgenic mouse with targeted deletion of PPARγ in arterial SMCs (*SM22α Cre PPARγ$^{flox/flox}$*). We documented, by PCR, gain of a new knockout transcript (300 bp) and almost complete loss of the 700-bp wild-type transcript in PASMCs and aorta isolated from *SM22α Cre PPARγ$^{flox/flox}$* mice (Figure 6A). Both the wild-type and the knockout transcript were found in lungs from *SM22α Cre PPARγ$^{flox/flox}$* mice, since the tissue contains several cell types besides SMCs. In contrast, only the wild-type transcript was detected in lung

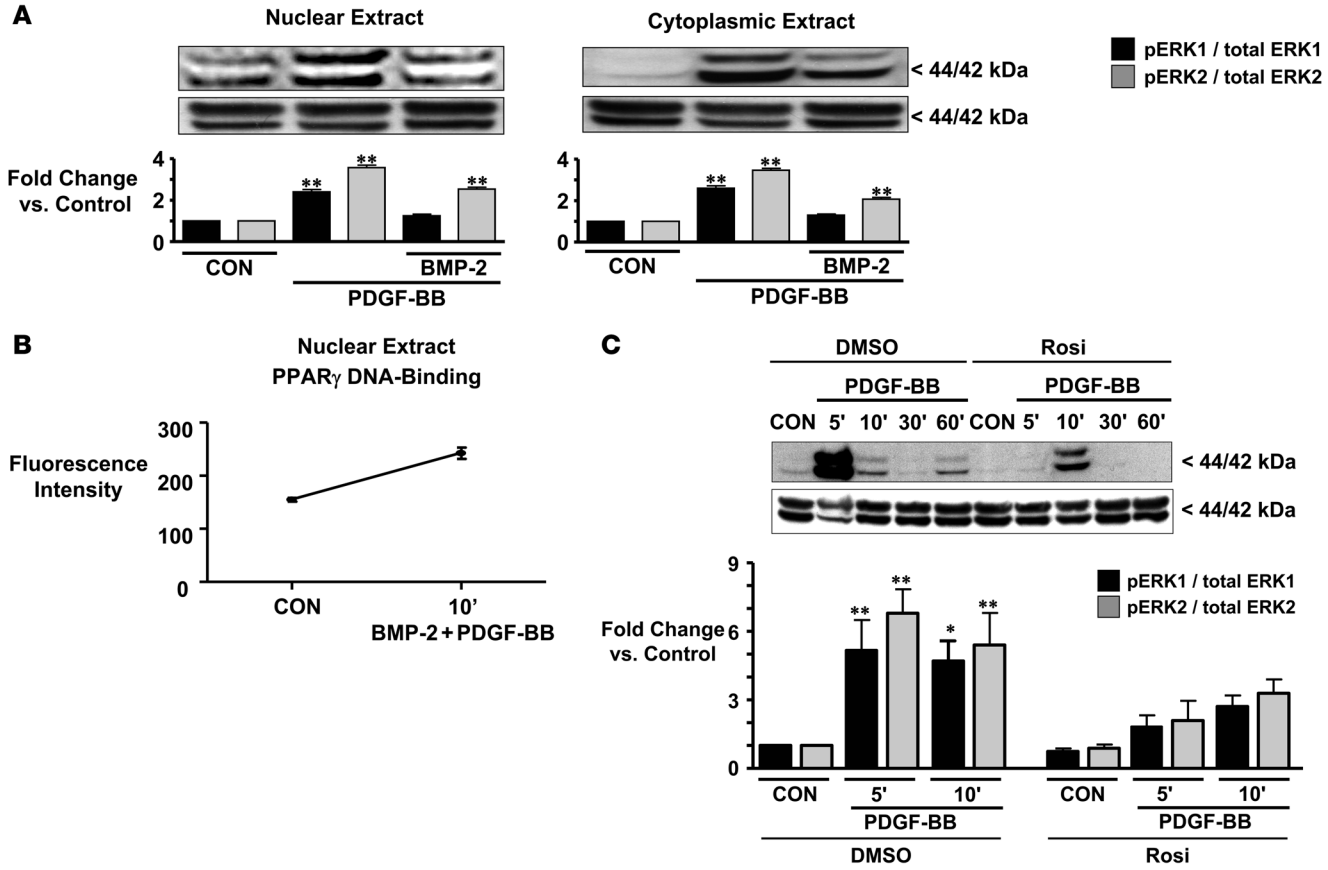

Figure 3

BMP-2 and rosiglitazone inhibit PDGF-BB–mediated ERK phosphorylation (**A** and **C**), and concomitant BMP-2 and PDGF-BB stimulation increases PPARγ DNA binding (**B**), in HPASMCs. Cells were preincubated with BMP-2 (10 ng/ml) for 30 minutes (**A** and **B**) or rosiglitazone (1 μM) for 24 hours (**C**), followed by PDGF-BB (20 ng/ml) stimulation for 10 minutes (**A** and **B**) or 5–60 minutes. (**C**) Western immunoblotting and PPARγ DNA binding assays are described in Methods and Figure 2. For protein levels in cell fractions (**A**) or cell lysates (**C**), bars represent mean ± SEM (n = 3 each). In **C**, all samples are compared with the DMSO control. For the PPARγ DNA binding assay (**B**), bars represent median ± SEM of triplicate measurements of 1 representative experiment of 3 independent experiments with similar results. *P < 0.05; **P < 0.01 versus control; ANOVA with Dunnett's post-hoc test.

tissue from littermate control mice (Figure 6A). We also confirmed knockout of PPARγ protein in PASMCs from *SM22α Cre PPARγ$^{flox/flox}$* mice (Figure 6B). BMP-2 stimulation of these murine PPARγ-deficient PASMCs revealed intact phospho-Smad1/5/8 signaling that occurred earlier (5–10 minutes; Figure 6C) than in human control PASMCs, where it was observed at 30 minutes (Supplemental Figure 4). Hence, the established BMP-2/phospho-Smad1/5/8 signaling pathway appears to be independent of PPARγ, since it occurs in PASMCs with deletion of PPARγ (Figure 6C).

Mice with targeted deletion of PPARγ in arterial SMCs (SM22α Cre PPARγ$^{flox/flox}$) have PAH. *SM22α Cre PPARγ$^{flox/flox}$* mice had elevated RV systolic pressure (RVSP) in room air when compared with controls (29.0 versus 21.5 mmHg; P < 0.001; Figure 7A). Systemic blood pressure, RV function (RV *dP/dt* maximum and minimum) and LV function (fractional shortening, ejection fraction), and cardiac output were not significantly different when comparing the 2 groups (Table 1). In association with elevated RVSP as a measure of PAH, *SM22α Cre PPARγ$^{flox/flox}$* mice also developed RV hypertrophy (RVH), as judged by the ratio of RV weight to that of the LV and septum (0.46 versus 0.26; P < 0.0001; Figure 7B) and the ratio of RV to body weight (P < 0001; Table 1). *SM22α Cre PPARγ$^{flox/flox}$* mice had a similar number of pulmonary arteries per 100 alveoli (Table 1) and per surface area (data not shown) but showed more muscularized pulmonary arteries at the alveolar wall level, when compared with littermate controls (Figure 7, C–E). The muscular thickening in small pulmonary arteries seen in lung sections from SMC PPARγ–deficient mice (Movat staining; Figure 7, D and E) was confirmed by immunohistochemistry with specific antibodies for α-SMA (Figure 7, F and G) and associated with an enhanced signal for proliferating cell nuclear antigen (PCNA; Figure 7, H and I) in PASMCs. LV end-diastolic inner diameter (LVIDD), LV end-diastolic posterior wall thickness (LVPWd), and end-diastolic interventricular septum thickness (IVSd) as measures of LV dilatation and LV hypertrophy (LVH) were not different between the 2 genotypes (Table 1). Thus, LV dysfunction does not account for the PAH in *SM22α Cre PPARγ$^{flox/flox}$* mice. *SM22α Cre PPARγ$^{flox/flox}$* mice had similar hematocrit and glucose values but slightly higher wbc counts than controls (Table 1).

Discussion

This report is the first indication to our knowledge that the antiproliferative effects of BMP-2/BMP-RII signaling in primary cells (i.e., PASMCs) can be attributed to activation of PPARγ and its

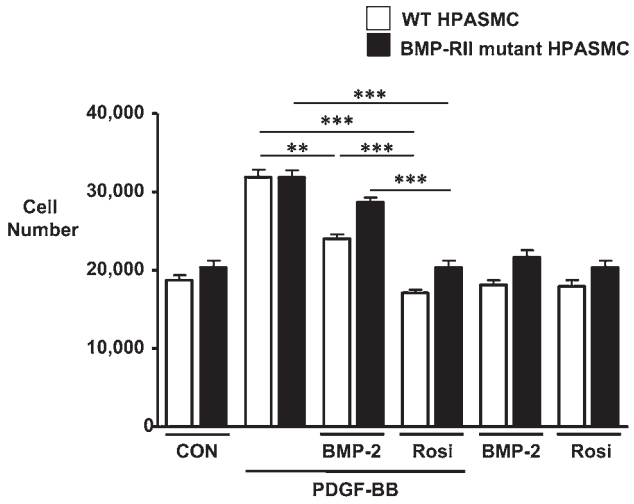

Figure 4
Antiproliferative effects of BMP-2 and the PPARγ agonist rosiglitazone on PDGF-BB–induced proliferation of human wild-type and BMP-RII mutant PASMCs. Control PASMCs were isolated from surgical resection specimens derived from patients undergoing lobectomy or pneumonectomy for suspected lung tumor. Additional peripheral pulmonary arteries (<1–2 mm external diameter) were obtained from a patient undergoing heart-lung transplantation for FPAH and known to harbor a mutation (W9X) in BMP-RII. The nature of the BMP-RII mutation, cell isolation, culture techniques, and cell counts are described in Methods and in Figure 1. HPASMCs were incubated for 48 hours in starvation media (0.1% FBS) and then stimulated with PDGF-BB (20 ng/ml) for 72 hours. BMP-2 (10 ng/ml) or rosiglitazone (1 μM) were added to quiescent cells 30 minutes prior to PDGF-BB stimulation. Bars represent mean ± SEM ($n = 3$). $^{**}P < 0.01$; $^{***}P < 0.001$ as indicated; ANOVA with Bonferroni's multiple comparison test. The number of PDGF-BB–stimulated cells was significantly higher than that of untreated control cells ($P < 0.001$).

putative transcription target apoE, a protein not previously known to be synthesized and secreted by SMCs (Figure 8A). Furthermore, we establish that endogenous expression of PPARγ in SMCs can protect against the spontaneous development of PAH. Our experiments using a PPARγ antagonist and PPARγ-deficient PASMCs further demonstrate that PPARγ is required for BMP-2–mediated inhibition of PASMC proliferation induced by PDGF-BB. By using RNAi and PASMCs with a known loss-of-function mutation of BMP-RII, we show that BMP-2 requires BMP-RII to block SMC proliferation and provide evidence that BMP-RII dysfunction that occurs with or without BMP-RII mutations (3, 4) could lead to unopposed mitogenic SMC stimulation by PDGF-BB and other growth factors (Figure 8B). BMP-RII dysfunction may, however, be rescued by PPARγ agonists such as pioglitazone or rosiglitazone (Figure 8C), as we have demonstrated in PDGF-BB–stimulated BMP-RII mutant HPASMCs.

In this study, we investigated whether BMP-2 and PDGF-BB might have opposing effects on the growth-inhibitory transcrip-

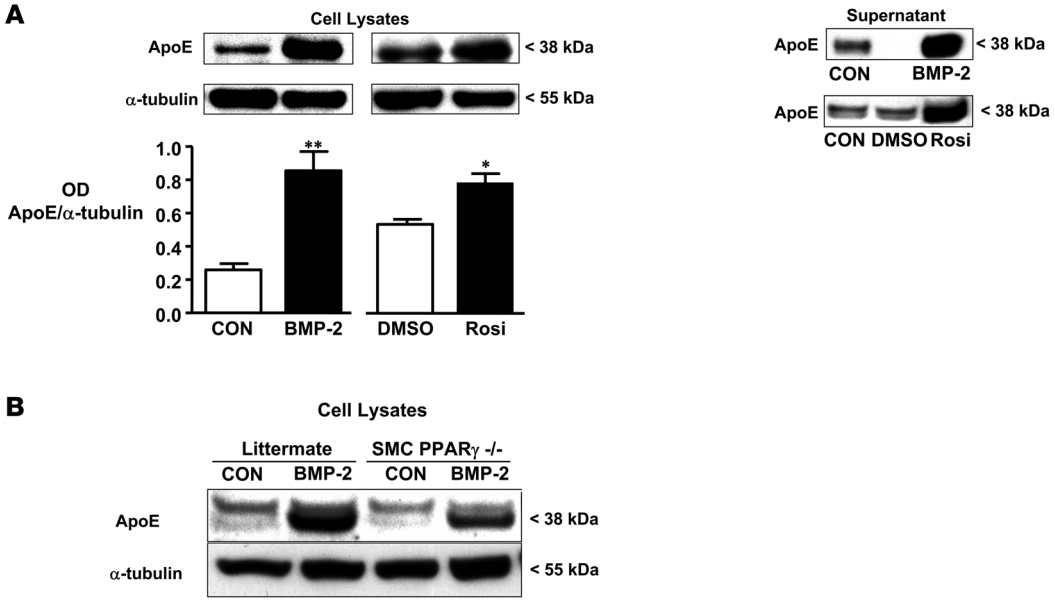

Figure 5
BMP-2 and the PPARγ agonist rosiglitazone induce apoE in PASMCs. (**A**) apoE protein expression in cell lysates (left) and apoE protein secretion in supernatant (right) induced by BMP-2 (10 ng/ml, 24 hours) and rosiglitazone (1 μM, 24 hours) were detected by immunoblotting as described in Methods (for cell lysates, densitometric values were corrected for equal loading using α-tubulin). For apoE secretion, the media of 3–4 cell culture flasks per condition were pooled and concentrated for the blots shown (representative of 2 independent experiments with similar results). (**B**) BMP-2–induced (10 ng/ml, 24 hours) upregulation of apoE in murine control PASMCs was reduced by half in PASMCs harvested from *SM22α Cre PPARγ*$^{flox/flox}$ mice. PASMCs were isolated from 5 littermate control and 5 *SM22α Cre PPARγ*$^{flox/flox}$ mice as described in Methods. PASMCs from each genotype were then pooled and subcultured prior to stimulation with BMP-2. The blot is representative of 2 independent experiments with similar results. For apoE protein levels in cell lysates (**A**), bars represent mean ± SEM ($n = 3$). $^{*}P < 0.05$; $^{**}P < 0.01$ versus control; unpaired 2-tailed *t* test.

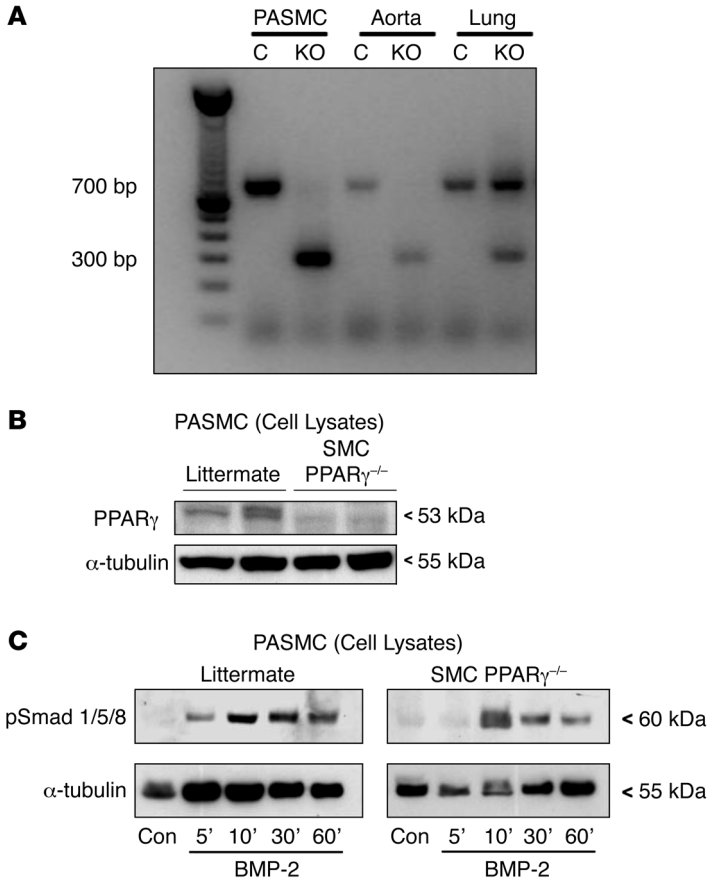

Figure 6
Mice with targeted deletion of PPARγ in SMCs maintain BMP-2–induced pSmad1/5/8 signaling. (**A** and **B**) Genotyping of mice with targeted deletion of PPARγ in SMCs. (**A**) PCR reactions showing gain of a 300-bp knockout transcript and almost complete loss of the 700-bp wild-type transcript in PASMCs and aorta from *SM22α Cre PPARγ*$^{flox/flox}$ mice. In the lung, which contains SMCs but also many other cell types, both transcripts are found in *SM22α Cre PPARγ*$^{flox/flox}$ mice, whereas only the wild-type transcript is detected in littermate control mice. (**B**) Western immunoblotting of PASMC lysates isolated from both littermate and *SM22α Cre PPARγ*$^{flox/flox}$ (SMC PPARγ$^{-/-}$) mice (n = 2 each) showed no detectable PPARγ protein expression when compared with control cells. (**C**) Both littermate control and SMC PPARγ$^{-/-}$ PASMCs were stimulated with BMP-2 (10 ng/ml) for 5–60 minutes as described in the legend for Figure 1, and phospho-Smad 1/5/8 protein expression was detected by immunoblotting as described in Methods (densitometric values were corrected for equal loading using α-tubulin). Data for 1 of 2 representative experiments with similar results are shown.

tion factor PPARγ and the growth-promoting MAPK nuclear phospho-ERK (30). We observed that BMP-2 activation of PPARγ in HPASMCs was independent of the phospho-Smad1/5/8 pathway but correlated with reduced nuclear phospho-ERK expression, presumably due to PPARγ activation of phosphatases (14, 15) or inhibition of phospho-ERK nuclear translocation (27). Conversely, PDGF-BB/PDGFR-β–mediated induction of nuclear phospho-ERK was associated with reduced PPARγ DNA binding, probably due to phosphorylation and inactivation of PPARγ at its N terminus (28) and/or enhancement of nuclear export (31) or ubiquitin/proteasome-mediated degradation and rapid turnover of PPARγ (32). Thus, it may be that continuous endogenous BMP-2/BMP-RII signaling is necessary as a gatekeeper to prevent inactivation of PPARγ and nuclear translocation of phospho-ERK in response to PDGF-BB/PDGFR-β stimulation.

Low-dose rosiglitazone and a physiological dose of recombinant apoE completely blocked PDGF-BB–induced proliferation of HPASMCs, consistent with previous work in *systemic* SMCs (12, 33). Since we showed that both BMP-2 and rosiglitazone induce apoE protein synthesis and secretion in HPASMCs, we reason that, in addition to lowering phospho-ERK in the nucleus, PPARγ-mediated induction of apoE inhibits PDGF-BB/PDGFR-β signaling (20, 21). The fact that some upregulation of apoE by BMP-2 occurs even in PPARγ-deficient SMCs indicates that apoE also can be regulated by a PPARγ-independent pathway. Further studies using apoE promoter-reporter assays would delineate the nature of PPARγ-mediated transcriptional activation of this target gene.

The *spontaneous* development of PAH in the *SM22α Cre PPARγ*$^{flox/flox}$ mice is in contrast to our observations that apoE$^{-/-}$ mice at similar age develop PAH only when fed a high-fat diet leading to insulin resistance (25). Since we found that the PPARγ agonist rosiglitazone can completely reverse PAH in the apoE$^{-/-}$ mouse, multiple other PPARγ-dependent mechanisms in addition to apoE induction may prevent PASMC proliferation and PAH in response to growth factors. In our previous study, we attributed the rescue effect of PPARγ activation to enhanced production of adiponectin, an adipocytokine that sequesters the ligand PDGF-BB, thereby inhibiting SMC proliferation and survival (34). However, we have not been able to detect adiponectin mRNA or protein expression in HPASMCs. Nonetheless, activated PPARγ can induce multiple other growth-inhibitory and proapoptotic gene products and repress growth-promoting factors in vascular cells (Figure 8C). For example, PPARγ activation blocks PDGF gene expression (35) and induces the expression of LRP (36), the receptor necessary for apoE-mediated suppression of PDGF-BB signaling (20, 21) (Figure 8, A and C). PPARγ activation also reduces levels of endothelin-1 (ET-1) (37) and the endogenous nitric oxide synthase inhibitor asymmetric dimethylarginine (ADMA) (38, 39), factors that are implicated in the pathobiology of PAH (39). Moreover, activated PPARγ stabilizes the cyclin-dependent kinase inhibitor p27^{KIP1} (40) and inhibits telomerase activity (41), retinoblastoma protein phosphorylation (40), and ultimately G_1 to S phase transition, cell-cycle progression, and vascular SMC proliferation (40). By blocking important survival pathways downstream of activated PDGFR-β, i.e., PI3K (42),

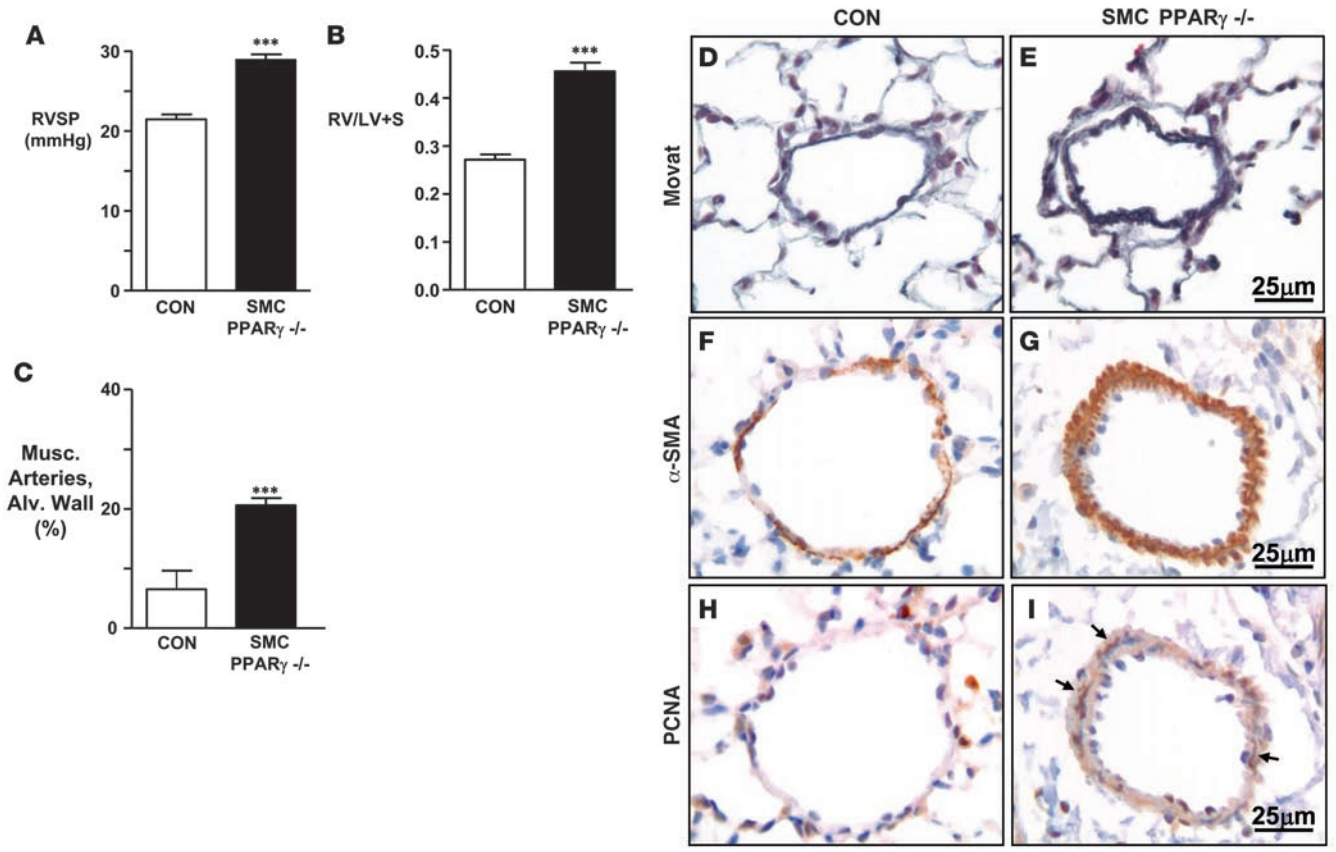

Figure 7

PAH in mice with targeted deletion of PPARγ in SMCs. Thirteen- to 15-week-old mice underwent RV catheterization, followed by organ harvest. (**A**) RVSP measurements, as described in Methods. (**B**) Right ventricular hypertrophy (RVH), measured as ratio of the weight of the RV to that of the LV plus septum (RV/LV+S), as described in Methods. (**C**) Muscularization of alveolar wall arteries (Musc. Arteries Alv. Wall), as described in Methods. (**D**) Representative photomicrographs of lung tissue (stained by Movat pentachrome) of 15-week-old mice showing a typical nonmuscular peripheral alveolar artery in a littermate control mouse. (**E**) A similar section in the *SM22α Cre PPARγ$^{flox/flox}$* (SMC PPARγ$^{-/-}$) mouse shows an alveolar wall artery surrounded by a rim of muscle. (**F–I**) Immunohistochemistry in serial lung tissue sections from littermate control (CON) and SMC PPARγ$^{-/-}$ mice stained for α-SMA (**F** and **G**) and proliferating cell nuclear antigen (PCNA; **H** and **I**). Arrows in **I** indicate enhanced PCNA staining in PASMCs. See also Table 1. Bars represent mean ± SEM (n = 5). ***P < 0.001 versus control; unpaired 2-tailed t test.

PPARγ agonists also lead to apoptosis of proliferating vascular cells (12, 43). In addition, it is known that PPARγ ligands impair production of matrix metalloproteinases (44) that can be activated by elastase (45). Our group has shown that inhibition of this proteolytic cascade not only prevents but also reverses advanced fatal PAH in rats (46).

Previous studies have shown beneficial effects of BMP-2 (47), PPARγ activation (reviewed in ref. 12), and apoE (18, 19) in preventing systemic vascular pathology, but our observations are the first indication to our knowledge that all 3 factors are linked. More recently, a connection between PPARγ and apoE has been made in patients with Alzheimer disease, in that the improvement of cognitive function with rosiglitazone is not apparent in patients who carry the APOE epsilon 4 allele (48). Hence, the novel axis we describe may be relevant in addressing mechanisms that underlie many different pathologic processes.

In summary, our data reveal a novel PPARγ/apoE axis downstream of BMP-2 signaling in HPASMCs. Failure to activate PPARγ in response to BMP-2 when there is BMP-RII dysfunction could place a patient at risk for the development or progression of PAH. We suggest that PPARγ agonists might rescue BMP-RII dysfunction and reverse SMC proliferation and vascular remodeling in PAH patients and may be useful antiproliferative agents even in those patients without BMP-RII dysfunction.

Methods

Additional and more detailed methods are provided in the supplemental materials.

Creation of mice with targeted deletion of PPARγ in arterial SMCs using the Cre-loxP system. We cross-bred SM22α promoter–driven Cre-transgenic mice with PPARγ homozygous floxed mice. Both strains were obtained from the Jackson Laboratory, and the cross resulted in *SM22α Cre PPARγ$^{flox/flox}$* (SMC PPARγ$^{-/-}$) mice. The offspring genotypes were determined by PCR (see Supplemental Methods). PCR conditions and primer information are available from the Jackson Laboratory. For the experiments involving PASMC isolation and subculture described below, apoE-deficient (B6.129P2-Apoetm1Unc/J) and C57BL/6 control mice were purchased from the Jackson Laboratory.

Genotyping/RT-PCR analysis. To detect the deletion of PPARγ exon 1 and exon 2, two primers were designed and located in exon A1 and exon

Table 1
Invasive hemodynamic, echocardiographic, heart weight, pulmonary artery, hematocrit, wbc, and blood glucose measurements in *SM22α PPARγ Cre*$^{flox/flox}$ (SMC PPARγ$^{-/-}$) and littermate control mice

	Littermate control	SMC PPARγ$^{-/-}$	*P*	*n*
Body weight (g)	22.5 ± 0.9	22.1 ± 1.2		8–10
Hemodynamics				
RVSP (mmHg)	21.5 ± 0.6	29.0 ± 0.6	$P < 0.001$	7–8
RV *dP/dt* max (mmHg/s)	1,439 ± 144	1,718 ± 143		7–8
RV *dP/dt* min (mmHg/s)	–1,228 ± 87	–1,405 ± 63		7–8
Systolic BP (mmHg)	105 ± 3.2	97 ± 3.1		9–10
MAP (mmHg)	85 ± 2.0	78 ± 3.1		9–10
Diastolic BP (mmHg)	74 ± 1.9	68 ± 3.1		9–10
Echocardiography				
Heart rate (bpm)	423 ± 22	411 ± 20		9–10
Ejection fraction (%)	72.7 ± 2.2	76.8 ± 1.2		9–10
Fractional shortening (%)	36.5 ± 1.8	39.8 ± 1.1		9–10
Cardiac output (ml/min)	35.3 ± 2.7	38.7 ± 3.6		9–10
LVIDD (mm)	3.58 ± 0.05	3.62 ± 0.10		9–10
LVISD (mm)	2.26 ± 0.09	2.19 ± 0.09		9–10
LVPWd (mm)	0.60 ± 0.04	0.58 ± 0.03		9–10
IVSd (mm)	0.56 ± 0.02	0.55 ± 0.02		9–10
Heart weight				
RV/LV+S	0.26 ± 0.01	0.46 ± 0.02	$P < 0.0001$	8–10
RV/body weight (×10^3)	0.88 ± 0.05	1.33 ± 0.05	$P < 0.0001$	8–10
Number and muscularization of pulmonary arteries				
No. of arteries/alveoli (%)	2.2 ± 0.2	2.3 ± 0.2		5–6
Musc. arteries, alv. wall (%)	6.5 ± 3.1	20.6 ± 1.2	$P = 0.0014$	5–6
Blood				
HCT (%)	48.7 ± 0.8	49.3 ± 1.0		8
wbc count (×10^3 cells/μl)	5.2 ± 0.8	7.4 ± 0.4	$P = 0.0168$	8–10
Glucose (mg/dl)	126.6 ± 6.2	122.8 ± 4.2		9–10

Thirteen- to 15-week-old male littermate control and SMC PPARγ$^{-/-}$ mice on regular chow in normoxia. Data are shown as mean ± SEM. Statistically significant differences ($P < 0.05$; unpaired 2-tailed *t* test) between genotypes are indicated. *dP/dt* max., maximal rate of pressure development (systolic RV function); *dP/dt* min., max. rate of pressure decay (diastolic RV function); MAP, mean arterial pressure; EF, ejection fraction; FS, fractional shortening; LVIDD, LV end-diastolic inner diameter; LVISD, LV end-systolic inner diameter; LVPWd, LV end-diastolic posterior wall thickness; IVSd, end-diastolic interventricular septum thickness; LV+S, LV plus septum; Alv., alveolar; Musc., muscularization; HCT, hematocrit.

4 of the *Pparg1* gene for RT-PCR to recognize the full-length (700 bp) and recombined mRNA (300 bp), as previously described (49) (for primers and PCR protocol, see Supplemental Methods). Total RNA was extracted from PASMCs, aorta, and lung with TRIzol reagent (Invitrogen). PASMCs were obtained from pulmonary arteries of *SM22α Cre PPARγ*$^{flox/flox}$ mice and littermate control mice and cultured for 10 days. Then RNA samples from the cells were reverse transcribed using the Superscript III Reverse Transcriptase kit (Invitrogen). PCR was applied to cDNA using a Taq DNA polymerase kit (Invitrogen), and transcripts were run on a 1% agarose gel.

Lentiviral shRNAi gene silencing of human BMP-RII. For long-term gene silencing of BMP-RII in HPASMCs, we constructed a pLentivirus 6 with an integrated short hairpin oligonucleotide directed against the mRNA of human BMP-RII, using an inducible H1 RNAi entry vector kit and a lentiviral RNAi expression system kit (K4920-00, K4943-00; Invitrogen) as described by the manufacturer (for details, see Supplemental Methods). Lentivirus was made and propagated in 293FT cells, and HPASMCs were transfected as described in Supplemental Methods. After 12 days of blasticidin selection, we confirmed an 85% stable knockdown of human BMP-RII compared with shLacZi control in HPASMCs (Supplemental Figure 1) and continued with further experiments.

Cell culture. Primary murine PASMCs were isolated from 13- to 15-week-old apoE$^{-/-}$ and C57BL/6 mice, as well as *SM22α Cre PPARγ*$^{flox/flox}$ and littermate control mice, using a modified elastase/collagenase digestion protocol as previously described (50). Primary HPASMCs were purchased from Cascade Biologics. Moreover, control PASMCs were isolated from surgical resection specimens derived from a patient undergoing lobectomy or pneumonectomy for suspected lung tumor. Additional PASMCs were obtained from a patient undergoing heart-lung transplantation for FPAH and known to harbor a mutation in BMP-RII (W9X), as previously described (51). The nature of the BMP-RII mutation, cell isolation, and culture techniques are described in Supplemental Methods.

Cell proliferation assays. For determination of cell number, PASMCs were seeded at 2.5 × 10^4 cells per well of a 24-well plate in 500 μl of growth medium and allowed to adhere overnight. The medium was removed and the cells washed 3 times with PBS prior to the addition of starvation media (DMEM, 0.1% FBS, penicillin/streptomycin) and incubated at 37°C, 5% CO_2 for 24 hours (murine PASMCs) or 48 hours (HPASMCs) prior to PDGF-BB stimulation (20 ng/ml) for 72 hours (treatments and concentrations are given in the figure legends). The media with or without growth factors and/or inhibitors was changed every 24 hours. Cells were washed twice with PBS and trypsinized in 150 μl of trypsin/EDTA for 7 minutes, followed by the addi-

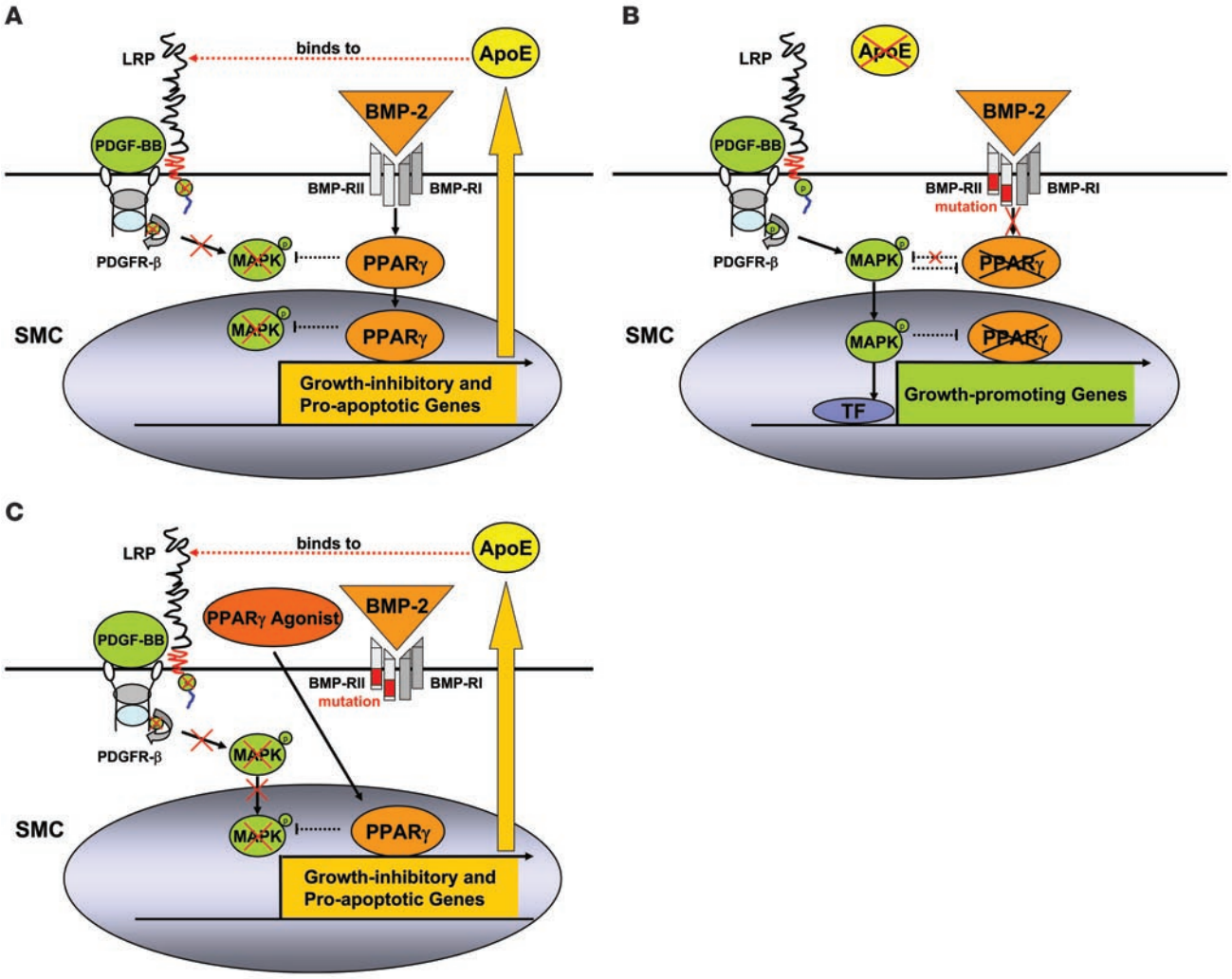

Figure 8

Model: A novel antiproliferative BMP-2/PPARγ/apoE axis protects against PAH. This schema incorporates the findings described in our article and the literature to date as discussed. (**A**) BMP-2 inhibits SMC proliferation via PPARγ and apoE. apoE impairs PDGF-BB/MAPK signaling by binding to LDL receptor–related protein (LRP), thereby initiating endocytosis and degradation of the LRP/PDGFR-β/PDGF-B complex. PPARγ induces LRP and other growth-inhibitory/proapoptotic genes in SMCs and inhibits cell-cycle and other growth-promoting genes such as telomerase, cyclin D1, and retinoblastoma protein. Moreover, PPARγ induces phosphatases that can directly inactivate phospho-ERK. (**B**) BMP-RII dysfunction promotes SMC proliferation and survival in PAH. Heightened PDGF-BB signaling leading to SMC proliferation is a key clinical feature of PAH. Deficiency of both apoE and LRP enhances mitogenic PDGF-BB/MAPK signaling. Loss-of-function mutations in the BMP-RII gene will decrease endogenous PPARγ activity, leading to unopposed MAPK signaling, SMC proliferation and survival, and ultimately development of PAH.TF, transcription factor. (**C**) PPARγ agonists can rescue BMP-RII dysfunction and reverse PAH. PPARγ agonists such as rosiglitazone or pioglitazone might reverse SMC proliferation and vascular remodeling in PAH patients with or without BMP-RII dysfunction via induction of apoE and other growth-inhibitory/proapoptotic genes (as indicated) and through repression of growth-promoting genes (not shown).

tion of 150 μl trypsin neutralizer (Cascade Biologics). The cells were then resuspended and counted in a hemacytometer (3–6 wells per condition, 4 counts per well). The biochemical MTT cell proliferation assay (ATCC) is described in Supplemental Methods. In cell proliferation studies, BMP-2 (10 ng/ml; Sigma-Aldrich), rosiglitazone (1 μM; Alexis), or recombinant human apoE (1–10 μM; Chemicon) were added to quiescent cells 30 minutes prior to mitogenic stimulation with PDGF-BB (human, 20 ng/ml; R&D Systems) for 72 hours. The PPARγ antagonist GW9662 (1 μM; Cayman) was added 24 hours prior to the addition of BMP-2. The media with or without growth factors and/or inhibitors was changed every 24 hours.

Protein expression and compartmental localization. Murine and human PASMCs (wild-type, shLacZi control, or shBMP-RIIi) were grown to 70% confluence and cultured in starvation media (DMEM, 0.1% FBS, 100 U/ml penicillin, 0.1 mg/ml streptomycin; Gibco; Invitrogen) for 24 and 48 hours, respectively. PDGF-BB, BMP-2, apoE, or rosiglitazone was added to quiescent cells for 5–60 minutes and for 24 hours (treatments and concentrations are stated in the figure legends). In addition to total cell lysates, subcellular fractions (nuclear matrix, nuclear extract, cytoplasmic extract) were prepared using a modified low-salt/high-salt protocol as previously described (52). For details, see Supplemental Methods.

apoE protein secretion. Quiescent HPASMCs were cultured in T75 cell culture flasks (75 cm^2) covered with minimal media (1 ml) and were then stimulated with BMP-2 (10 ng/ml) or rosiglitazone (1 μM) for 24 hours. The supernatant media was collected from 3 cell culture flasks per con-

dition, pooled, and concentrated using an Amicon-4 Centriprep device (Millipore). Protein extracts were then prepared as described in Supplemental Methods, and 20 μg protein per sample was loaded for SDS-PAGE immunoblotting (Invitrogen).

Western immunoblotting. Preparation of subcellular fractions (nuclear matrix, nuclear extract, cytoplasmic extract) and whole-cell lysates (protein extracts) as well as immunoblotting techniques are described in Supplemental Methods. Primary antibodies against phospho-ERK1/2, ERK 1/2, phospho-Smad1/5/8, Smad1 (all Cell Signaling Technology), PPARγ (Santa Cruz Biotechnology Inc.), apoE (Abcam), BMP-RII (BD Biosciences — Pharmingen), and α-tubulin (Sigma-Aldrich) were used.

PPARγ DNA binding assay. A multiplex transcription factor DNA binding assay (Marligen Biosciences) was performed as previously described (53). Briefly, nuclear extracts were incubated with a mixture of biotinylated DNA probes representing different transcription factor binding sites (e.g., for PPARγ, 5′-TGACCTTTGACCTAGAA-3′), each containing a distinct single-stranded sequence that serves as a capture tag. Following the transcription factor binding reactions, samples were incubated with proprietary reagents to digest any DNA probes not bound to transcription factors. Reactions were then incubated with a mix containing spectrally distinct bead sets, and intact biotinylated probes were captured onto corresponding bead surfaces by capture-tag and anti-tag sequence interactions. Beads were then washed using a filter plate and stained with streptavidin-PE. The fluorescent signal associated with transcription factor binding sites localized on the surface of spectrally distinct beads was measured using Luminex-100 instrumentation. Each reaction was carried out in triplicate, so that 300 different data points per sample were obtained for analysis.

Experimental design for studies in transgenic mice. *SM22α Cre PPARγ$^{flox/flox}$* or littermate control mice were maintained on regular chow with free access to drinking water. All studies were carried out in 13- to 15-week-old mice under a protocol approved by the Animal Care Committee of Stanford University following the guidelines of the American Physiological Society.

Hemodynamic measurements. RVSP and RV *dP/dt* measurements were performed in 15-week-old nonventilated mice under isoflurane anesthesia (1.5%–2.5%, 2 l O_2/min) by inserting a 1.4 F catheter (Millar Instruments) via the right jugular vein as described previously (25). Systemic blood pressure was determined in nonanesthetized, 14- to 15-week-old mice by the tail cuff method using the BP 2000 analysis system (Visitech Systems). Cardiac output and function were measured in 13- to 15-week-old mice by echocardiography under isoflurane anesthesia (1%, 1 l O_2/min) with an ultrasound machine (Vivid 7; GE Medical Systems) using a 13-MHz linear array transducer (see Supplemental Methods).

RVH and LVH. RVH was measured as described previously (54) by the weight of the RV relative to LV plus septum. LVH was measured as absolute weight of the LV plus septum relative to body weight. LV dilatation was assessed by echocardiographic M-mode measurement of the LVIDD.

Lung tissue preparation. Lungs were perfused with normal saline, fixed in 10% formalin overnight, and then embedded in paraffin for routine histology (H&E, elastin van Gieson, Movat pentachrome), as previously described (25, 54). A subset of left lungs (approximately half) were injected with barium-gelatin via pulmonary artery–inserted tubing (25) to label peripheral pulmonary arteries for morphometric analysis (see Supplemental Methods).

Morphometric analysis. Barium-injected, transverse left lung step sections were stained by the elastin van Gieson method. From all mice, we took the same full section in the mid-portion of the barium-injected left lung parallel to the hilum and embedded it in the same manner. Pulmonary artery muscularization was assessed at ×400 magnification by calculating the proportion of fully and partially muscularized peripheral (alveolar wall) pulmonary arteries to total peripheral pulmonary arteries in 5 random fields (1 field = ×200 magnification). The total number of alveolar wall and duct arteries was expressed as both the ratio of number of pulmonary arteries per 100 alveoli and number of pulmonary arteries per surface area (5 random fields at ×200 magnification). Approximately 1,000 alveoli were counted per animal. All measurements were carried out by investigators blinded to genotype and condition.

Immunohistochemistry. Paraffin-embedded sections were deparaffinized in xylene and rehydrated through graded alcohol. Antigen retrieval was performed using a heat-mediated epitope retrieval method by heating the sections in citrate buffer (10 mM sodium citrate, 0.05% Tween-20, pH 6.0) for 10 minutes at 95°C and then allowing the sections to cool to room temperature. Sections were then incubated with primary antibodies specific for PCNA and α-SMA (Abcam) overnight at 4°C. Staining was then completed using the Vectastain Elite ABC Kit (Vector Laboratories) according to the manufacturer's instructions, using 3,3-diaminobenzidine as a substrate for peroxidase, and counterstained with hematoxylin.

Fasting whole-blood measurements. Tail vein puncture was performed in nonanesthetized, overnight-starved mice, followed by immediate, duplicate whole-blood glucose measurements with a glucometer (FreeStyle; Abbott), to rule out any influence of the SMC-targeted PPARγ knockout on glucose hemostasis. Additional blood was obtained by cardiac puncture after the hemodynamic measurements. White blood cell count and hematocrit were assessed by the Stanford Animal Facility Laboratories (see Supplemental Methods).

Statistics. Values from multiple experiments are expressed as mean ± SEM. Statistical significance was determined using 1-way ANOVA. When only 2 groups were compared, statistical differences were assessed with the unpaired 2-tailed *t* test. A *P* value of less than 0.05 was considered as significant. The number of samples or animals in each group is indicated in the figure legends.

Acknowledgments

We thank Pete Clausen (Marligen Biosciences) for help with the multiplex DNA binding assay and data analysis. This work was supported by a Postdoctoral Fellowship from the American Heart Association/Pulmonary Hypertension Association (0425943H) to G. Hansmann; the NIH (1-R01-HL074186-01) and the Dwight and Vera Dunlevie Endowed Professorship to M. Rabinovitch; a National Heart, Lung, and Blood Institute National Research Service Award (2-T32-HL007708-14) to J.M. Bekker; and a Predoctoral Fellowship from Boehringer Ingelheim Funds to S. Schellong. N.W. Morrell received grant funding from the British Heart Foundation.

Received for publication April 25, 2007, and accepted in revised form February 6, 2008.

Address correspondence to: Marlene Rabinovitch, Vera Moulton Wall Center for Pulmonary Vascular Disease, Stanford University School of Medicine, CCSR Building, Room 2245B, 269 Campus Drive, Stanford, California 94305-5162, USA. Phone: (650) 723-8239; Fax: (650) 723-6700; E-mail: marlener@stanford.edu.

1. Merklinger, S.L., Jones, P.L., Martinez, E.C., and Rabinovitch, M. 2005. Epidermal growth factor receptor blockade mediates smooth muscle cell apoptosis and improves survival in rats with pulmonary hypertension. *Circulation.* **112**:423–431.
2. Schermuly, R.T., et al. 2005. Reversal of experimental pulmonary hypertension by PDGF inhibition. *J. Clin. Invest.* **115**:2811–2821.
3. Lane, K.B., et al. 2000. Heterozygous germline mutations in BMPR2, encoding a TGF-beta receptor, cause familial primary pulmonary hypertension. The International PPH Consortium. *Nat. Genet.* **26**:81–84.
4. Deng, Z., et al. 2000. Familial primary pulmonary hypertension (gene PPH1) is caused by mutations

in the bone morphogenetic protein receptor-II gene. *Am. J. Hum. Genet.* **67**:737–744.
5. Newman, J.H., et al. 2004. Genetic basis of pulmonary arterial hypertension: current understanding and future directions. *J. Am. Coll. Cardiol.* **43**:33S–39S.
6. Humbert, M., et al. 2002. BMPR2 germline mutations in pulmonary hypertension associated with fenfluramine derivatives. *Eur. Respir. J.* **20**:518–523.
7. Roberts, K.E., et al. 2004. BMPR2 mutations in pulmonary arterial hypertension with congenital heart disease. *Eur. Respir. J.* **24**:371–374.
8. Atkinson, C., et al. 2002. Primary pulmonary hypertension is associated with reduced pulmonary vascular expression of type II bone morphogenetic protein receptor. *Circulation.* **105**:1672–1678.
9. Galetto, R., et al. 2001. Identification of a peroxisome-proliferator-activated-receptor response element in the apolipoprotein E gene control region. *Biochem. J.* **357**:521–527.
10. Ameshima, S., et al. 2003. Peroxisome proliferator-activated receptor gamma (PPARgamma) expression is decreased in pulmonary hypertension and affects endothelial cell growth. *Circ. Res.* **92**:1162–1169.
11. Geraci, M.W., et al. 2001. Gene expression patterns in the lungs of patients with primary pulmonary hypertension: a gene microarray analysis. *Circ. Res.* **88**:555–562.
12. Marx, N.N., Duez, H.H., Fruchart, J.C., and Staels, B.B. 2004. Peroxisome proliferator-activated receptors and atherogenesis: regulators of gene expression in vascular cells. *Circ. Res.* **94**:1168–1178.
13. Gilde, A.J., Fruchart, J.C., and Staels, B. 2006. Peroxisome proliferator-activated receptors at the crossroads of obesity, diabetes, and cardiovascular disease. *J. Am. Coll. Cardiol.* **48**:A24–A32.
14. Benkirane, K., Amiri, F., Diep, Q.N., El Mabrouk, M., and Schiffrin, E.L. 2006. PPAR-gamma inhibits ANG II-induced cell growth via SHIP2 and 4E-BP1. *Am. J. Physiol. Heart Circ. Physiol.* **290**:H390–H397.
15. Wakino, S., et al. 2001. Peroxisome proliferator-activated receptor gamma ligands inhibit mitogenic induction of p21(Cip1) by modulating the protein kinase Cdelta pathway in vascular smooth muscle cells. *J. Biol. Chem.* **276**:47650–47657.
16. Akiyama, T.E., et al. 2002. Conditional disruption of the peroxisome proliferator-activated receptor gamma gene in mice results in lowered expression of ABCA1, ABCG1, and apoE in macrophages and reduced cholesterol efflux. *Mol. Cell. Biol.* **22**:2607–2619.
17. Yue, L., Rasouli, N., Ranganathan, G., Kern, P.A., and Mazzone, T. 2004. Divergent effects of peroxisome proliferator-activated receptor gamma agonists and tumor necrosis factor alpha on adipocyte ApoE expression. *J. Biol. Chem.* **279**:47626–47632.
18. Zeleny, M., Swertfeger, D.K., Weisgraber, K.H., and Hui, D.Y. 2002. Distinct apolipoprotein E isoform preference for inhibition of smooth muscle cell migration and proliferation. *Biochemistry.* **41**:11820–11823.
19. Ishigami, M., Swertfeger, D.K., Granholm, N.A., and Hui, D.Y. 1998. Apolipoprotein E inhibits platelet-derived growth factor-induced vascular smooth muscle cell migration and proliferation by suppressing signal transduction and preventing cell entry to G1 phase. *J. Biol. Chem.* **273**:20156–20161.
20. Boucher, P., Gotthardt, M., Li, W.P., Anderson, R.G., and Herz, J. 2003. LRP: role in vascular wall integrity and protection from atherosclerosis. *Science.* **300**:329–332.
21. Newton, C.S., et al. 2005. Platelet-derived growth factor receptor-beta (PDGFR-beta) activation promotes its association with the low density lipoprotein receptor-related protein (LRP). Evidence for co-receptor function. *J. Biol. Chem.* **280**:27872–27878.
22. Lassila, M., et al. 2004. Imatinib attenuates diabetes-associated atherosclerosis. *Arterioscler. Thromb. Vasc. Biol.* **24**:935–942.
23. Humbert, M., et al. 1998. Platelet-derived growth factor expression in primary pulmonary hypertension: comparison of HIV seropositive and HIV seronegative patients. *Eur. Respir. J.* **11**:554–559.
24. Ghofrani, H.A., Seeger, W., and Grimminger, F. 2005. Imatinib for the treatment of pulmonary arterial hypertension. *N. Engl. J. Med.* **353**:1412–1413.
25. Hansmann, G., et al. 2007. Pulmonary arterial hypertension is linked to insulin resistance and reversed by peroxisome proliferator-activated receptor-gamma activation. *Circulation.* **115**:1275–1284.
26. Ghosh, S.S., et al. 2003. PPARgamma ligand attenuates PDGF-induced mesangial cell proliferation: role of MAP kinase. *Kidney Int.* **64**:52–62.
27. Goetze, S., et al. 2001. Peroxisome proliferator-activated receptor-gamma ligands inhibit nuclear but not cytosolic extracellular signal-regulated kinase/mitogen-activated protein kinase-regulated steps in vascular smooth muscle cell migration. *J. Cardiovasc. Pharmacol.* **38**:909–921.
28. Hu, E., Kim, J.B., Sarraf, P., and Spiegelman, B.M. 1996. Inhibition of adipogenesis through MAP kinase-mediated phosphorylation of PPARgamma. *Science.* **274**:2100–2103.
29. Ishihara, K., Tsutsumi, K., Kawane, S., Nakajima, M., and Kasaoka, T. 2003. The receptor for advanced glycation end-products (RAGE) directly binds to ERK by a D-domain-like docking site. *FEBS Lett.* **550**:107–113.
30. Sarjeant, J.M., et al. 2003. Apolipoprotein D inhibits platelet-derived growth factor-BB-induced vascular smooth muscle cell proliferated by preventing translocation of phosphorylated extracellular signal regulated kinase 1/2 to the nucleus. *Arterioscler. Thromb. Vasc. Biol.* **23**:2172–2177.
31. Burgermeister, E., et al. 2007. Interaction with MEK causes nuclear export and downregulation of peroxisome proliferator-activated receptor gamma. *Mol. Cell. Biol.* **27**:803–817.
32. Floyd, Z.E., and Stephens, J.M. 2002. Interferon-gamma-mediated activation and ubiquitin-proteasome-dependent degradation of PPARgamma in adipocytes. *J. Biol. Chem.* **277**:4062–4068.
33. Ishigami, M., et al. 2000. Apolipoprotein E inhibition of vascular smooth muscle cell proliferation but not the inhibition of migration is mediated through activation of inducible nitric oxide synthase. *Arterioscler. Thromb. Vasc. Biol.* **20**:1020–1026.
34. Arita, Y., et al. 2002. Adipocyte-derived plasma protein adiponectin acts as a platelet-derived growth factor-BB-binding protein and regulates growth factor-induced common postreceptor signal in vascular smooth muscle cell. *Circulation.* **105**:2893–2898.
35. Zhang, J., Fu, M., Zhao, L., and Chen, Y.E. 2002. 15-Deoxy-prostaglandin J(2) inhibits PDGF-A and -B chain expression in human vascular endothelial cells independent of PPAR gamma. *Biochem. Biophys. Res. Commun.* **298**:128–132.
36. Gauthier, A., Vassiliou, G., Benoist, F., and McPherson, R. 2003. Adipocyte low density lipoprotein receptor-related protein gene expression and function is regulated by peroxisome proliferator-activated receptor gamma. *J. Biol. Chem.* **278**:11945–11953.
37. Martin-Nizard, F., et al. 2002. Peroxisome proliferator-activated receptor activators inhibit oxidized low-density lipoprotein-induced endothelin-1 secretion in endothelial cells. *J. Cardiovasc. Pharmacol.* **40**:822–831.
38. Wakino, S., et al. 2005. Pioglitazone lowers systemic asymmetric dimethylarginine by inducing dimethylarginine dimethylaminohydrolase in rats. *Hypertens. Res.* **28**:255–262.
39. Kielstein, J.T., et al. 2005. Asymmetrical dimethylarginine in idiopathic pulmonary arterial hypertension. *Arterioscler. Thromb. Vasc. Biol.* **25**:1414–1418.
40. Wakino, S., et al. 2000. Peroxisome proliferator-activated receptor gamma ligands inhibit retinoblastoma phosphorylation and G1--> S transition in vascular smooth muscle cells. *J. Biol. Chem.* **275**:22435–22441.
41. Ogawa, D., et al. 2006. Activation of peroxisome proliferator-activated receptor gamma suppresses telomerase activity in vascular smooth muscle cells. *Circ. Res.* **98**:e50–e59.
42. Vantler, M., Caglayan, E., Zimmermann, W.H., Baumer, A.T., and Rosenkranz, S. 2005. Systematic evaluation of anti-apoptotic growth factor signaling in vascular smooth muscle cells. Only phosphatidylinositol 3′-kinase is important. *J. Biol. Chem.* **280**:14168–14176.
43. Bruemmer, D., et al. 2003. Regulation of the growth arrest and DNA damage-inducible gene 45 (GADD45) by peroxisome proliferator-activated receptor gamma in vascular smooth muscle cells. *Circ. Res.* **93**:e38–e47.
44. Worley, J.R., et al. 2003. Metalloproteinase expression in PMA-stimulated THP-1 cells. Effects of peroxisome proliferator-activated receptor-gamma (PPAR gamma) agonists and 9-cis-retinoic acid. *J. Biol. Chem.* **278**:51340–51346.
45. Nagase, H., Enghild, J.J., Suzuki, K., and Salvesen, G. 1990. Stepwise activation mechanisms of the precursor of matrix metalloproteinase 3 (stromelysin) by proteinases and (4-aminophenyl)mercuric acetate. *Biochemistry.* **29**:5783–5789.
46. Cowan, K.N., et al. 2000. Complete reversal of fatal pulmonary hypertension in rats by a serine elastase inhibitor. *Nat. Med.* **6**:698–702.
47. Nakaoka, T., et al. 1997. Inhibition of rat vascular smooth muscle proliferation in vitro and in vivo by bone morphogenetic protein-2. *J. Clin. Invest.* **100**:2824–2832.
48. Risner, M.E., et al. 2006. Efficacy of rosiglitazone in a genetically defined population with mild-to-moderate Alzheimer's disease. *Pharmacogenomics J.* **6**:246–254.
49. Hevener, A.L., et al. 2003. Muscle-specific Pparg deletion causes insulin resistance. *Nat. Med.* **9**:1491–1497.
50. Fouty, B.W., et al. 2001. p27(Kip1) is important in modulating pulmonary artery smooth muscle cell proliferation. *Am. J. Respir. Cell Mol. Biol.* **25**:652–658.
51. Yang, X., Lee, P.J., Long, L., Trembath, R.C., and Morrell, N.W. 2007. BMP4 induces HO-1 via a Smad-independent, p38MAPK-dependent pathway in pulmonary artery myocytes. *Am. J. Respir. Cell Mol. Biol.* **37**:598–605.
52. Mitani, Y., Zaidi, S.H., Dufourcq, P., Thompson, K., and Rabinovitch, M. 2000. Nitric oxide reduces vascular smooth muscle cell elastase activity through cGMP-mediated suppression of ERK phosphorylation and AML1B nuclear partitioning. *FASEB J.* **14**:805–814.
53. Shurin, G.V., et al. 2005. Loss of new chemokine CXCL14 in tumor tissue is associated with low infiltration by dendritic cells (DC), while restoration of human CXCL14 expression in tumor cells causes attraction of DC both in vitro and in vivo. *J. Immunol.* **174**:5490–5498.
54. Zaidi, S.H., You, X.M., Ciura, S., Husain, M., and Rabinovitch, M. 2002. Overexpression of the serine elastase inhibitor elafin protects transgenic mice from hypoxic pulmonary hypertension. *Circulation.* **105**:516–521.

SUPPLEMENTARY METHODS

Mice Genotyping/RT-PCR Analysis. To detect the deletion of PPARγ exon 1 and exon 2, two primers (5'-primer: gtcacgttctgacaggactgtgtgac; 3'-primer: tatcactggagatctccgccaacagc) were designed to correspond to exon A1 and exon 4 of the PPARγ1 gene. RT-PCR could then be carried out to detect the full length 700bp transcript or the 300bp transcript containing the deletion as previously described (1). Total RNA was extracted from PASMC, aorta and lung with Trizol reagent (Invitrogen, Cat. # 15596-026). PASMC were obtained from pulmonary arteries of *SM22α Cre PPARγ $^{flox/flox}$* mice *(SMC PPARγ -/-)* and littermate control mice after 10 days in cell culture (5 mice per genotype and experiment). 3μg total RNA (1μg from aorta) was treated with DNase I for 30 min at 37ºC (Invitrogen, Cat# 18047019) followed by heating at 70°C for 15min (DNase I inactivation). After confirming appropriate RNA quality, RNA samples were subsequently reverse-transcribed (RT) by using the Superscript III reverse transcriptase kit (Invitrogen, Cat# 18080-044). 2μg RNA (0.5 from aorta) from each sample was incubated with 1ul Oligo dT at 70ºC for 10min and then put on ice. Samples were then incubated with 1xRT buffer, 1μl of 0.1M DTT, 1μl of 10μM dNTPs, and 1μl of Superscript III in a total 20μl volume at 50ºC for 1 hour. RT was stopped by heating samples at 70ºC for 15 min. After incubating the samples for 20 min. with 1μl of RNase H at 37ºC, the cDNA was subjected to the PCR reaction using Taq DNA polymerase kit (Invitrogen, Cat#10342-020). 5μl of RT product from each sample was used to mix with 3μl of 10 x buffer, 1μl of 50 mM $MgCl_2$, 0.5 μl of 10mM dNTPs, 1μl of each primer(20μM) and 1μl of Taq DNA polymerase in a total 30μl volume. Hot start PCR reaction was used at 94ºC for 3 min., followed by 35 cycles of 94ºC 30 sec, 65ºC 30 sec, 72ºC 1min. and then 72ºC 10min. incubation. PCR products were then run on a 1% agarose gel.

Lentiviral small hairpin RNAi gene silencing (shRNAi against human BMP-RII): For longterm gene silencing of human BMP-RII, we constructed a pLentivirus 6 with an integrated small hairpin oligonucleotide (bottom 5' to 3': (DNA) - AAA AGC AGA TGG ACG CAT GGA ATA TTT CGA TAT TCC ATG CGT CCA TCT GC; top 5' to 3': (DNA) – AAA AGG ACA ATA TTA TGC TCG AAA GTT CGC TTT CGA GCA TAA TAT TGT CC) directed against the mRNA of human BMP-RII, using an inducible H1 RNAi entry vector kit (Invitrogen #K4920-00). Lentivirus was made and propagated with a lentiviral RNAi expression system kit (Invitrogen, #K4943-00), by transfecting 293FT cells with the shRNA-H1-TO-human BMP-RII pLenti6 construct using Lipofectamine 2000 (Invitrogen) and Vira Power Packaging Mix (Invitrogen, #K4944-00) according to the manufacturer's instructions. Virus-containing supernatants were harvested 48 and 72h posttransfection, ultra-filtered (Milipore, centricon Plus-70), and titrated on HT1080 cells (ATCC). A multiplicity of infection (MOI) of one was used for transfection of human PASMC (Cascade biologics, Portland,

OR) with shBMP-RII pLenti6 (see Supplementary Figure 1 online) following the manufacturer's instructions: Cells were incubated with virus mix and polybrene (8μg/ml) for 6h, and then changed to full growth-medium. Forty-eight hours after the beginning of transfection, blasticidin (3μg/ml) was added to Medium 231 medium including 100U/ml Penicillin, 0.1mg/ml streptomycin and smooth muscle growth supplement (SMGS, Cascade Biologics, Portland, OR). A kill curve for blasticidin had been performed on HPASMC and revealed cell death in untransfected HPASMC by day 5 of blasticidin incubation (3μg/ml). By day 12 of blasticidin selection, we confirmed by q-PCR a 85% stable knock down of BMP-RII in shBMP-RIIi vs. shLacZi (control) transfected HPASMC.

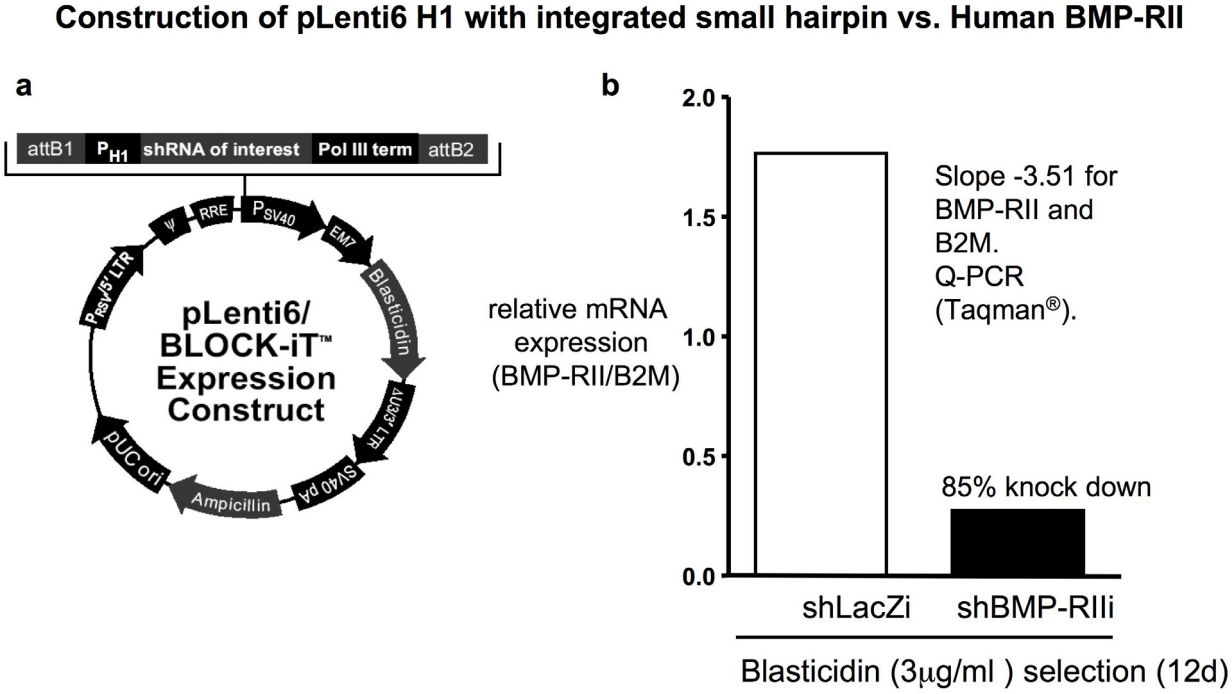

Supplementary Figure 1 **a,** Construction of a pLentivirus 6 (pLenti 6) with integrated small hairpin oligonucleotide *vs.* human bone morphogenetic protein receptor II (shBMP-RIIi). For longterm gene silencing of human BMP-RII, we constructed a pLentivirus 6 with an integrated small hairpin oligonucleotide (for details see Supplementary Methods below) directed against the mRNA of human BMP-RII, using an inducible H1 RNAi entry vector kit and lentiviral RNAi expression system kit (Invitrogen #K4920-00, #K4943-00). **b,** Lentivirus was made and propagated in 293FT cells and human PASMC were transfected as described in the Supplementary Methods below. After 12 days blasticidin selection, we confirmed a 85% stable knock down of human BMP-RII vs. shLacZi control in human PASMC.

Abbreviations, Supplementary Figure 1a: attB1, attB2: DNA recombination sequences that permit recombinational cloning of the gene of interest from a Gateway® entry clone (Invitrogen). **P_{H1}**, human H1 promotor: Expression of the shRNA of interest from pENTR™/H1/TO (or a suitable destination vector following LR recombination) is controlled by the human H1 promoter. The endogenous human H1 promoter normally controls expression of H1 RNA, the RNA component of human RNase P involved in tRNA processing. This particular promoter to control vector-based expression of shRNA molecules in mammalian cells was choosen for the following reasons: 1.) The promoter is recognized by RNA Polymerase III and controls high-level, constitutive expression of shRNA. 2.) The promoter is active in most mammalian cell types. 3.) The promoter is a type III Pol III promoter in that all elements required to control expression of the shRNA are located upstream of the transcription start site. **Pol III term**, RNA polymerase III. **P_{SV40}**, SV40 early promoter and origin: Allows high-level expression of the selection marker and episomal replication in cells expressing the SV40 large T antigen. **EM7** promoter: synthetic prokaryotic promoter for expression of the selection marker in E. coli. **Blasticidin resistance gene**: permits selection of stably transduced mammalian cell lines. **ΔU3/HIV-1 truncated 3′ LTR**: Allows viral packaging but self-inactivates the 5′ LTR for biosafety purposes. The element also contains a polyadenylation signal for transcription termination and polyadenylation of mRNA in transduced cells. **SV40 pA**, SV40 polyadenylation signal. **Ampicillin** resistance gene (β-lactamase): allows selection of the plasmid in *E. coli*. **pUC ori**: permits high-copy replication and maintenance in *E. coli*. **P_{RSV}/5' LTR**, Rous Sarcoma Virus (RSV) enhancer/promoter: Allows Tat-independent production of viral mRNA. HIV-1 truncated 5′ LTR: Permits viral packaging and reverse transcription of the viral mRNA. **Ψ**, HIV-1 psi (ψ) packaging signal: Allows viral packaging. **RRE**, HIV-1 Rev response element (RRE): Permits Rev-dependent nuclear export of unspliced viral mRNA.

Small interfering (si) RNA gene silencing of human BMP-RII. To achieve effective gene knockdown, siRNA duplexes specific for BMP-RII (Dharmacon on-target plus; accession number NM_001204) were transfected into human PASMCs using Lipofectamine 2000 (Invitrogen) following the manufacturer's protocol. Knockdown efficiency was evaluated 48 hours later by measuring protein levels in cell lysates via immunoblotting. Transfection of nontargeting siRNA duplexes (siCONTROL, Dharmacon, Inc) was performed simultaneously to serve as control in all experiments.

Cell Culture and Functional Assays: *Primary murine PASMC were isolated from* 5 male 14-15-week old mice of apoE deficient (apoE -/-) and C57Bl/6 mice, as well as *SM22α Cre PPARγ $^{flox/flox}$* (SMC PPARγ -/-) mice and littermate control mice, using a modified protocol as previously described (2): The main extralobular pulmonary arteries were dissected, cleaned from adherent tissue, cut in small pieces and digested for 90 min. in dispersion media containing 0.53mg/ml

elastase (Roche), 0.53mg/ml collagenase II (Worthington), 2 mg/ml albumin (Sigma), 0.2mg/ml soybean trypsin inhibitor (Worthington), 40μM $CaCl_2$, in HBSS buffer (Gibco). PASMCs were then cultured in DMEM (Gibco) containing FBS (20% for 3 days, then reduced to 10%), 2mM L-glutamine and 100U/ml Penicillin, 0.1mg/ml streptomycin. Passages 3-4 were used for further studies. Smooth muscle cell identity was verified by positive immunohistochemistry staining for SMα-actin (Sigma Aldrich, St. Louis, MO) (>95% of cells stained positive for SMα-actin). PASMC were grown to 70% confluence in DMEM and then cultured for 24h in starvation media (DMEM, 0.1% FBS, 2mM L-glutamine, 100U/ml Penicillin, 0.1mg/ml streptomycin).

Primary human PASMC were purchased from Cascade Biologics (Portland, OR) and maintained cell culture flasks (25-150cm^2) containing Medium 231, Smooth Muscle Growth Supplement (SMGS), 100U/ml penicillin G, 0.1mg/ml Streptomycin sulfate, and 0.25μg/ml Amphotericin B (PSA Solution) (all Cascade Biologics). Cells were received at passage 3 and used between passages 5 and 9. Moreover, normal PASMC were isolated from surgical resection specimens derived from patients undergoing lobectomy or pneumonectomy for suspected lung tumor (control). Only uninvolved tissue was used. PASMC were explanted peripheral pulmonary arteries (<1-2mm external diameters, as previously described (3, 4). Cells were maintained in 10% FBS/DMEM and used for experiments between passages 4 and 6. Additional PASMC were obtained from a patient undergoing heart-lung transplantation for familial PAH and known to harbor a mutation in the BMP-RII receptor. The isolate used was obtained from a patient in which a premature stop codon is inserted in place of tryptophan at position of the amino acid sequence (W9X). The smooth muscle phenotype of isolated cells was confirmed by positive immunofluorescence with antibodies to anti-α-smooth muscle actin antibody (IA4) and anti–smooth muscle specific myosin (hsm-v), as described(5).

Cell Counts: PASMC were seeded at 2.5x10^4 cells per well of a 24-well plate in 500μl of growth medium and allowed to adhere overnight. The medium was removed and the cells washed 3 times with PBS prior to the addition of starvation media (DMEM, 0.1% FBS, penicillin/streptomycin) and incubated at 37°C, 5% CO2 for 24h (murine PASMC) or 48h (human PASMC) prior to PDGF-BB stimulation for 0h and 72h (treatments and concentrations stated in the figure legends). Cells were washed twice with PBS and trypsinized in 150μl of Trypsin/EDTA for 7min., followed by the addition of 150μl trypsin neutralizer (all Cascade Biologics, Portland, OR). The cells were then resuspended and counted in a hemacytometer (3-6 wells per condition, 4 counts per well).

MTT Cell Proliferation Assay (ATCC, Manassas, VA): 3 x 10^3 HPASMC per well were seeded and allowed to adhere on a 96-well plate overnight. After removal of the medium, the cells were washed 3 times with PBS prior to the addition of Opti-MEM I (Gibco, Gaithersburg, MD) containing

0.1% FBS, penicillin/streptomycin, and incubated at 37°C, 5% CO2 for 48h prior to stimulation. The cells were stimulated with PDGF-BB (20ng/ml) for 72h and then incubated with the yellow MTT (3-(4, 5-dimethylthiazolyl-2)-2, 5-diphenyltetrazolium bromide) for 6h at 37°C, followed by the addition of detergent (room temperature, stored overnight in the dark). The absorbance was measured in a microtiter plate reader (Biorad, Hercules, CA) at 570nm the next day.

Western immunoblotting. *Preparation of total cell lysates.* PASMC were washed three times with ice-cold PBS. Cell lysates were prepared by adding boiling lysis buffer (10mM Tris HCl, 1% SDS, PMSF 0.2mM, protease and phosphatase inhibitor cocktails (Sigma-Aldrich, St. Louis, MO), phosphatase inhibitors cocktails #1 and #2) to the cells, scraping into a 1.5ml microcentrifuge tube and boiling for 10min. prior to centrifugation. The supernatants were transferred to fresh microcentrifuge tubes and stored – 80°C.

Preparation of subcellular fractions (nuclear matrix, nuclear extract, cytoplasmic extract) were performed using a modified low-salt-high-salt-protocol as previously described (6, 7). HPASMC were washed and then scraped in ice-cold PBS. After centrifugation (1850g, 10min., 4°C), the cell pellet was washed again in PBS. After spin down, the cells were then lysed by resupension in hypotonic buffer (HEPES 10mM, $MgCl_2$ x 6 H_2O 1.5mM, KCl 19mM, PMSF 0.2mM, DTT 0.5mM), cell swelling on ice for 20min., followed by 15 strokes with a Dounce homogenizer (B pestle). Nuclei were then pelleted at 3300g for 15min., 4°C. *For cytoplasmic extract preparation*, 0.11 vol. of 10X cytoplasmatic extract buffer (HEPES 300mM, $MgCl_2$ x 6 H_2O 30mM, NaCl 1.4M) was added to the supernatant. After high speed centrifugation at 20,000g for 30min. at 4°C, the supernatant was designated as cytoplasmic extract and stored at – 80°C. *For nuclear extract preparation*,1/2 packed nuclear volume of high salt buffer (HEPES 20mM, $MgCl_2$ x 6 H_2O1.5mM, NaCl 800mM, glycerol 25%, EDTA-Na 0.2mM, PMSF 0.2mM, DTT 0.5mM) was added dropwise to the nuclear pellet, vortexed for 40min. at 4°C., then centrifuged at 20,000g for 30min. at 4°C. The resulting supernatant was designated as nuclear extract and stored at – 80°C. *For nuclear matrix extract preparation*, 1/2 packed nuclear volume (pnv) of high salt buffer was added. The pellet was boiled for 10min, and the nuclear matrix fraction was extracted by vortexing in 2x packed nuclear volume (pnv) SDS buffer for 60min. at 20°C. After centrifugation at 20,000g for 30min., 4°C, the salt resistant supernatant was designated as nuclear matrix fraction and stored at – 80°C. All buffers contained protease and phosphatase inhibitors (Sigma-Aldrich, phosphatase inhibitor cocktails #1 and #2).

Protein concentration was determined by the Lowry protein assay (Biorad, Hercules, CA). Equal amounts of protein were loaded onto each lane of a 4-12% Bis-Tris gel and subjected to electrophoresis under reducing conditions. After blotting, PVDF-membranes (Invitrogen, Carlsbad, CA) were blocked for 1h (milkpowder 5% in TBS/tween 0.1-0.2%) and incubated with rabbit

polyclonal antibodies raised against ERK 1/2 (Cell Signaling, Danvers, MA), , pSmad 1/5/8 or total Smad1 (both Cell Signaling, Danvers, MA), or mouse monoclonal antibodies against phosphoERK 1/2 (Cell Signaling), PPARγ (Santa Cruz, Santa Cruz, CA), apolipoprotein E (Abcam, Cambridge, MA) or BMP-RII (BD Biosciences Pharmingen, San Jose, CA). Binding of secondary HRP-antibodies were visualized by ECL or ECL plus chemiluminescent (Amersham, Princeton, NJ). Normalization for total cell protein was performed by re-probing the membrane with a mouse monoclonal antibody against α-tubulin (Sigma-Aldrich, St. Louis, MO). Normalization for total protein in cell fractions was achieved by correcting for Ponceau S stain.

PPARγ-DNA-Binding Assay. A multiplex transcription factor (TF) assay (Marligen Biosciences, Ijamsville, MD) was performed as previously described (8, 9). Briefly, multiple biotin labeled TF DNA probes (DNA multiplex probe mix) are mixed with one nuclear extract protein sample to allow transcription factor-DNA binding. In the following digestion step, DNA sequences that are not bound (and "protected") by specific transcription factors are destroyed by proprietary reagents. A mix of colored beads (1000 of each color per specific transcription factor) with attached DNA-oligonucleotides complimentary to a sequence in the specific TF DNA probes is added to the tube. Then, DNA binding sites hybridize to their respective beads (PPARγ core binding site: 5'-TGACCTTTGACC-3') and the entire sample is measured in a Luminex-100 instrumentation (Luminex, Houston, TX) that reads at least 100 signals per colored bead type. Nuclear extract samples were run in triplicate so that 300 different data points are collected for each DNA binding site.

Immunohistochemistry/Confocal Microscopy. Serum starved Human PASMC were seeded on 4-chamber slides (250μl), stimulated with BMP-2 (10ng/ml), washed and fixated with paraformaldehyde 4% at room temperature, incubated in blocking buffer (5% goat serum, 0.02% BSA, Triton X-100 0.1% in TBS) for 30min., and then incubated with primary polyclonal antibody (rabbit anti human) against phosphoERK1/2 (Cell Signalling, Danvers, MA) overnight at 4°C. The fixed cells were then carefully washed three times, and incubated with secondary antibody (goat anti rabbit, Alexa 488, Molecular Probes/Invitrogen, Carlsbad, CA), and again washed three times. For mounting, antifade-DAPI (Component A, slow fade-antifade kit S-24635, Mol. Probes/Invitrogen) was given on the cover slips, and slides were sealed with colorless nail polish. Images were acquired on a Zeiss LSM 510 two-photon confocal laser scanning microscope. Confocal micrographs were processed with Openlab 3.1.4 and Volocity 3.0 software (Improvision, Coventry, UK).

Hemodynamic Measurements in Mice. RV catheterisation: A 1.4 F catheter (Millar Instruments, Houston, Texas) was inserted into the right jugular vein and then placed into the RV free cavity, as previously described (10). Using the PowerLab/4SP recording unit (AD Instruments, Colorado Springs, CO), 3-5 tracings at different time points were averaged to determine the RVSP, maximal rate of pressure development (dp/dt max.; RV systolic function) and maximal rate of pressure decay (dp/dt min.; RV diastolic function). *Systemic blood pressure measurements (tail cuff method):* At least 5 recordings per mouse were averaged to determine systolic BP, MAP and diastolic BP. *Echocardiography:* Fractional shortening (FS) and heart rate (HR) were determined in M-mode. Ejection fraction (EF) and cardiac output (CO) were estimated using the Teichholz formula (11).

Lung tissue preparation. After abdominal aortic dissection, lungs were perfused in vivo by injecting 5ml normal saline into the beating RV. Lungs were tracheally injected with 10% formalin, fixed overnight, and then embedded either in paraffin for standard histology (Hematoxylin & Eosin, Elastic van Gieson, Movat pentachrome). Prior to fixation, a subset of left lungs were infused with barium-gelatin via the central PA (12) to label peripheral pulmonary arteries for morphometric analysis. The barium was infused by hand with similar endpoints of pre-capillary filling of all small vessels at alveolar duct and wall level. The total number of peripheral arteries was calculated as a ratio of number of arteries per surface area (5 random fields per slide) and per 100 alveoli in each field (200x magnification). Muscularized and non-muscularized peripheral (alveolar wall) pulmonary arteries were counted at 400x magnification in 5 random fields per lung. (200x magnfication = 1 field)

SUPPLEMENTARY DATA

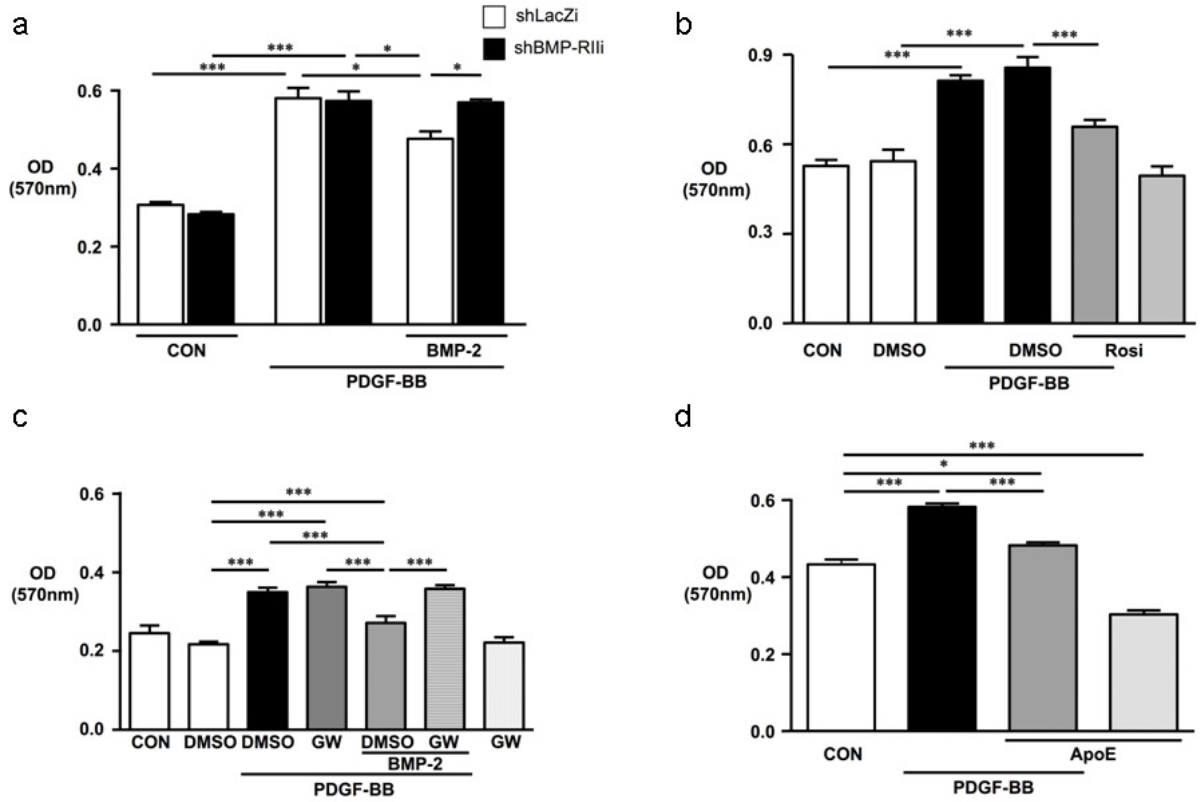

Supplementary Figure 2 BMP-2 (**a,c**), the PPARγ agonist rosiglitazone (**b**), and apolipoprotein E (**d**) inhibit proliferation of human pulmonary artery smooth muscle cells (PASMC) induced by PDGF-BB (20ng/ml). **a**, Recombinant BMP-2 inhibits proliferation in LacZi control but not in shBMR2i PASMC in which BMP-receptor II expression is suppressed by shRNAi pLenti 6. **b,** Rosiglitazone (1μM) blocks human PASMC proliferation. The expansion of the y axis reflects higher baseline OD values. **c**, The inhibitory effect of BMP-2 on human PASMC proliferation is lost in the presence of the irreversible PPARγ antagonist GW9662 (1μM). **d**, recombinant apolipoprotein E (apoE 10μM) inhibits human PASMC proliferation. Starvation, stimulation with PDGF-BB and MTT assay as described under methods. Bars represent mean±SEM (n = 4-8; n = 12-14 for PDGF-BB in Fig. 2b and 2d). ∗ $p < 0.05$; ∗∗∗ $p < 0.001$.

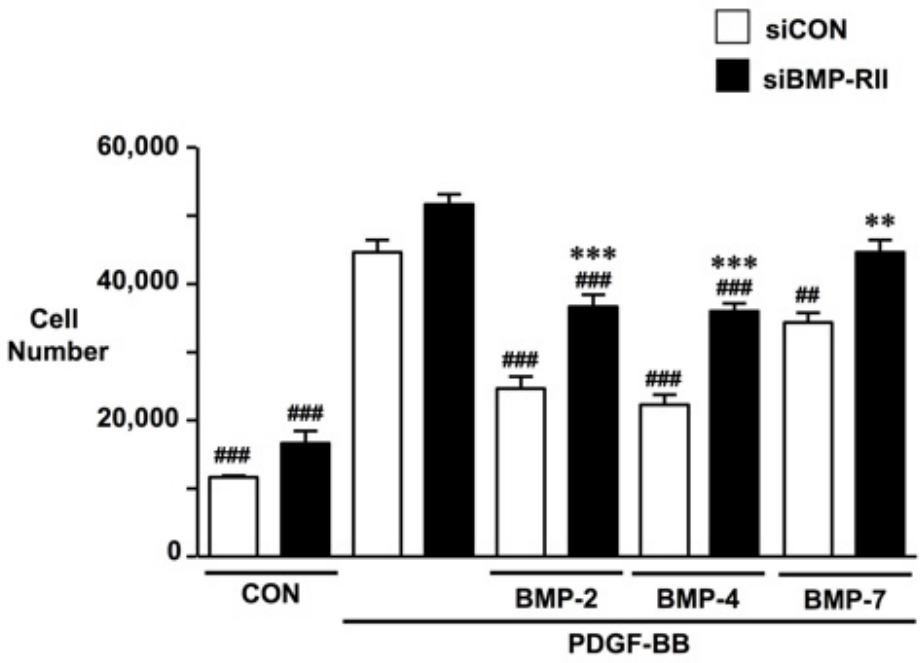

Supplementary Figure 3 Antiproliferative effects of BMP-2, BMP-4, and BMP-7 in sicontrol and siBMP-RII (knock down) human PASMC. To achieve effective gene knockdown, siRNA duplexes specific for BMP-RII were transfected into human PASMCs using Lipofectamine 2000 (Invitrogen). Knock-down efficiency was evaluated 48 hours later by measuring protein levels in cell lysates by western immunoblotting. Transfection of nontargeting siRNA duplexes (siCONTROL, Dharmacon, Inc) was performed simultaneously to serve as a control in all experiments. PASMC were seeded at $2.5x10^4$ cells per well of a 24-well plate in 500µl of growth medium and allowed to adhere overnight. The cells were washed with PBS prior to the addition of starvation media (0.1% FBS) and incubated for 48h, and then stimulated with PDGF-BB (20ng/ml) for 72h. BMP-2, BMP-4 and BMP-7 (all 10ng/ml) were added to quiescent cells 30min. prior to PDGF-BB stimulation. Cell numbers in controls at time points 0h and 72h were not significantly different. Bars represent mean±SEM (n = 3). ANOVA with Bonferroni's multiple comparison test. ## $p < 0.01$; ### $p < 0.001$ denote comparisons with PDGF-BB stimulation of either siCON or siBMP-RII cells, in the absence of BMPs. * $p < 0.05$; ** $p < 0.01$; *** $p < 0.001$ denote comparisons between siCON and siBMP-RII for each ligand (BMP-2, BMP-4, BMP-7).

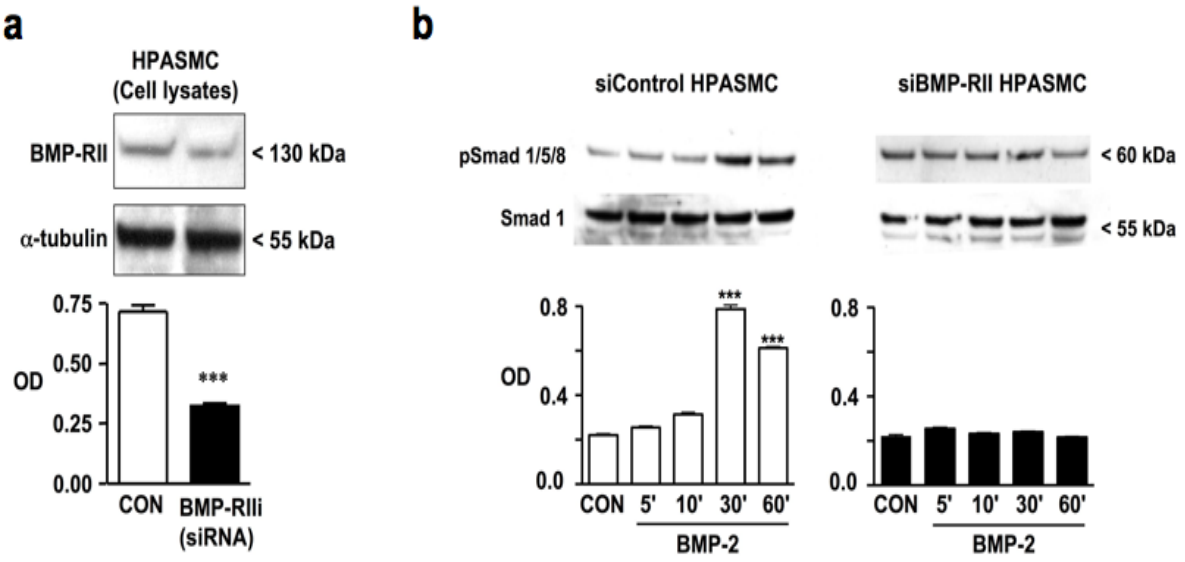

Supplementary Figure 4. Knock-down of human BMP-RII prevents BMP-2 mediated phosphoSmad 1/5/8 (pSmad 1/5/8) signalling in human PASMC. **a**, Knock-down of human BMP-RII protein expression by small interfering RNA in human PASMC. To achieve effective gene knockdown, siRNA duplexes specific for BMP-RII were transfected into human PASMCs using Lipofectamine 2000. Nontargeting siRNA duplexes were used for control transfections (see Supplementary Methods). **b**, BMP-2 (10ng/ml) stimulation for 30min. induces Smad1/5/8 phosphorylation in siControl but not in siBMP-RII (knock-down) human PASMC. Of note, Smad 1/5/8 phosphorylation occurs after BMP-2 mediated activation of PPARγ (see Figure 2d, main manuscript). Cell culture, total cell lysate preparation and Western immunoblotting are described in the (Supplementary) Methods section. Arbitrary OD values (densitometry): Bars represent mean±SEM (n = 3). Unpaired two-tailed t-test (**a**) and ANOVA with Bonferroni's multiple comparison test (**b**). *** $p < 0.001$ versus control.

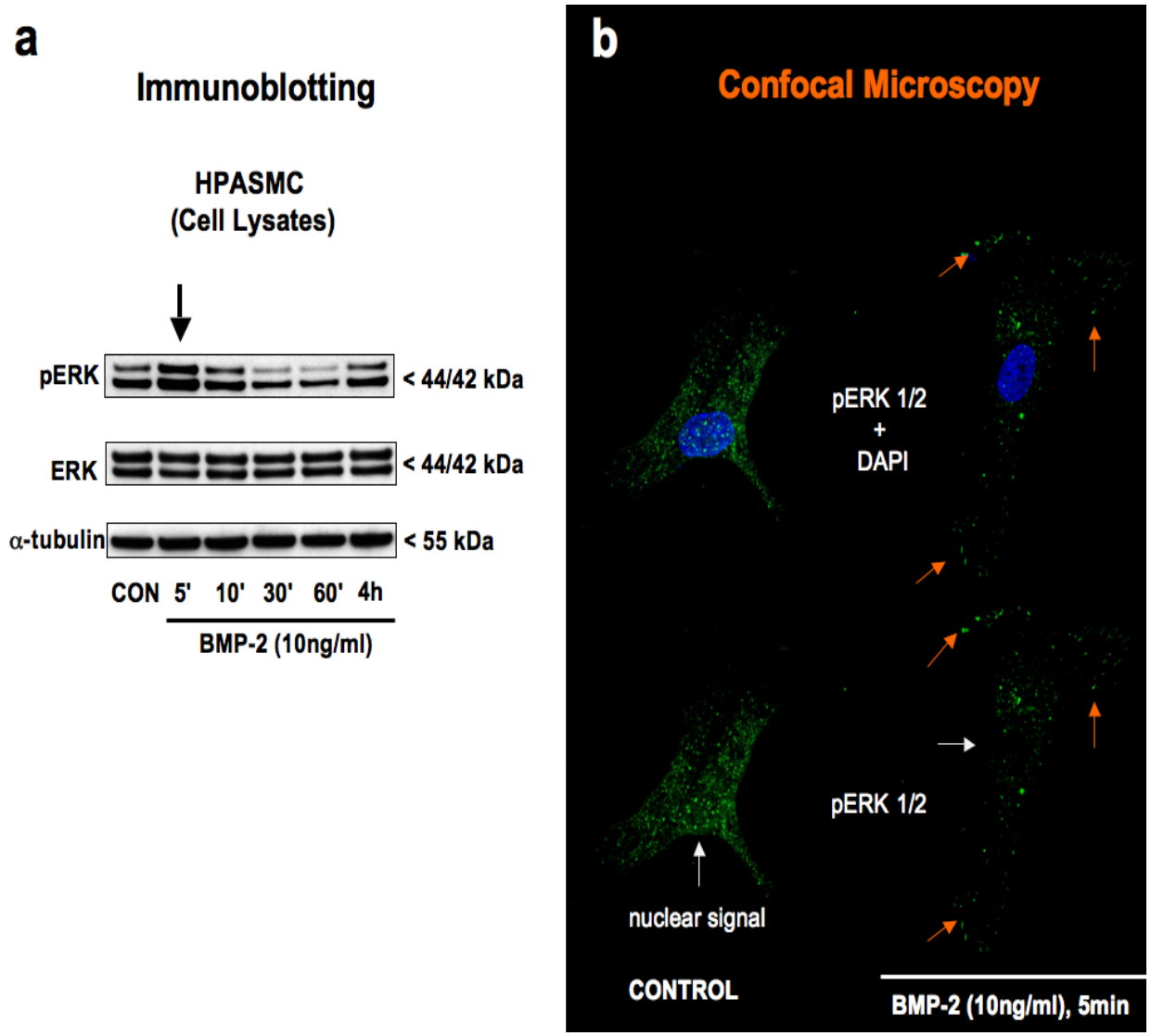

Supplementary Figure 5. BMP-2 induces rapid extra-nuclear ERK1/2 phosphorylation that is accompanied by a strong signal at the cyoplasmic membrane. **a**, Western immunoblotting of total cell lysates: pERK1, pERK2, total ERK1, total ERK2, as well as α-tubulin (2nd loading control). Human PASMC were stimulated with BMP-2 (10ng/ml) for 5-60min., and 4h (n=2). Cell culture and preparation of total cell lysates (which include the cytoplasmic membrane fraction) as described in the Methods section. **b**, Immunohistochemistry/confocal microscopy. DAPI = nuclear DNA stain, bright green = pERK 1/2 stain (see Methods section). BMP-2 stimulation (5min.) impairs the nuclear signal of pERK (white arrows). This is accompanied by strong pERK 1/2 staining at the cytoplasmic membrane (orange arrows). Of note, the decrease in nuclear pERK staining (white arrow) on BMP-2 stimulation (5min.) is timely coinciding with the decrease of pERK in nuclear extracts (see Figure 2b, main manuscript).

References (Supplement)

1. Hevener, A.L., He, W., Barak, Y., Le, J., Bandyopadhyay, G., Olson, P., Wilkes, J., Evans, R.M., and Olefsky, J. 2003. Muscle-specific Pparg deletion causes insulin resistance. *Nat Med* 9:1491-1497.
2. Fouty, B.W., Grimison, B., Fagan, K.A., Le Cras, T.D., Harral, J.W., Hoedt-Miller, M., Sclafani, R.A., and Rodman, D.M. 2001. p27(Kip1) is important in modulating pulmonary artery smooth muscle cell proliferation. *Am J Respir Cell Mol Biol* 25:652-658.
3. Yang, X., Long, L., Southwood, M., Rudarakanchana, N., Upton, P.D., Jeffery, T.K., Atkinson, C., Chen, H., Trembath, R.C., and Morrell, N.W. 2005. Dysfunctional Smad signaling contributes to abnormal smooth muscle cell proliferation in familial pulmonary arterial hypertension. *Circ Res* 96:1053-1063.
4. Wharton, J., Davie, N., Upton, P.D., Yacoub, M.H., Polak, J.M., and Morrell, N.W. 2000. Prostacyclin analogues differentially inhibit growth of distal and proximal human pulmonary artery smooth muscle cells. *Circulation* 102:3130-3136.
5. Morrell, N.W., Upton, P.D., Kotecha, S., Huntley, A., Yacoub, M.H., Polak, J.M., and Wharton, J. 1999. Angiotensin II activates MAPK and stimulates growth of human pulmonary artery smooth muscle via AT1 receptors. *Am J Physiol* 277:L440-448.
6. Dignam, J.D., Lebovitz, R.M., and Roeder, R.G. 1983. Accurate transcription initiation by RNA polymerase II in a soluble extract from isolated mammalian nuclei. *Nucleic Acids Res* 11:1475-1489.
7. Mitani, Y., Zaidi, S.H., Dufourcq, P., Thompson, K., and Rabinovitch, M. 2000. Nitric oxide reduces vascular smooth muscle cell elastase activity through cGMP-mediated suppression of ERK phosphorylation and AML1B nuclear partitioning. *Faseb J* 14:805-814.
8. Hodge, D.R., Peng, B., Pompeia, C., Thomas, S., Cho, E., Clausen, P.A., Marquez, V.E., and Farrar, W.L. 2005. Epigenetic silencing of manganese superoxide dismutase (SOD-2) in KAS 6/1 human multiple myeloma cells increases cell proliferation. *Cancer Biol Ther* 4:585-592.
9. Shurin, G.V., Ferris, R.L., Tourkova, I.L., Perez, L., Lokshin, A., Balkir, L., Collins, B., Chatta, G.S., and Shurin, M.R. 2005. Loss of new chemokine CXCL14 in tumor tissue is associated with low infiltration by dendritic cells (DC), while restoration of human CXCL14 expression in tumor cells causes attraction of DC both in vitro and in vivo. *J Immunol* 174:5490-5498.
10. Hansmann, G., Wagner, R.A., Schellong, S., Perez, V.A., Urashima, T., Wang, L., Sheikh, A.Y., Suen, R.S., Stewart, D.J., and Rabinovitch, M. 2007. Pulmonary arterial hypertension is linked to insulin resistance and reversed by peroxisome proliferator-activated receptor-gamma activation. *Circulation* 115:1275-1284.
11. Teichholz, L.E., Kreulen, T., Herman, M.V., and Gorlin, R. 1976. Problems in echocardiographic volume determinations: echocardiographic-angiographic correlations in the presence of absence of asynergy. *Am J Cardiol* 37:7-11.
12. Ye, C.L., and Rabinovitch, M. 1991. Inhibition of elastolysis by SC-37698 reduces development and progression of monocrotaline pulmonary hypertension. *Am J Physiol* 261:H1255-1267.

2.2 Pulmonary Arterial Hypertension Is Linked To Insulin Resistance And Reversed By PPARγ Activation

Patients with PAH have reduced expression of PPARγ and apoE in lung tissues, and deficiency of both has been linked to insulin resistance (IR). In *systemic* vascular SMC, apoE and adiponectin[83], a PPARγ target in adipocytes[43], inhibit PDGF-BB-induced SMC proliferation and migration[93, 112], both key features in the pathogenesis of PAH. ApoE internalizes the PDGFR-β[94, 95, 113] and adiponectin sequesters the ligand PDGF-B[114]. Thus, in association with insulin resistance, reduced levels of apoE[93] and adiponectin[112] can be expected to enhance PDGF-BB-signaling (see introduction **1.3**, **Figure 1**). In accordance with these observations, diabetic apoE deficient mice (apoE -/-) show pronounced PDGF-BB-signaling and neointimal thickening of the arterial vessel wall[96]. We hypothesized that these factors would have similar effects on *pulmonary* arterial SMC (PASMC), consequently leading to PAH.

ApoE -/- and C57Bl/6 Mice on Regular Chow Have Similar RVSP and RV Mass. First, we assessed 15-week-old male and female apoE -/- on regular chow for the presence and severity of PAH. Values of RVSP, a measure of PAH, and of RV/LV+S ratio, a measure of RVH, were similar in apoE -/- and C57Bl/6 control mice. Moreover, there were no significant differences in RVSP or RV/LV+S ratio between genders of either genotype.

ApoE -/- Mice on High Fat Diet Develop PAH. An 11-week high fat (HF) diet treatment did not significantly increase RVSP in 15-week old C57Bl/6 mice. In contrast, apoE -/- mice on high fat diet for the same duration developed PAH as indicated by significant elevation in RVSP, with males having higher values than females. In addition, only male apoE -/- mice on high fat diet had RVH and enhanced peripheral PA muscularization when compared to C57Bl/6 controls. A direct comparison revealed a more severe PAH phenotype in the male vs. female apoE-/- mice on high fat diet in that RVSP (28.9 vs. 24.9mmHg; $p=0.0014$), RVH (RV/LV+S ratio 0.41 vs. 0.29; $p=0.0093$) and peripheral muscularization (47.8 vs. 35.4%; $p=0.0371$) were significantly greater. RV systolic function (RV dp/dt max.) was augmented in apoE -/- mice of both genders and reflected the elevated RVSP compared to C57Bl/6 controls. RV diastolic function (RV dp/dt min.) was greater in both male (trend) and female ($p<0.05$) apoE -/- when compared to C57Bl/6 mice of the same gender. Systemic blood pressure, cardiac output, left ventricular function (indicated by left ventricular end diastolic pressure; LVEDP 2-5mmHg) and hematocrit were similar in both genotypes. Thus, elevation of RVSP in apoE -/- compared to C57Bl/6 mice likely reflected an elevation in pulmonary vascular resistance.

PA Atherosclerosis in the ApoE-/- Mice Does Not Cause Significant PA Stenosis. Further studies were carried out to determine whether apoE -/- mice on high fat (HF) diet developed - in addition to

neomuscularization of peripheral pulmonary arteries - occlusive atheromata accounting for the elevated RVSP and RVH, when compared to C57Bl/6 mice. ApoE -/- mice of both genders on HF diet showed atheromata on histology and on computed tomography (micro-CT), affecting the large pulmonary arteries in a non-occlusive manner (see Circulation, 2007; Supplementary Figure 1). Similar features have been described in pathological specimens of adult patients with PAH[115]. However, the cholesterol levels and the presence of atheroma were similar in male and female apoE deficient mice, but only male apoE -/- developed insulin resistance and severe PAH, i.e., a combination of marked RVSP elevation, RVH and enhanced peripheral PA muscularization. We therefore suggest that apoE deficiency, hypoadiponectinemia, and the related insulin resistance (see below), rather than pulmonary atherosclerosis itself, were the major causes of PAH.

Insulin Resistance Is Associated with More Severe PAH in Male ApoE-/- Mice. We focused our attention on possible differences in the lipid profile and markers of insulin resistance associated with the more severe PAH phenotype in apoE -/- *vs.* C57Bl/6 mice, and in particular in male *vs.* female apoE -/- mice. Higher plasma cholesterol was observed in male and female apoE -/- mice compared to C57Bl/6 controls on HF diet. Also, apoE -/- mice had moderately higher triglyceride levels that were similar in male and female apoE -/- and independent of the diet (see Circulation, 2007; Supplementary Tables 1 and 2). However, only in male apoE -/- but not in female apoE -/- mice on HF diet, did we observe features consistent with insulin resistance, i.e., elevated fasting blood glucose and insulin levels when compared to C57Bl/6 controls.

Because of the concordance of insulin resistance and the more severe PAH phenotype in male vs. female apoE -/- mice, we investigated whether the females had higher plasma levels of the insulin-sensitizing adipocytokine adiponectin. While the high fat diet resulted in a marked increase in adiponectin levels in control C57Bl/6 mice of both genders, this marked upregulation was absent in apoE -/- mice. It is therefore possible that the release of adiponectin from adipocytes in response to high fat diet is - to some extent - apoE-dependent. However, female mice of both genotypes had >50 % higher plasma adiponectin concentration than their male counterparts. Since testosterone inhibits the secretion of adiponectin in adipocytes[116], we hypothesized that higher adiponectin levels - in association with lack of insulin resistance - may account for the less severe pulmonary vascular phenotype in female apoE -/- mice on HF diet.

PPARγ Activation Elevates Plasma Adiponectin, Improves Insulin Sensitivity and Reverses PAH. On the basis of these data we reasoned that the presence of PAH may be determined by the inability to sufficiently raise adiponectin levels in association with high fat diet, and that the severity of the disease may be a function of the degree of hyperinsulinemia and hyperglycemia We therefore hypothesized that treating the pulmonary hypertensive, insulin-resistant male apoE -/- mice with a

PPARγ agonist – to increase plasma adiponectin and improve insulin sensitivity - might arrest disease progression or reverse PAH. Thus, we treated 15-week-old male apoE -/- and C57Bl/6 control mice on HF diet with rosiglitazone, at a dose of 10mg/kg per day, incorporated into their food. Four-week treatment with rosiglitazone resulted in much higher plasma adiponectin levels in C57Bl/6 control (5-fold) and apoE -/- mice (8-fold) when compared to untreated animals of the same genotype. The higher plasma adiponectin concentration in treated *vs.* untreated apoE -/- mice was associated with lower blood glucose (control level), indicating improved insulin sensitivity in apoE -/- mice treated with rosiglitazone.

In addition to the induction of plasma adiponectin and improvement of insulin sensitivity, a 4-week course of rosiglitazone treatment resulted in full regression of PAH (RVSP at control level), RV hypertrophy (RV/LV+S ratio), and peripheral PA muscularization at alveolar wall level in apoE -/- mice that were insulin resistant before treatment. Rosiglitazone, given for 4 weeks, caused no significant differences in systemic blood pressure, heart rate, LV systolic function (fractional shortening, ejection fraction), cardiac output, and RV function. Other measurements such as hematocrit and WBC count were also similar in treated and untreated animals. There was, however, a tendency for rosiglitazone to cause mild LV dilatation and increased LV mass in both C57Bl/6 control and apoE -/- mice. All the features described above were sustained following a 10-week rosiglitazone treatment period, suggesting that the effect was not transient.

Recombinant Apolipoprotein E and Adiponectin Inhibit PASMC Proliferation. To support possible roles of apoE and adiponectin in protecting against the development of PAH (see introduction **1.3**, **Figure 1**), we showed that both proteins inhibit PDGF-BB-induced proliferation of PASMC from control and apoE-/- mice. The likely mechanism by which apoE deficiency leads to the development of PAH appears to be facilitated PDGF-BB signaling. From studies in systemic vascular SMC, we know PDGF-BB signaling is suppressed when apoE binds to the LRP, thereby initiating endocytosis and degradation of the LRP–PDGFR-β–PDGF-BB complex[94, 95, 113]. We have shown here that PDGF-BB-induced proliferation is also suppressed by apoE in PASMC, suggesting a similar mechanism may be present in the pulmonary vasculature. In diabetic apoE -/- mice, PDGFR-β signaling is increased in vascular SMC, and systemic vascular disease can be reversed by the PDGFR tyrosine kinase inhibitor imatinib[96]. We[32] and others[30] have shown that blockade of tyrosine kinase activity selective to the epidermal growth factor receptor [32] or the PDGF receptor[30] reverses experimental PAH and vascular remodeling caused by the toxin monocrotaline in rats.

In association with insulin resistance, the male mice (apoE -/- and C57Bl/6) had lower levels of adiponectin than the female mice. This is in keeping with a recent study demonstrating that testosterone inhibits the secretion of adiponectin in adipocytes[43]. Adiponectin reverses insulin

resistance[83], and is independently associated with a reduced risk of type 2 diabetes in apparently healthy individuals[84]. Morevover, adiponectin – in its high molecular weight form – binds PDGF-B, thereby reducing PDGF-B bioavailability[114] and mitogenic post-receptor function in vascular SMC[112] (see introduction **1.3**, **Figure 1**). Adiponectin has been shown to be a transcriptional target of PPARγ in adipocytes[43]. Since previous studies used the PPARγ agonist rosiglitazone to suppress intimal thickening in the apoE-/- mouse[117], we reasoned that it might also be effective in preventing disease progression or reversing PAH. Indeed, treatment of male apoE -/- mice with rosiglitazone increased plasma adiponectin, improved insulin sensitivity, and led to sustained regression of PAH, RVH, and abnormal muscularization of distal pulmonary arteries. The source of adiponectin in our model is likely from visceral and subcutaneous as well as perivascular adipocytes[86]. To support a mechanistic relationship between apoE and adiponectin deficiency on the one hand, and PAH with enhanced muscularization of peripheral PA on the other, we showed that recombinant apoE and adiponectin inhibited PDGF-BB-induced proliferation of cultured wildtype and apoE -/- PASMC.

While a link between insulin resistance and systemic cardiovascular disease is evident in both clinical[70] and experimental studies[45, 82], this report is the first indication that there may be a possible link with PAH. If insulin resistance does contribute to the pathobiology of PAH in humans (see our clinical study under **2.3**), it will be an extremely important relationship, owing to the steadily increasing number of children, adolescents[69] and adults[70] with the "metabolic syndrome".

This study[118] identified several new factors which may be involved in the pathogenesis of PAH, and a potential treatment. We acknowledge that it is difficult to separate out the effects of apoE deficiency and insulin resistance (IR) in our animal model, and to extrapolate the potential impact of a successful experimental treatment to human disease. Most recently we could demonstrate that apoE -/- mice on regular diet develop PAH with age in the absence of IR, indicating apoE deficiency may be an independent risk factor for PAH (Hansmann G et al., unpublished data, presented at SPR/PAS, Honolulu, 05/2008). Nevertheless, it will be important to examine whether insulin resistance, dyslipidemia, impaired apoE function, and low adiponectin levels are risk factors for the progression of PAH in humans[119]. It will also be of interest to investigate a relationship between genetic and molecular mechanisms that underlie IR, apoE and adiponectin levels, and known PAH pathways, e.g. those downstream of BMP-RII. Taken together these data suggest a beneficial effect from the addition of PPARγ agonists to the treatment regimen for PAH patients.

Cited own reference, reproduced with permission from Wolters Kluwer (Lippincott Williams & Wilkins):

Hansmann G, Wagner RA, Schellong S, de Jesus Perez VA, Urashima T, Wang L, Sheikh AY, Suen RS, Stewart DJ, Rabinovitch M (2007) Pulmonary arterial hypertension is linked to insulin resistance and reversed by PPARγ activation. **Circulation** 115: 1275-1284 *epub March 5, 2007*

Vascular Medicine

Pulmonary Arterial Hypertension Is Linked to Insulin Resistance and Reversed by Peroxisome Proliferator–Activated Receptor-γ Activation

Georg Hansmann, MD; Roger A. Wagner, MD, PhD; Stefan Schellong, BA; Vinicio A. de Jesus Perez, MD; Takashi Urashima, MD; Lingli Wang, MD; Ahmad Y. Sheikh, MD; Renée S. Suen, BSc; Duncan J. Stewart, MD; Marlene Rabinovitch, MD

Background—Patients with pulmonary arterial hypertension (PAH) have reduced expression of apolipoprotein E (apoE) and peroxisome proliferator–activated receptor-γ in lung tissues, and deficiency of both has been linked to insulin resistance. ApoE deficiency leads to enhanced platelet-derived growth factor signaling, which is important in the pathobiology of PAH. We therefore hypothesized that insulin-resistant apoE-deficient ($apoE^{-/-}$) mice would develop PAH that could be reversed by a peroxisome proliferator–activated receptor-γ agonist (eg, rosiglitazone).

Methods and Results—We report that $apoE^{-/-}$ mice on a high-fat diet develop PAH as judged by elevated right ventricular systolic pressure. Compared with females, male $apoE^{-/-}$ were insulin resistant, had lower plasma adiponectin, and had higher right ventricular systolic pressure associated with right ventricular hypertrophy and increased peripheral pulmonary artery muscularization. Because male $apoE^{-/-}$ mice were insulin resistant and had more severe PAH than female $apoE^{-/-}$ mice, we treated them with rosiglitazone for 4 and 10 weeks. This treatment resulted in markedly higher plasma adiponectin, improved insulin sensitivity, and complete regression of PAH, right ventricular hypertrophy, and abnormal pulmonary artery muscularization in male $apoE^{-/-}$ mice. We further show that recombinant apoE and adiponectin suppress platelet-derived growth factor-BB–mediated proliferation of pulmonary artery smooth muscle cells harvested from $apoE^{-/-}$ or C57Bl/6 control mice.

Conclusions—We have shown that insulin resistance, low plasma adiponectin levels, and deficiency of apoE may be risk factors for PAH and that peroxisome proliferator–activated receptor-γ activation can reverse PAH in an animal model. **(*Circulation*. 2007;115:1275-1284.)**

Key Words: apolipoproteins ■ glucose ■ hypercholesterolemia ■ hypertension, pulmonary ■ insulin ■ metabolism ■ PPAR gamma

Although insulin resistance is associated with systemic cardiovascular disease,[1–3] it has not been implicated as a predisposing factor in pulmonary arterial hypertension (PAH). Several findings, however, support such an association. Patients with idiopathic PAH have reduced pulmonary mRNA expression of peroxisome proliferator–activated receptor gamma (PPARγ),[4] a ligand-activated nuclear receptor and transcription factor that regulates adipogenesis and glucose metabolism.[5–7] They also have reduced pulmonary mRNA expression of apolipoprotein E (apoE),[8] a protective factor known to reduce circulating oxidized low-density lipoprotein and atherogenesis in the vessel wall.[9] Deficiency of both PPARγ and apoE has been linked to insulin resistance and the metabolic syndrome.[7,9] Elevated levels of several circulating factors that are normally repressed by PPARγ are associated with insulin resistance[3] and implicated in the pathobiology of PAH. These include interleukin-6,[10,11] fractalkine,[12,13] monocyte chemoattractant protein-1,[14] endothelin-1 (ET-1),[15–17] and the endogenous nitric oxide synthase inhibitor asymmetric dimethylarginine (ADMA).[18,19]

Clinical Perspective p 1284

Heightened signaling by platelet-derived growth factor-BB (PDGF-BB)/mitogen-activated protein kinase leading to smooth muscle cell (SMC) proliferation and migration is also a key clinical feature of pulmonary vascular disease.[20–22] With apoE deficiency, abundant oxidized low-density lipoprotein[23] and PDGF-BB[23] were shown to induce mitogen-

Received September 8, 2006; accepted December 29, 2006.

From the Department of Pediatrics, Division of Pediatric Cardiology (G.H., S.S., V.A.D.J.P., T.U., L.W., M.R.), Department of Medicine, Division of Cardiovascular Medicine (R.A.W.), and Department of Cardiovascular Surgery (A.Y.S.), Stanford University School of Medicine, Stanford, Calif, and Department of Medicine, Division of Cardiology, University of Toronto, Toronto, Ontario, Canada (R.S.S., D.J.S.).

The online-only Data Supplement, consisting of expanded Methods and tables, is available with this article at http://circ.ahajournals.org/cgi/content/full/CIRCULATIONAHA.106.663120/DC1.

Correspondence to Dr Marlene Rabinovitch, Vera Moulton Wall Center for Pulmonary Vascular Disease, Stanford University School of Medicine, CCSR 2245B, 269 Campus Dr, Stanford, CA 94305-5162. E-mail marlener@stanford.edu

Circulation **is available at http://www.circulationaha.org** **DOI: 10.1161/CIRCULATIONAHA.106.663120**

activated protein kinase, transcription of growth-promoting genes (eg, cyclin D1), and subsequently proliferation and migration of systemic vascular SMCs.[23,24] Interestingly, high glucose concentrations induce mitogen-activated protein kinase/phosphatidylinositol 3-kinase (PI3K)–dependent up-regulation of PDGF receptor-β (PDGFR-β) and potentiate SMC migration in response to PDGF-BB.[24] In concert with PI3K, PDGFR-β/mitogen-activated protein kinase-signaling also leads to SMC resistance to apoptosis.[25]

In systemic vascular SMCs, apoE and adiponectin,[26] a PPARγ target in adipocytes,[7] inhibit PDGF-BB–induced SMC proliferation and migration.[23,27] ApoE internalizes the PDGFR-β,[28–30] and adiponectin sequesters the ligand PDGF-BB.[31] Thus, in association with insulin resistance, reduced levels of apoE[23] and adiponectin[27] can be expected to enhance PDGF-BB signaling. In accordance with these observations, diabetic apoE-deficient (apoE$^{-/-}$) mice show pronounced PDGF-BB signaling and neointimal thickening of the arterial vessel wall.[32] We hypothesized that these factors would have similar effects on pulmonary arterial SMCs (PASMCs), consequently leading to PAH.

PPARγ agonists are clinically used to make cells insulin sensitive, thereby obviating the detrimental effects of insulin resistance related to hyperlipidemia, inflammation, and mitogenesis in the vessel wall.[33] Rosiglitazone, a PPARγ ligand of the thiazolidinedione class, enhances insulin-mediated glucose uptake and inhibits proliferation and migration of systemic SMCs induced by PDGF-BB.[33,34] We therefore hypothesized that PAH would develop in apoE$^{-/-}$ insulin-resistant mice but that the disease process would be attenuated or reversed by a PPARγ agonist (eg, rosiglitazone).

In the present study, we show that apoE deficiency, in association with a high-fat (HF) diet, leads to both insulin resistance and PAH. Male apoE$^{-/-}$ mice had more severe PAH (ie, higher right ventricular systolic pressure [RVSP], right ventricular hypertrophy [RVH], and enhanced peripheral PA muscularization) associated with insulin resistance and lower plasma adiponectin levels compared with female apoE$^{-/-}$ mice. Because testosterone inhibits the secretion of adiponectin in adipocytes,[35] we hypothesized that elevation of this vasoprotective adipocytokine may account for the less severe vascular phenotype in female apoE$^{-/-}$ mice. We therefore treated male apoE$^{-/-}$ mice with rosiglitazone and documented 8-fold-higher plasma adiponectin levels, improved insulin sensitivity, and complete regression of PAH, RVH, and abnormal PA muscularization. To further establish a direct link between apoE and adiponectin and SMC proliferation and survival, we treated murine (apoE$^{-/-}$ and wild-type) PASMCs in culture with recombinant apoE and adiponectin. We showed that both proteins inhibit PDGF-BB–induced proliferation in apoE$^{-/-}$ and wild-type PASMCs. Our data therefore suggest that insulin resistance and deficiency of apoE and/or adiponectin may be risk factors for PAH that can be reversed by PPARγ activation.

Methods

Expanded Methods and Results sections are given in the online Data Supplement.

Experimental Design

ApoE$^{-/-}$ mice (B6.129P2-Apoetm1Unc/J) and C57Bl/6 control mice were obtained from Jackson Laboratories (Bar Harbor, Me). At 4 weeks of age, the mice were either continued on regular chow or switched to HF diet (Dyets No. 101511, Dyets Inc, Bethlehem, Pa) for a maximum of 21 weeks. For the nontreatment study, 15-week-old male and female mice (apoE$^{-/-}$, C57Bl/6 controls) on either diet were studied. For the rosiglitazone treatment study, 15-week-old male mice (apoE$^{-/-}$, C57Bl/6 controls) on HF diet were used. Half of the animals received rosiglitazone (GlaxoSmithKline, Research Triangle Park, NC) 10 mg/kg body weight per day PO incorporated into the food for 4 or 10 weeks. All protocols were approved by the Stanford Animal Care Committee.

Hemodynamic Measurements

Measurements of RVSP and RV dP/dt were performed by jugular vein catheterization (1.4F, Millar Instruments Inc, Houston, Tex) under isoflurane anesthesia (1.5% to 2.5%) using a closed-chest technique in unventilated mice at 15, 19, and 25 weeks of age. Left ventricular (LV) end-diastolic pressure was determined by LV catheterization via the left carotid artery under isoflurane anesthesia. Systemic blood pressure was determined by the tail-cuff method in nonanesthesized mice. Measurements of cardiac output and function were performed by echocardiography.

RVH and LV Hypertrophy

RVH was measured by the weight of the RV relative to LV+septum. LV hypertrophy was measured as absolute weight of the LV plus septum. LV dilatation was assessed by echocardiographic M-mode measurement of the LV end-diastolic inner diameter.

Lung Tissue Preparation

Lungs were perfused with normal saline, fixed in 10% formalin overnight, and then either embedded in paraffin for standard histology or frozen for Oil-red-O staining. A subset of left lungs (approximately half) were barium infused via PA-inserted tubing to label peripheral PAs for morphometric analysis and micro–computed tomography (CT) imaging.

Morphometric Analysis

Transverse left lung sections were stained by elastic van Gieson and Movat pentachrome stains. From all mice, we took the same full section in the mid portion of the lung parallel to the hilum and embedded it in the same manner. Muscularization was assessed in barium-injected left lung sections by calculating the proportion of fully and partially muscularized peripheral (alveolar wall) PAs to total peripheral PAs. All measurements were done blinded to genotype and condition.

Micro-CT Imaging

A custom-built eXplore Locus RS120 Micro CT Scanner (GE Health Care, Ontario, Canada) was used to acquire nondestructing 3-dimensional images of barium-infused whole-lung specimens. Images were scanned at 49-μm resolution and 720 views (70 kV [peak], 50 mAmps, 30-ms single image acquisition time) and reconstructed with the eXplore Reconstruction Utility, and volumes were viewed and rendered with the GE Health Care MicroView software.

Fasting Whole-Blood and Plasma Measurements

We performed tail vein puncture in nonanesthetized, overnight-starved mice, followed by duplicate whole-blood glucose measurements with a glucometer (Freestyle/Abbott). Fasting blood plasma was obtained via retro-orbital bleeding or cardiac puncture. White blood cell count and hematocrit were assessed by the Stanford Animal Facility Laboratories. Hemoglobin A1c was measured by Esoterix (Calabasa Hills, Calif). Plasma ET-1 was measured by ELISA. Plasma ADMA levels were determined by high-performance liquid tomography at Oxonon Bioanalysis Inc (Oakland, Calif). All

other plasma measurements were done in duplicate at Linco Diagnostics (St Charles, Mo).

Cell Culture

Primary murine PASMCs were isolated from apoE$^{-/-}$ and C57Bl/6 mice using a modified elastase/collagenase digestion protocol as previously described.[36] Murine PASMCs were grown to 70% confluence and cultured in starvation media (DMEM, 0.1% FBS, 100 U/mL penicillin, 0.1 mg/mL streptomycin) for 24 hours. Recombinant apoE (Chemicon International, Temecula, Calif) and adiponectin (BioVision, Mountain View, Calif) were added to quiescent cells 30 minutes before mitogenic stimulation with PDGF-BB (R&D Systems, Minneapolis, Minn).

Cell Proliferation Assays

For cell counts, PASMCs were seeded at 2.5×10^4 cells per well of a 24-well plate in growth medium and allowed to adhere overnight. The medium was removed, and the cells were washed 3 times with PBS and incubated in starvation media for 24 hours, followed by PDGF-BB stimulation (20 ng/mL) for 0 and 72 hours. Cells were then washed with PBS, trypsinized, resuspended, and counted in a hemacytometer.

Statistical Analysis

Values from multiple experiments are expressed as mean±SEM. Using the Kohmogorov-Smirnov test and larger data sets from previous studies, we could show that the measured values were approximately normally distributed. Statistical significance was determined using 1-way ANOVA, followed by Bonferroni's multiple-comparison test unless stated otherwise. A value of $P<0.05$ was considered significant. The significance of our data also was confirmed by the nonparametric Mann-Whitney test. The number in each group is indicated in the column graphs and in the figure legends. For some of the metabolic measurements such as blood glucose, which did not require invasive blood draws, a larger number of animals could be assessed, resulting in minor unevenness in the numbers reported.

All authors had full access to and take full responsibility for the integrity of the data. All authors have read and agree to the manuscript as written.

Results

ApoE$^{-/-}$ and C57Bl/6 Mice on Regular Chow Have Similar RVSPs and RV Mass

First, we assessed 15-week-old male and female apoE$^{-/-}$ mice on regular chow for the presence and severity of PAH. Values of RVSP, a measure of PAH, and of RV/LV+septum ratio, a measure of RVH, were similar in apoE$^{-/-}$ and C57Bl/6 control mice. Moreover, no significant differences were observed in RVSP or RV/LV+septum ratio between genders of either genotype (Table 1).

ApoE$^{-/-}$ Mice on HF Diet Develop PAH

An 11-week HF diet treatment did not significantly increase RVSP in 15-week old C57Bl/6 mice (Table 1). In contrast, apoE$^{-/-}$ mice on HF diet for the same duration developed PAH as judged by significant elevation in RVSP, with males having higher values than females (Figure 1A and Table 1). In addition, only male apoE$^{-/-}$ mice on HF diet had RVH and enhanced peripheral PA muscularization (Figure 1B and 1C) compared with C57Bl/6 controls ($P<0.001$). A direct comparison revealed a more severe PAH phenotype in the male versus female apoE$^{-/-}$ mice on HF diet in that RVSP (28.9 versus 24.9 mm Hg; $P=0.0014$), RVH (RV/LV+septum ratio, 0.41 versus 0.29; $P=0.0093$), and peripheral muscularization (47.8 versus 35.4%; $P=0.0371$) were significantly greater (Figure 1A through 1C, unpaired 2-tailed *t* test). RV systolic function (RV dP/dtmax) was augmented in apoE$^{-/-}$ mice of both genders and reflected the elevated RVSP compared with C57Bl/6 controls (Table 1). RV diastolic function (RV dP/dtmin) was greater in both male (trend) and female ($P<0.05$) apoE$^{-/-}$ mice compared with C57Bl/6 mice of the same gender. Systemic blood pressure, cardiac output, LV function (indicated by LV end-diastolic pressure of 2 to 5 mm Hg), and hematocrit were similar in both genotypes (Table 1). Thus, the elevation of RVSP in apoE$^{-/-}$ compared with C57Bl/6 mice likely reflected an elevation in pulmonary vascular resistance.

PA Atherosclerosis in the ApoE$^{-/-}$ Mice Does Not Cause Significant PA Stenosis

Further studies were carried out to determine whether apoE$^{-/-}$ mice on HF diet developed, in addition to neomuscularization of peripheral PAs, occlusive atheroma accounting for the elevated RVSP and RVH compared with C57Bl/6 mice. Micro-CT imaging of barium-injected lungs revealed an irregularly shaped main PA vessel wall in male and female apoE$^{-/-}$ mice on HF diet but excluded PA branch stenosis as contributing to the RVSP elevation (Figure 1F and 1G). This feature was associated with nonocclusive atherosclerotic lesions only in large intrapulmonary arteries (diameter ≥500 μm) in apoE$^{-/-}$ mice of both genders on HF diet (see Figure I in the online Data Supplement). Atherosclerotic lesions were neither seen in C57Bl/6 control mice on HF diet nor in mice of both genotypes on regular chow.

Insulin Resistance Is Associated With More Severe PAH in Male ApoE$^{-/-}$ Mice

We focused our attention on possible differences in the lipid profile and markers of insulin resistance associated with the more severe PAH phenotype in apoE$^{-/-}$ versus C57Bl/6 mice, particularly in male versus female apoE$^{-/-}$ mice. Higher plasma cholesterol (mainly non–high-density lipoprotein cholesterol) was observed in male and female apoE$^{-/-}$ mice compared with C57Bl/6 controls on HF diet. In addition, apoE$^{-/-}$ mice had moderately higher triglyceride levels that were similar in male and female apoE$^{-/-}$ mice and independent of the diet (Tables I and II in the online Data Supplement). However, only in male apoE$^{-/-}$ and not female apoE$^{-/-}$ mice on HF diet did we observe features consistent with insulin resistance (ie, elevated fasting blood glucose and insulin levels), compared with C57Bl/6 controls (Figure 2).

Because of the concordance of insulin resistance and the more severe PAH phenotype in male versus female apoE$^{-/-}$ mice, we investigated whether the females had higher plasma levels of the insulin-sensitizing adipocytokines adiponectin and leptin. Although the HF diet resulted in a marked increase in adiponectin and leptin levels in control C57Bl/6 mice of both genders, this marked upregulation was absent in apoE$^{-/-}$ mice (for adiponectin, see Figure 2A and 2B; for leptin, see Tables I and II in the online Data Supplement). It is therefore possible that the release of adiponectin and leptin from adipocytes in response to HF diet is to some extent apoE dependent. However, female mice of both genotypes had

TABLE 1. RVSP and Heart Weight Measurements in C57Bl/6 (Control) and ApoE$^{-/-}$ Mice on Regular Chow and Hemodynamic, Echocardiographic, and Heart Weight Measurements in C57Bl/6 (Control) and ApoE$^{-/-}$ Mice on HF Diet

	Control Males	ApoE$^{-/-}$ Males	Control Females	ApoE$^{-/-}$ Females	*P*	n
Mice on regular chow						
RVSP, mm Hg	20.6±0.8	23.2±0.6	19.7±1.5	22.5±0.8		4–5
RV, mg	26.5±1.3‡	24.9±1.4†	17.9±0.9	18.1±0.7	CM vs CF,‡ AM vs AF†	4–5
RV/LV+S	0.26±0.01	0.30±0.01	0.26±0.01	0.27±0.02		4–5
LV+S, mg	101.0±2.7‡	84.6±4.3*	69.2±2.7	68.6±2.2	CM vs AM,* CM vs CF,‡ AM vs AF*	4–5
Mice on HF diet						
Hemodynamics						
RVSP, mm Hg	20.6±0.5	28.9±0.6‡	20.5±0.9	24.9±0.6†	AM vs CM,‡ AM vs AF,† AF vs CF†	4–5
RV dP/dtmax, mm Hg/s	1132±82	1754±62*	950±206	1513±125*	AM vs CM,* AF vs CF*	4–5
RV dP/dtmin, mm Hg/s	−951±86	−1396±72	−753±173	−1279±96*	AF vs CF*	4–5
Systolic BP, mm Hg	92±1.9	99±2.6	83±5.4	96±1.3		4–5
MAP, mm Hg	79±1.4	85±2.9	77±3.5	86±1.5		4–5
Diastolic BP, mm Hg	73±1.6	77±4.4	71±3.4	80±1.8		4–5
LVEDP, mm Hg	2.4±0.5	2.8±0.2	2.5±0.3	2.7±1.2		4–5
Echocardiography						4–5
Heart rate, bpm	398±29.6	370±22.5	447±27	408±36		4–5
EF, %	74±0.7	77.6±5.4	70.2±2.4	85.7±2.6*	AF vs CF*	4–5
FS, %	37.5±0.6	42.0±6.2	34.3±1.9	51.2±2.9†	AF vs CF†	4–5
CO, mL/min)	30.0±2.1	29.1±5.5	24.3±2.2	24.7±3.8		4–5
LVIDD, mm	3.4±0.06	3.4±0.28	3.1±0.02	3.0±0.13		4–5
LVISD, mm	2.1±0.02	2.0±0.33	2.0±0.06	1.5±0.16		4–5
Heart weight						
RV, mg	19.5±1.3	33.0±4.0†	18.1±0.5	18.0±1.1	AM vs CM,† AM vs AF†	4
RV/LV+S	0.25±0.02	0.41±0.03‡	0.24±0.01	0.29±0.01	AM vs CM,‡ AM vs AF†	4
LV+S, mg	79.3±0.3	81.3±8.3*	74.8±1.4	60.9±2.0	AM vs AF*	4
Blood						
HCT, %	47.1±0.8	44.5±0.9	42.4±2.6	44.8±0.8		4–5
WBC, 10^3 cells/μL	2.1±0.5	1.4±0.4	2.3±0.6	1.2±0.2		4–5

Fifteen-week-old male and female mice on regular chow or HF diet for 11 weeks in normoxia. Statistically significant differences between C57Bl/6 (control) and apoE$^{-/-}$ mice of either gender and between genders of the same genotype are indicated. Values are mean±SEM. CM indicates control males; AM, apoE$^{-/-}$ males; CF, control females; AF, apoE$^{-/-}$ females; S, septum; BP, blood pressure; MAP, mean arterial pressure; LVEDP, LV end-diastolic pressure (determined by left carotid artery/LV catheterization); EF, ejection fraction; FS, fractional shortening; CO, cardiac output; LVIDD, LV end-diastolic inner diameter; LVISD, LV end-systolic inner diameter; HCT, hematocrit; and WBC, white blood cell count.

*$P<0.05$; †$P<0.01$; ‡$P<0.001$.

~50% higher plasma adiponectin levels than their male counterparts (Figure 2A and 2B). Gender differences in leptin levels were difficult to ascertain because of considerable variability in the individual values (Tables I and II in the online Data Supplement). Because testosterone inhibits the secretion of adiponectin in adipocytes,[35] we hypothesized that higher adiponectin levels, in association with lack of insulin resistance, may account for the less severe pulmonary vascular phenotype in female apoE$^{-/-}$ mice on a HF diet.

PPARγ Activation Elevates Plasma Adiponectin, Improves Insulin Sensitivity, and Reverses PAH

On the basis of these data, we reasoned that the presence of PAH may be determined by the inability to sufficiently raise adiponectin levels in association with a HF diet (Figure 2A and 2B) and that the severity of the disease may be a function of the degree of hyperinsulinemia and hyperglycemia (Figure 2C through 2F). We therefore hypothesized that treating the pulmonary hypertensive, insulin-resistant male apoE$^{-/-}$ mice with a PPARγ agonist to increase plasma adiponectin and improve insulin sensitivity might arrest disease progression or reverse PAH. Thus, we treated 15-week-old male apoE$^{-/-}$ and C57Bl/6 control mice on a HF diet with rosiglitazone 10 mg $\cdot$ kg^{-1} $\cdot$ d^{-1} incorporated into their food. The effects of both 4- and 10-week treatments on RVSP, RVH, and metabolic features were assessed. Four-week treatment with rosiglitazone resulted in much higher plasma adiponectin levels in C57Bl/6 control (5-fold) and apoE$^{-/-}$ (8-fold) mice compared with untreated animals of the same genotype (Figure 3A). The higher plasma adiponectin in treated versus untreated apoE$^{-/-}$ mice was associated with lower blood glucose (control level), indicating improved insulin sensitivity in apoE$^{-/-}$ mice treated with rosiglitazone (Figure 3A, 3C, and 3E).

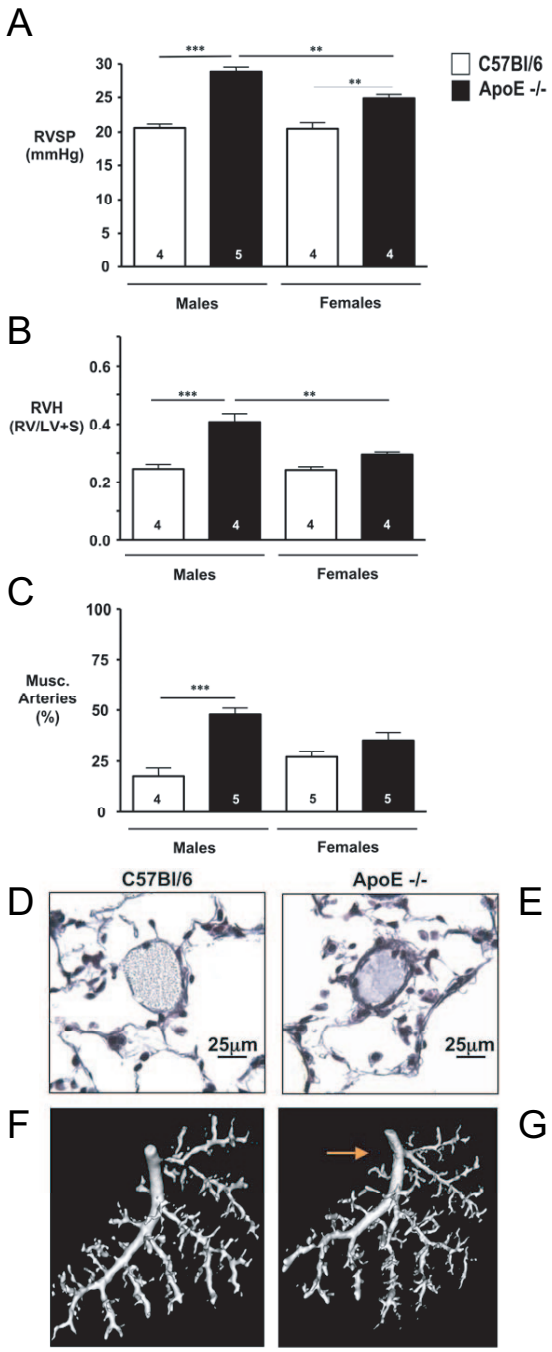

Figure 1. Pulmonary hypertension in apoE$^{-/-}$ mice on HF diet in normoxia. Fifteen-week-old male mice on HF diet for 11 weeks. A, RVSP. B, RVH, measured as ratio of the weight of the right ventricle (RV) to that of left ventricle (LV) plus septum (S). C, Muscularization of alveolar wall arteries. Bars represent mean±SEM (n=4–5 as indicated in column graphs). *P<0.05; **P<0.01; and ***P<0.001. D and E, Representative photomicrographs of lung tissue (stained by Movat pentachrome) of 15-week-old male mice on HF diet showing a typical nonmuscular peripheral alveolar artery in a C57B1/6 mouse (D). A similar section in the apoE$^{-/-}$ mouse shows an alveolar wall artery surrounded by a rim of muscle (E). F and G, Micro-CT imaging of barium-injected pulmonary arteries (PA). Representative irregularly shaped main PA wall is observed in apoE$^{-/-}$ mouse on HF diet (arrow), but significant PA stenoses are excluded in C57B1/6 control (F) and apoE$^{-/-}$ mice (G).

RVSP in untreated C57Bl/6 and apoE$^{-/-}$ mice over this period of time was not significantly different from the baseline values observed in the 15-week-old mice of the initial study (see Figure 1A compared with Figure 3B and Table 1 versus Table 2). In addition to the induction of plasma adiponectin and improvement of insulin sensitivity, a 4-week course of rosiglitazone treatment resulted in lower RVSP, RV mass (RV/LV+septum ratio), and percentage of muscularized arteries at the alveolar wall level that were similar to those in C57Bl/6 control mice (Figure 3B, 3D, and 3F). Because we started treatment at a time when the insulin-resistant male apoE$^{-/-}$ mice already had elevated RVSP, RVH, and peripheral PA muscularization, our findings indicate that we had induced regression of PAH. Rosiglitazone given for 4 weeks caused no significant differences in systemic blood pressure, heart rate, LV systolic function (fractional shortening, ejection fraction), cardiac output, and RV systolic and diastolic function (Table 2). Other measurements such as hematocrit and white blood cell count also were similar in treated and untreated animals. There was, however, a tendency for rosiglitazone to cause mild LV dilatation and increased LV mass in both C57Bl/6 control and apoE$^{-/-}$ mice (Table 2).

All the features described above were sustained after a 10-week rosiglitazone treatment period, suggesting that the effect was not transient. However, at this time point, hematocrit was slightly lower in both control and apoE$^{-/-}$ mice treated with rosiglitazone (Table III in the online Data Supplement). Decreased hematocrit and a tendency for LV dilatation and increased LV mass have been previously reported in the clinical setting as minor side effects of rosiglitazone treatment.[37]

Rosiglitazone Does Not Regulate Plasma ET-1 and ADMA in ApoE$^{-/-}$ Mice

ET-1 and ADMA were measured in blood plasma after a 4-week treatment with rosiglitazone. Plasma ET-1 levels were lower in treated than in untreated C57Bl/6 mice. However, ET-1 levels were lower in apoE$^{-/-}$ compared with C57Bl/6 mice and were not affected by rosiglitazone. ADMA levels were in the normal murine range, not different between genotypes, and not altered by rosiglitazone treatment (Table 2).

Recombinant ApoE and Adiponectin Inhibit PASMC Proliferation

To support possible roles of apoE and adiponectin in protecting against the development of PAH, we showed that both proteins inhibit PDGF-BB–induced proliferation of PASMCs harvested from both C57Bl/6 control and apoE$^{-/-}$ mice (Figure 4A and 4B).

Discussion

Although a link between insulin resistance and systemic cardiovascular disease is evident in both clinical[2] and experimental studies,[3,33] this report is the first indication that there may be a possible link with PAH. If insulin resistance does contribute to the pathobiology of PAH in humans, it will be an extremely important relationship owing to the steadily increasing number of children, adolescents,[1] and adults[2] with

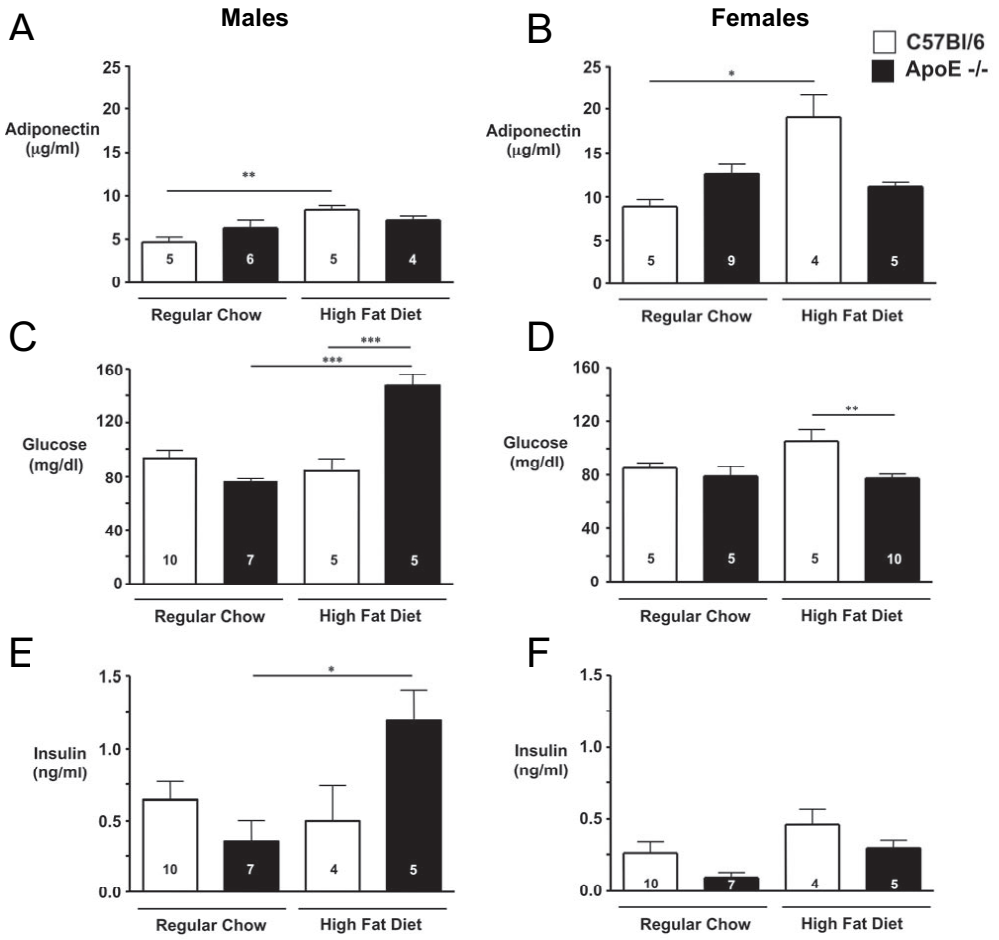

Figure 2. Male but not female apoE$^{-/-}$ mice develop insulin resistance and hypoadiponectinemia on HF diet. Plasma adiponectin (A,B), blood glucose (C, D), and plasma insulin (E, F). Overnight-starved 15-week-old male (A, C, E) and female (B, D, F) C57Bl/6 and apoE$^{-/-}$ mice, on regular chow or HF diet for 11 weeks. Note that C57Bl/6 mice but not apoE$^{-/-}$ mice of both genders upregulate their adiponectin levels when exposed to HF diet. Bars represent mean±SEM (n=5–10 as indicated in column graphs). *$P<0.05$; **$P<0.01$; and ***$P<0.001$.

the metabolic syndrome, which includes insulin resistance as a key element.

ApoE$^{-/-}$ mice of both genders on HF showed atheroma on histology and on micro-CT, affecting the large PAs in a nonocclusive manner. Similar features have been described in pathological specimens of adult patients with PAH.[38] However, the cholesterol levels and the presence of atheroma were similar in male and female apoE$^{-/-}$ mice, but only male apoE$^{-/-}$ developed insulin resistance and severe PAH (ie, a combination of marked RVSP elevation, RVH, and enhanced peripheral PA muscularization). We therefore suggest that apoE deficiency, hypoadiponectinemia, and the related insulin resistance, rather than pulmonary atherosclerosis itself, were the major causes of PAH.

The level of PAH seen in our model, with an RVSP baseline elevation of 7 to 9 mm Hg over controls for males on a HF diet in normoxia, was not based on LV dysfunction and is comparable to[39] or even greater than[40,41] that in the relatively few murine models of PAH described to date. The sole exception is the inducible vascular SMC dominant-negative bone-morphogenetic protein receptor II (BMP-RII) transgenic mouse. However, values in the control mice of this BMP-RII model also were quite elevated, consistent with the relative "hypoxia" at Denver altitude.[42]

The likely mechanism by which apoE deficiency leads to the development of PAH appears to be facilitated by PDGF-BB signaling. From studies in systemic vascular SMCs, we know that PDGF-BB signaling in SMCs is suppressed when apoE binds to the low-density lipoprotein receptor–related protein (LRP), thereby initiating endocytosis and degradation of the LRP–PDGFR-β–PDGF-BB complex.[28–30] We have shown here that PDGF-BB–induced proliferation also is suppressed by apoE in PASMCs, suggesting that a similar mechanism may be present in the pulmonary vasculature. In diabetic apoE$^{-/-}$ mice, PDGFR-β signaling is increased in vascular SMCs, and systemic vascular disease can be reversed by the PDGFR tyrosine kinase inhibitor imatinib.[32] We[40] and others[21] have shown that blockade of tyrosine kinase activity selective to the epidermal growth factor receptor[40] or the PDGFR[21] reverses experimental PAH and vascular remodeling caused by the toxin monocrotaline in rats.

In association with insulin resistance, the male mice (apoE$^{-/-}$ and C57Bl/6) had lower levels of adiponectin than

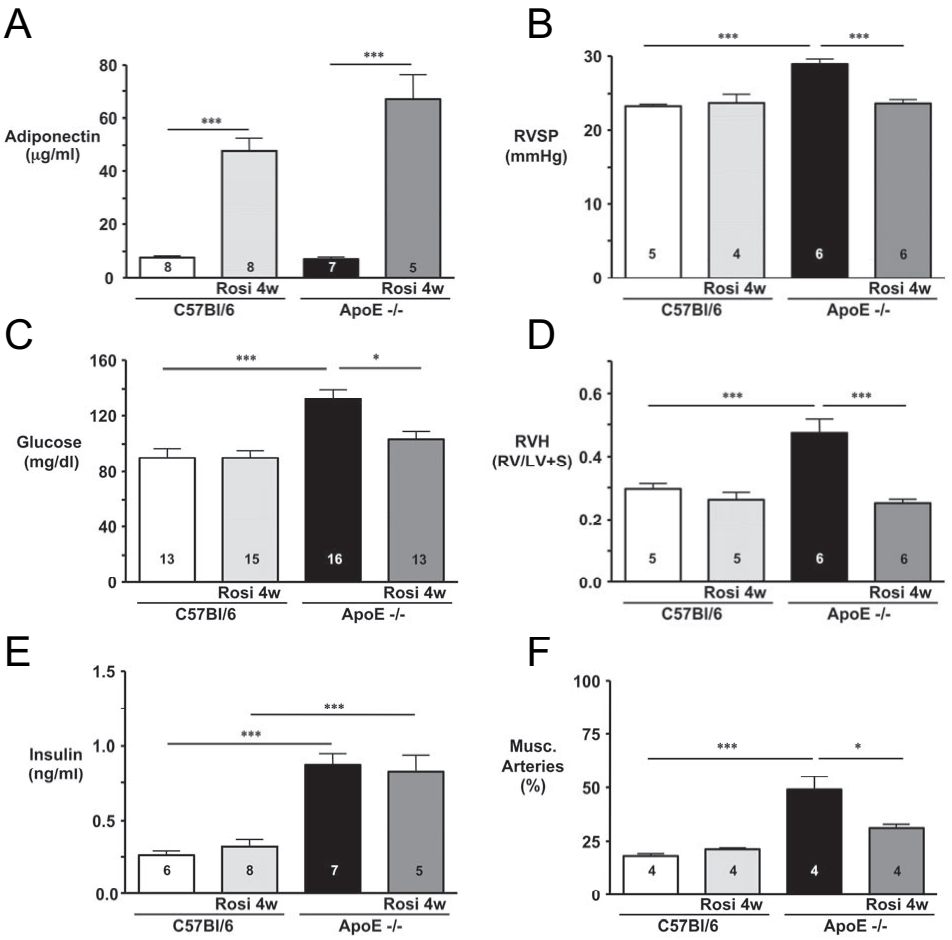

Figure 3. Four-week treatment with the PPARγ agonist rosiglitazone reverses PAH, increases plasma adiponectin, and induces insulin sensitivity. Measurements of plasma adiponectin (A), blood glucose (C) and plasma insulin (E), RVSP (B), RVH (D), and muscularization of alveolar wall arteries (F). Nineteen-week-old male C57Bl/6 and apoE$^{-/-}$ mice, all on HF diet for 15 weeks, were used. Bars represent mean±SEM (n=4–16 as indicated in column graphs). *$P<0.05$; **$P<0.01$; and ***$P<0.001$.

the female mice. This finding is in keeping with a recent study demonstrating that testosterone inhibits the secretion of adiponectin in adipocytes.[35] Adiponectin reverses insulin resistance[26] and is independently associated with a reduced risk of type 2 diabetes mellitus in apparently healthy individuals.[43] Moreover, the high-molecular-weight form of adiponectin binds PDGF-BB, thereby reducing PDGF-BB bioavailability[31] and mitogenic postreceptor function in vascular SMCs.[27] Adiponectin has been shown to be a transcriptional target of PPARγ in adipocytes.[7] Because previous studies used the PPARγ agonist rosiglitazone to suppress intimal thickening in the apoE$^{-/-}$ mouse,[44] we reasoned that it might also be effective in preventing disease progression or reversing PAH. Indeed, treatment of male apoE$^{-/-}$ mice with rosiglitazone increased plasma adiponectin, improved insulin sensitivity, and led to sustained regression of PAH, RVH, and abnormal muscularization of distal PAs. The source of adiponectin in our animal model is likely from visceral and subcutaneous as well as perivascular adipocytes.[17] To further support a mechanistic relationship between apoE and adiponectin deficiency on the one hand and PAH with enhanced muscularization of peripheral arteries on the other, we showed that both recombinant apoE and adiponectin inhibited PDGF-BB–induced proliferation of cultured murine wild-type and apoE$^{-/-}$ PASMCs.

In addition to elevating adiponectin levels and thus causing sequestration of PDGF-BB, PPARγ activation blocks PDGF gene expression[45] and PDGF-BB–mediated systemic SMC proliferation and migration.[33,34] This is likely to occur via inhibition of phosphorylated extracellular-regulated kinase nuclear translocation[46] and/or induction of protein phosphatases[47] that reduce phosphorylated extracellular-regulated kinase. Furthermore, PPARγ induces expression of LRP,[48] the receptor necessary for apoE-mediated suppression of PDGF-BB signaling.[28–30] By blocking important survival pathways downstream of activated PDGFR-β (eg, PI3K),[25] rosiglitazone could also induce apoptosis of proliferating vascular cells.[33,49]

We considered the possibility that PPARγ activation might impair the expression of ET-1[15] and the endogenous nitric oxide synthase inhibitor ADMA,[18] both of which have previously been linked to clinical PAH[16,19] and insulin resistance.[17,18] However, although it is not surprising that rosiglitazone decreased ET-1 levels in the C57Bl/6 mice, we expected the apoE$^{-/-}$ mice to have higher levels of ET-1 under control conditions. In the present study, however, we

TABLE 2. Hemodynamic, Echocardiographic, Heart Weight, Hematocrit, and Other Blood Measurements in Male C57Bl/6 (Control) and ApoE$^{-/-}$ Mice After Treatment With Rosiglitazone for 4 Weeks

Parameter	Control	Control Rosi	ApoE$^{-/-}$	ApoE$^{-/-}$ Rosi	*P*	n
Hemodynamics						
RVSP, mm Hg	23.3±0.2	23.8±1.2	28.9±0.6‡	23.7±0.5‡	A vs C,‡ AR vs A‡	4–6
RV dP/dtmax, mm Hg/s	1543±59	1762±170	1489±154	1668±155		4–6
RV dP/dtmin, mm Hg/s	−1207±104	−1575±198	−1665±147	−1569±128		4–6
Systolic BP, mm Hg	103±3.4	95±2.4	108±4.0	100±2.3		7–8
MAP, mm Hg	85±3.3	78±2.6	90±4.2	80.6±3.2		7–8
Diastolic BP, mm Hg	75±3.3	70±2.8	81±4.4	71±3.9		7–8
Echocardiography						
Heart rate, bpm	369±15.9	356±24.8	295±10.5*	334±16.6	A vs C*	5–7
EF, %	70.0±1.3	70.1±2.3	69.8±1.0	64.4±1.1		5–7
FS, %	34.2±1.0	34.5±1.8	34.1±0.7	30.2±0.8		5–7
CO, mL/min	39.0±3.2	48.7±4.6	32.0±2.6	40.8±2.5		5–7
LVIDD, mm	3.91±0.07	4.27±0.08*	3.97±0.11	4.20±0.06	CR vs C*	5–7
LVISD, mm	2.59±0.04	2.80±0.11	2.63±0.10	2.96±0.07		5–7
LVPWd, mm	0.60±0.03	0.75±0.08	0.72±0.05	0.64±0.06		5–7
IVSd, mm	0.61±0.05	0.58±0.04	0.70±0.06	0.62±0.04		5–7
Heart weight						
RV, mg	27.2±1.2	30.8±3.7	39.5±5.6	26.2±1.7		5–6
RV/LV+S	0.30±0.02	0.26±0.02	0.47±0.04†	0.25±0.01‡	A vs C,† AR vs A‡	5–6
LV+S, mg	92.2±1.4	116.8±6.2*	82.5±6.4	103.5±3.7*	CR vs C,* AR vs A*	5–6
Blood						
HCT, %	45.7±3.5	41.1±2.5	49.7±1.3	51.2±1.5*	AR vs CR*	5–7
WBC, $10^3/\mu$L	5.5±2.2	3.8±1.2	2.0±0.4	3.6±1.0		5–7
ET-1, fmol/L	35.8±5.5	12.5±1.9	11.5±0.9*	14.5±1.4*	A vs C,* CR vs C*	3–5
ADMA, μmol/L	0.24±0.02	0.29±0.05	0.22±0.02	0.21±0.02		4–7

Nineteen-week-old male mice on HF diet for 15 weeks, untreated or treated with rosiglitazone for 4 weeks, in normoxia. Statistically significant differences between C57Bl/6 (control) and apoE$^{-/-}$ mice of either group and between treated and untreated mice of the same genotype are indicated. ET-1 and ADMA were measured in blood plasma. Systemic blood pressure was measured at 24 weeks of age (ie, after treatment with rosiglitazone for 9 weeks). Values are mean±SEM. C indicates control; CR, control treated with rosiglitazone (Rosi); A, ApoE$^{-/-}$; AR, ApoE$^{-/-}$ treated with rosiglitazone; BP, blood pressure; MAP, mean arterial pressure; EF, ejection fraction; FS, fractional shortening; CO, cardiac output; LVIDD, LV end-diastolic inner diameter; LVISD, LV end-systolic inner diameter; LVPWd, LV end-diastolic posterior wall thickness; IVSd, end-diastolic interventricular septum thickness; S, septum; HCT, hematocrit; and WBC, white blood cell count.

*$P<0.05$; †$P<0.01$; ‡$P<0.001$.

could not relate the reversal of PAH with rosiglitazone to a decrease in either ET-1 or ADMA plasma level.

Recently, we made the interesting observation that BMP-2 induces nuclear shuttling and DNA binding of PPARγ in human PASMCs.[50] Loss-of-function mutations in the BMP-RII gene frequently occur in cases of familial and idiopathic PAH, and our preliminary results suggest that this would decrease endogenous PPARγ activity. Hence, a strategy

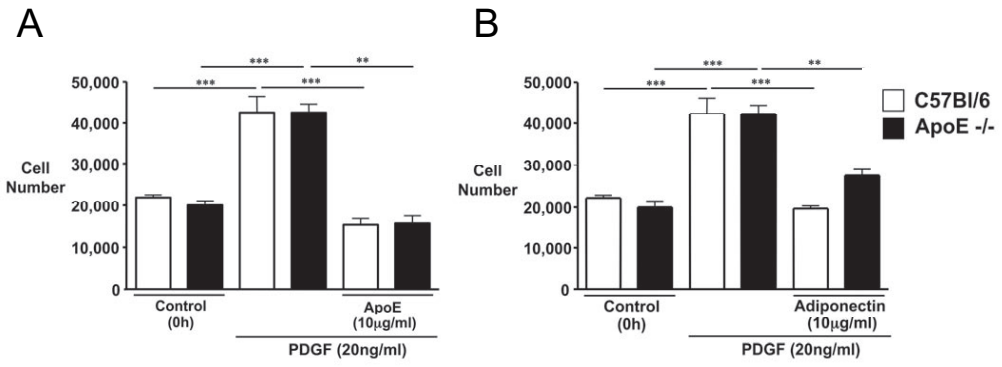

Figure 4. Recombinant apoE (A) and adiponectin (B) inhibit PDGF-BB–induced (20 ng/mL) proliferation of murine PASMC harvested both from C57Bl/6 and apoE$^{-/-}$ mice. Bars represent mean±SEM (n=3). *$P<0.05$; **$P<0.01$; and ***$P<0.001$.

aimed at activating PPARγ could reverse the PAH phenotype. However, the inheritance pattern of BMPR-II is that of a dominant gene with low penetrance in that only ≈20% of affected family members develop the disease.[51] This underscores the importance of environmental modifiers like insulin resistance that could potentiate BMP-RII dysfunction. It also is possible that abnormalities in downstream effectors of BMP-2 such as PPARγ and its targets may contribute to the development of disease.

The present study identified several new factors that may be involved in the pathogenesis of PAH and a potential treatment. We acknowledge that it is difficult to separate the effects of apoE deficiency and insulin resistance in our animal model and to extrapolate the potential impact of a successful experimental treatment to human disease. Therefore, it is important to examine whether insulin resistance, hyperlipidemia, impaired apoE function, and low adiponectin levels are risk factors for the progression of PAH in humans. It will also be of interest to investigate a relationship between molecular mechanisms that underlie insulin resistance, apoE and adiponectin levels, and known PAH pathways (eg, those downstream of BMP-RII). Taken together, these data might suggest a beneficial effect from the addition of PPARγ agonists to the treatment regimen for PAH patients.

Acknowledgments

We thank Tim Doyle for help with micro-CT imaging and Grant Hoyt for excellent technical assistance.

Sources of Funding

This work was supported by NIH (1-R01-HL074186–01) and the Dwight and Vera Dunlevie Endowed Professorship (Dr Rabinovitch), a postdoctoral fellowship from the American Heart Association/Pulmonary Hypertension Association (0425943H to Dr Hansmann), NIH grant HL876445–03 (Dr Wagner), and a predoctoral fellowship from Boehringer Ingelheim Funds (S. Schellong).

Disclosures

None.

References

1. Weiss R, Dziura J, Burgert TS, Tamborlane WV, Taksali SE, Yeckel CW, Allen K, Lopes M, Savoye M, Morrison J, Sherwin RS, Caprio S. Obesity and the metabolic syndrome in children and adolescents. *N Engl J Med*. 2004;350:2362–2374.
2. Eckel RH, Grundy SM, Zimmet PZ. The metabolic syndrome. *Lancet*. 2005;365:1415–1428.
3. Lazar MA. The humoral side of insulin resistance. *Nat Med*. 2006;12:43–44.
4. Ameshima S, Golpon H, Cool CD, Chan D, Vandivier RW, Gardai SJ, Wick M, Nemenoff RA, Geraci MW, Voelkel NF. Peroxisome proliferator-activated receptor gamma (PPARgamma) expression is decreased in pulmonary hypertension and affects endothelial cell growth. *Circ Res*. 2003;92:1162–1169.
5. He W, Barak Y, Hevener A, Olson P, Liao D, Le J, Nelson M, Ong E, Olefsky JM, Evans RM. Adipose-specific peroxisome proliferator-activated receptor gamma knockout causes insulin resistance in fat and liver but not in muscle. *Proc Natl Acad Sci U S A*. 2003;100:15712–15717.
6. Hevener AL, He W, Barak Y, Le J, Bandyopadhyay G, Olson P, Wilkes J, Evans RM, Olefsky J. Muscle-specific PPARg deletion causes insulin resistance. *Nat Med*. 2003;9:1491–1497.
7. Lehrke MM, Lazar MAMA. The many faces of PPARgamma. *Cell*. 2005;123:993–999.
8. Geraci MW, Moore M, Gesell T, Yeager ME, Alger L, Golpon H, Gao B, Loyd JE, Tuder RM, Voelkel NF. Gene expression patterns in the lungs of patients with primary pulmonary hypertension: a gene microarray analysis. *Circ Res*. 2001;88:555–562.
9. Greenow K, Pearce NJ, Ramji DP. The key role of apolipoprotein E in atherosclerosis. *J Mol Med*. 2005;83:329–342.
10. Combs CK, Johnson DE, Karlo JC, Cannady SB, Landreth GE. Inflammatory mechanisms in Alzheimer's disease: inhibition of beta-amyloid-stimulated proinflammatory responses and neurotoxicity by PPARgamma agonists. *J Neuroscience*. 2000;20:558–567.
11. Humbert M, Monti G, Brenot F, Sitbon O, Portier A, Grangeot-Keros L, Duroux P, Galanaud P, Simonneau G, Emilie D. Increased interleukin-1 and interleukin-6 serum concentrations in severe primary pulmonary hypertension. *Am J Respir Crit Care Med*. 1995;151:1628–1631.
12. Imaizumi T, Matsumiya T, Tamo W, Shibata T, Fujimoto K, Kumagai M, Yoshida H, Cui XF, Tanji K, Hatakeyama M, Wakabayashi K, Satoh K. 15-Deoxy-D12,14-prostaglandin J2 inhibits CX3CL1/fractalkine expression in human endothelial cells. *Immunol Cell Biol*. 2002;80:531–536.
13. Balabanian K, Foussat A, Dorfmuller P, Durand-Gasselin I, Capel F, Bouchet-Delbos L, Portier A, Marfaing-Koka A, Krzysiek R, Rimaniol AC, Simonneau G, Emilie D, Humbert M. CX(3)C chemokine fractalkine in pulmonary arterial hypertension. *Am J Respir Crit Care Med*. 2002;165:1419–1425.
14. Ikeda Y, Yonemitsu Y, Kataoka C, Kitamoto S, Yamaoka T, Nishida K, Takeshita A, Egashira K, Sueishi K. Anti-monocyte chemoattractant protein-1 gene therapy attenuates pulmonary hypertension in rats. *Am J Physiol Heart Circ Physiol*. 2002;283:H2021–H2028.
15. Martin-Nizard F, Furman C, Delerive P, Kandoussi A, Fruchart JC, Staels B, Duriez P. Peroxisome proliferator-activated receptor activators inhibit oxidized low-density lipoprotein-induced endothelin-1 secretion in endothelial cells. *J Cardiovasc Pharmacol*. 2002;40:822–831.
16. Giaid A, Yanagisawa M, Langleben D, Michel RP, Levy R, Shennib H, Kimura S, Masaki T, Duguid WP, Stewart DJ. Expression of endothelin-1 in the lungs of patients with pulmonary hypertension. *N Engl J Med*. 1993;328:1732–1739.
17. Yudkin JS, Eringa E, Stehouwer CD. "Vasocrine" signalling from perivascular fat: a mechanism linking insulin resistance to vascular disease. *Lancet*. 2005;365:1817–1820.
18. Stühlinger MC, Abbasi F, Chu JW, Lamendola C, McLaughlin TL, Cooke JP, Reaven GM, Tsao PS. Relationship between insulin resistance and an endogenous nitric oxide synthase inhibitor. *JAMA*. 2002;287:1420–1426.
19. Kielstein JT, Bode-Böger SM, Hesse G, Martens-Lobenhoffer J, Takacs A, Fliser D, Hoeper MM. Asymmetrical dimethylarginine in idiopathic pulmonary arterial hypertension. *Arterioscler Thromb Vasc Biol*. 2005;25:1414–1418.
20. Humbert M, Monti G, Fartoukh M, Magnan A, Brenot F, Rain B, Capron F, Galanaud P, Duroux P, Simonneau G, Emilie D. Platelet-derived growth factor expression in primary pulmonary hypertension: comparison of HIV seropositive and HIV seronegative patients. *Eur Respir J*. 1998;11:554–559.
21. Schermuly RT, Dony EE, Ghofrani HA, Pullamsetti S, Savai R, Roth M, Sydykov A, Lai YJ, Weissmann N, Seeger W, Grimminger F. Reversal of experimental pulmonary hypertension by PDGF inhibition. *J Clin Invest*. 2005;115:2811–2821.
22. Ghofrani HA, Seeger W, Grimminger F. Imatinib for the treatment of pulmonary arterial hypertension. *N Engl J Med*. 2005;353:1412–1413.
23. Ishigami M, Swertfeger DK, Granholm NA, Hui DY. Apolipoprotein E inhibits platelet-derived growth factor-induced vascular smooth muscle cell migration and proliferation by suppressing signal transduction and preventing cell entry to G1 phase. *J Biol Chem*. 1998;273:20156–20161.
24. Campbell M, Allen WE, Silversides JA, Trimble ER. Glucose-induced phosphatidylinositol 3-kinase and mitogen-activated protein kinase-dependent upregulation of the platelet-derived growth factor-beta receptor potentiates vascular smooth muscle cell chemotaxis. *Diabetes*. 2003;52:519–526.
25. Vantler M, Caglayan E, Zimmermann WH, Baumer AT, Rosenkranz S. Systematic evaluation of anti-apoptotic growth factor signaling in vascular smooth muscle cells: only phosphatidylinositol 3′-kinase is important. *J Biol Chem*. 2005;280:14168–14176.
26. Yamauchi T, Kamon J, Waki H, Terauchi Y, Kubota N, Hara K, Mori Y, Ide T, Murakami K, Tsuboyama-Kasaoka N, Ezaki O, Akanuma Y, Gavrilova O, Vinson C, Reitman ML, Kagechika H, Shudo K, Yoda M, Nakano Y, Tobe K, Nagai R, Kimura S, Tomita M, Froguel P, Kadowaki T. The fat-derived hormone adiponectin reverses insulin resistance associated with both lipoatrophy and obesity. *Nat Med*. 2001;7:941–946.

27. Arita Y, Kihara S, Ouchi N, Maeda K, Kuriyama H, Okamoto Y, Kumada M, Hotta K, Nishida M, Takahashi M, Nakamura T, Shimomura I, Muraguchi M, Ohmoto Y, Funahashi T, Matsuzawa Y. Adipocyte-derived plasma protein adiponectin acts as a platelet-derived growth factor-BB-binding protein and regulates growth factor-induced common postreceptor signal in vascular smooth muscle cell. *Circulation*. 2002;105:2893–2898.
28. Boucher P, Gotthardt M, Li WP, Anderson RG, Herz J. LRP: role in vascular wall integrity and protection from atherosclerosis. *Science*. 2003; 300:329–332.
29. Boucher P, Gotthardt M. LRP and PDGF signaling: a pathway to atherosclerosis. *Trends Cardiovasc Med*. 2004;14:55–60.
30. Newton CS, Loukinova E, Mikhailenko I, Ranganathan S, Gao Y, Haudenschild C, Strickland DK. Platelet-derived growth factor receptor-beta (PDGFR-beta) activation promotes its association with the low density lipoprotein receptor-related protein (LRP): evidence for co-receptor function. *J Biol Chem*. 2005;280: 27872–27878.
31. Wang Y, Lam KS, Xu JY, Lu G, Xu LY, Cooper GJ, Xu A. Adiponectin inhibits cell proliferation by interacting with several growth factors in an oligomerization-dependent manner. *J Biol Chem*. 2005;280:18341–18347.
32. Lassila M, Allen TJ, Cao Z, Thallas V, Jandeleit-Dahm KA, Candido R, Cooper ME. Imatinib attenuates diabetes-associated atherosclerosis. *Arterioscler Thromb Vasc Biol*. 2004;24:935–942.
33. Marx NN, Duez HH, Fruchart JCJ-C, Staels BB. Peroxisome proliferator-activated receptors and atherogenesis: regulators of gene expression in vascular cells. *Circ Res*. 2004;94:1168–1178.
34. Law RRE, Goetze SS, Xi XXP, Jackson SS, Kawano YY, Demer LL, Fishbein MMC, Meehan WWP, Hsueh WWA. Expression and function of PPARgamma in rat and human vascular smooth muscle cells. *Circulation*. 2000;101:1311–1318.
35. Xu A, Chan KW, Hoo RL, Wang Y, Tan KC, Zhang J, Chen B, Lam M, Tse C, Cooper GJ, Lam KS. Testosterone selectively reduces the high molecular weight form of adiponectin by inhibiting its secretion from adipocytes. *J Biol Chem*. 2005;280:18073–18080.
36. Fouty BW, Grimison B, Fagan KA, Le Cras TD, Harral JW, Hoedt-Miller M, Sclafani RA, Rodman DM. p27(Kip1) is important in modulating pulmonary artery smooth muscle cell proliferation. *Am J Respir Cell Mol Biol*. 2001;25:652–658.
37. St John Sutton M, Rendell M, Dandona P, Dole JF, Murphy K, Patwardhan R, Patel J, Freed M. A comparison of the effects of rosiglitazone and glyburide on cardiovascular function and glycemic control in patients with type 2 diabetes. *Diabetes Care*. 2002;25:2058–2064.
38. Wagenvoort CA. Pulmonary atherosclerosis. In: Wagenvoort CA, Heath D, Edwards JE, eds. *The Pathology of the Pulmonary Vasculature*. Springfield, Ill: Charles C Thomas; 1964:58–59.
39. Guignabert C, Izikki M, Tu LI, Li Z, Zadigue P, Barlier-Mur AM, Hanoun N, Rodman D, Hamon M, Adnot S, Eddahibi S. Transgenic mice overexpressing the 5-hydroxytryptamine transporter gene in smooth muscle develop pulmonary hypertension. *Circ Res*. 2006;98:1323–1330.
40. Merklinger SL, Jones PL, Martinez EC, Rabinovitch M. Epidermal growth factor receptor blockade mediates smooth muscle cell apoptosis and improves survival in rats with pulmonary hypertension. *Circulation*. 2005;112:423–431.
41. Long L, MacLean MR, Jeffery TK, Morecroft I, Yang X, Rudarakanchana N, Southwood M, James V, Trembath RC, Morrell NW. Serotonin increases susceptibility to pulmonary hypertension in BMPR2-deficient mice. *Circ Res*. 2006;98:818–827.
42. West J, Fagan K, Steudel W, Fouty B, Lane K, Harral J, Hoedt-Miller M, Tada Y, Ozimek J, Tuder R, Rodman DM. Pulmonary hypertension in transgenic mice expressing a dominant-negative BMPRII gene in smooth muscle. *Circ Res*. 2004;94:1109–1114.
43. Spranger J, Kroke A, Möhlig M, Bergmann MM, Ristow M, Boeing H, Pfeiffer AF. Adiponectin and protection against type 2 diabetes mellitus. *Lancet*. 2003;361:226–228.
44. Phillips JW, Barringhaus KG, Sanders JM, Yang Z, Chen M, Hesselbacher SS, Czarnik AC, Ley K, Nadler J, Sarembock IJ. Rosiglitazone reduces the accelerated neointima formation after arterial injury in a mouse injury model of type 2 diabetes. *Circulation*. 2003;108:1994–1999.
45. Zhang J, Fu M, Zhao L, Chen YE. 15-Deoxy-prostaglandin J(2) inhibits PDGF-A and -B chain expression in human vascular endothelial cells independent of PPAR gamma. *Biochem Biophys Res Commun*. 2002;298:128–132.
46. Goetze S, Kintscher U, Kim S, Meehan WP, Kaneshiro K, Collins AR, Fleck E, Hsueh WA, Law RE. Peroxisome proliferator-activated receptor-gamma ligands inhibit nuclear but not cytosolic extracellular signal-regulated kinase/mitogen-activated protein kinase-regulated steps in vascular smooth muscle cell migration. *J Cardiovasc Pharmacol*. 2001;38:909–921.
47. Wakino S, Kintscher U, Liu Z, Kim S, Yin F, Ohba M, Kuroki T, Schonthal AH, Hsueh WA, Law RE. Peroxisome proliferator-activated receptor gamma ligands inhibit mitogenic induction of p21(Cip1) by modulating the protein kinase Cdelta pathway in vascular smooth muscle cells. *J Biol Chem*. 2001;276:47650–47657.
48. Gauthier A, Vassiliou G, Benoist F, McPherson R. Adipocyte low density lipoprotein receptor-related protein gene expression and function is regulated by peroxisome proliferator-activated receptor gamma. *J Biol Chem*. 2003;278:11945–11953.
49. Bruemmer D, Yin F, Liu J, Berger JP, Sakai T, Blaschke F, Fleck E, Van Herle AJ, Forman BM, Law RE. Regulation of the growth arrest and DNA damage-inducible gene 45 (GADD45) by peroxisome proliferator-activated receptor gamma in vascular smooth muscle cells. *Circ Res*. 2003;93:e38–e47.
50. Hansmann G, Rabinovitch M. Bone morphogenetic protein 2 (BMP-2) activates the transcription factor, peroxisome proliferator-activated receptor gamma (PPARγ), in human pulmonary artery smooth muscle cells (HPASMC). *Circulation*. 2005;112:II-154. Abstract.
51. Lane KB, Machado RD, Pauciulo MW, Thomson JR, Phillips JA 3rd, Loyd JE, Nichols WC, Trembath RC. Heterozygous germline mutations in BMPR2, encoding a TGF-beta receptor, cause familial primary pulmonary hypertension: the International PPH Consortium. *Nat Genet*. 2000;26:81–84.

CLINICAL PERSPECTIVE

Recent studies document an increased incidence of metabolic syndrome and associated insulin resistance in children, adolescents, and adults, placing them at risk for systemic cardiovascular disease. Insulin resistance also may be linked to pulmonary arterial hypertension (PAH) because reduced expression of apolipoprotein E (apoE) and peroxisome proliferator–activated receptor-γ (PPARγ), which is associated with insulin resistance, is observed in lung tissues from PAH patients. Decreased levels of apoE and the PPARγ target adiponectin may enhance platelet-derived growth factor-BB signaling in pulmonary artery smooth muscle cells in a manner similar to that observed in systemic smooth muscle cells. In keeping with these observations, we now report a novel animal model in which PAH is linked to insulin resistance and reversed by PPARγ activation. Male apoE-deficient ($apoE^{-/-}$) mice on a high-fat diet do not upregulate the insulin sensitizers adiponectin and leptin (in contrast to control mice) but instead develop insulin resistance and severe PAH. Female $apoE^{-/-}$ mice on high-fat diet have higher adiponectin levels and less severe PAH than male $apoE^{-/-}$ mice. A 4-week treatment with the PPARγ agonist rosiglitazone led to an 8-fold increase in plasma adiponectin, improved insulin sensitivity, and complete regression of PAH in male insulin-resistant $apoE^{-/-}$ mice. We also document that apoE and adiponectin inhibit platelet-derived growth factor-BB–induced proliferation of pulmonary artery smooth muscle cells in culture. Our data suggest that insulin resistance, low plasma adiponectin levels, and apoE deficiency may be risk factors for PAH that can be reversed by PPARγ activation. Hence, PPARγ agonists could be given consideration in the treatment of PAH patients, particularly those with documented insulin resistance.

Supplementary Methods

Experimental Design. At 4 weeks of age, the mice were either continued on regular chow or switched to non-cholate-containing high fat diet, which included 21% anhydrous milk fat and 0.15% cholesterol (Dyets #101511, Dyets Inc.) for a maximal period of 21 weeks. *For the non-treatment study*, 15-week-old male and female mice (ApoE -/-, C57Bl/6 controls) on either diet were studied in room air (FiO_2 0.21). *For the rosiglitazone treatment study,* the drug dose per kg high fat diet was based on our own measurements of food intake (3g daily food intake per mouse) and a previous publication[1]. During the course of the study, the drug dose was adjusted once to weight gain in both mouse strains. All studies were carried out under a protocol approved by the Stanford Animal Care Committee following the guidelines of the American Physiological Society.

Hemodynamic Measurements. *RV and LV catheterization:* Measurements of RVSP and RV dp/dt were performed under isoflurane anesthesia (1.5-2.5%) using a closed chest technique in unventilated mice at 15, 19 and 25 weeks of age. Briefly, a 1.4 F catheter (Millar Instruments, Houston, Texas) was inserted into the right jugular vein and then placed into the free RV cavity. Using the PowerLab/4SP recording unit (AD Instruments, Colorado Springs, CO), 3-5 simultaneous tracings from different time points were taken to determine the individual RVSP, maximal rate of pressure development (RV dp/dt max.; RV systolic function) and maximal rate of pressure decay (RV dp/dt min.; RV diastolic function). Left ventricular enddiastolic pressure (LVEDP) was determined by direct LV catheterization under isoflurane anesthesia (2.5%). Briefly, a 1.4F catheter tip (Millar Instruments, Houston, TX) was inserted through the left carotid artery and advanced in a retrograde fashion past the aortic valve, into the left ventricular cavity. The catheter was adjusted to lie in the left ventricular outflow tract and tracings were evaluated in real time to ensure adequate catheter placement. Data were recorded using the PowerLab system (ADInstruments, Colorado Springs, CO). LVEDP was determined using PVAN 3.4 software (Millar Instruments, Houston, TX). *Systemic blood pressure* was determined in non-anesthetized mice by the tail cuff method using the BP 2000 analysis system (Visitech Systems, Apex, NC). At least 5 recordings per mouse were taken to determine systolic BP, MAP and diastolic BP. *Echocardiography:* Measurements of cardiac output and function were performed by echocardiography in mice anesthetized with ketamine (70 mg/kg i.p.) and xylazine (12 mg/kg i.p.) using an ultrasound machine (Vivid 7, GE Medical Systems) equipped with a 13 MHZ linear array transducer. Fractional shortening (FS) and heart rate (HR) were determined in M-mode. Ejection fraction (EF) and cardiac output (CO) were estimated using the Teichholz formula[2]. In addition to the invasively measured RV dp/dt., the Tei-Index ([isovolumetric contraction time + isovolumetric relaxation time]/ ejection time) was calculated in a subset of animals to reveal any potential RV dysfunction[3, 4].

Right and Left Ventricular Hypertrophy. Right ventricular hypertrophy (RVH) was measured as described[5] by the weight of the right ventricle relative to left ventricle (LV) + septum. Left ventricular hypertrophy (LVH) was measured as absolute weight of the LV plus septum, and as enddiastolic interventricular septum thickness (IVSd) by echocardiographic M-mode imaging. LV dilatation was assessed by echocardiographic M-mode measurement of the LV enddiastolic inner diameter.

Lung tissue preparation. After abdominal aortic dissection, lungs were perfused *in vivo* by injecting 5ml normal saline into the beating RV. Lungs were tracheally injected with 10% formalin, fixed overnight, and then embedded either in paraffin for standard histology (Hematoxylin & Eosin, Elastic van Gieson, Movat pentachrome) or treated with sucrose-gradient solution (15-30%) and frozen in OCT (Tissue Tek) for Oil-red-O (fat) staining[6]. Prior to fixation, a subset of left lungs (approximately half) were barium-infused via PA-inserted tubing[7] to label peripheral pulmonary arteries for morphometric analysis and micro-CT-imaging. The barium was infused by hand with similar gross and microscopic endpoints of pre-capillary filling of all small vessels at alveolar duct and wall level.

Morphometric Analysis. Transverse left lung sections (3 step sections, 200μm apart) were stained by Elastic van Gieson and Movat pentachrome. Muscularized and non-muscularized peripheral (alveolar wall) pulmonary arteries were counted in 5-10 random views per lung.

Micro-CT-Imaging. A custom-built eXplore Locus RS120 Micro CT Scanner (GE Health Care, Ontario, Canada) was used to acquire non-destructing 3-D images of barium-infused [7] whole lung specimens.

Oil-red-O (fat) Staining. Oild-red-O (fat) staining of fresh frozen lung sections was performed as previously described [6].

Cell Culture and Functional Assays: *Primary murine PASMC were isolated from* 5 male 14-15-week old mice of either genotype on regular chow and used for one culture: The main extralobular pulmonary arteries were dissected, cleaned from adherent tissue, cut in small pieces and digested for 90 min. in dispersion media containing 0.53mg/ml elastase (Roche), 0.53mg/ml collagenase II (Worthington), 2mg/ml albumin (Sigma), 0.2mg/ml soybean trypsin inhibitor (Worthington), 40 μM $CaCl_2$, in HBSS buffer (Gibco). PASMC were then cultured in DMEM (Gibco) containing FBS (20% for 3 days, then reduced to 10%), 2mM L-glutamine and 100U/ml Penicillin, 0.1mg/ml streptomycin. Passages 3-4 were used for further studies. Smooth muscle cell identity was verified by positive immunohistochemistry staining for SM α-actin (Sigma) (> 95% of cells stained positive for SM α-actin). PASMC were grown to 70% confluence and then cultured for 24h in

starvation media (DMEM, 0.1% FBS, 2mM L-glutamine, 100U/ml Penicillin, 0.1mg/ml streptomycin). The media with or without growth factors and/or inhibitors was changed every 24h.

Cell Counts: PASMC were seeded at $2.5x10^4$ cells per well of a 24-well plate in 500µl of growth medium and allowed to adhere overnight. The medium was removed and the cells washed 3 times with PBS prior to the addition of starvation media (DMEM, 0.1% FBS, penicillin/streptomycin) and incubated at 37°C, 5% CO_2 for 24 (murine PA SMC) or 48h (human PA SMC) prior to PDGF-BB stimulation for 0h and 72h (treatments and concentrations stated in the figure legends). Cells were washed twice with PBS and trypsinized in 150µl of Trypsin/EDTA (Cascade Biologics) for 7min., followed by the addition of 150µl trypsin neutralizer (Cascade Biologics). The cells were then resuspended and counted in a hemacytometer (4 counts per well and condition).

Whole blood and blood plasma measurements. Since even brief isoflurane exposure elevates plasma glucose levels in mice *in vivo* [8], we performed tail vein puncture in non-anesthetized, overnight-starved mice followed by immediate, duplicate whole blood glucose measurements with a glucometer (Freestyle/Abbott). Fasting blood plasma was obtained either via retroorbital bleeding or – in a subset of mice – by cardiac puncture, either after cervical dislocation or under isoflurane anesthesia. Fasting plasma adiponectin and insulin levels were determined by radioimmunosorbent assay (RIA), plasma leptin values as duplicate measurements by a multiplex cytokine assay at Linco Diagnostics (St. Charles, MO). Plasma endothelin-1 was assessed by enzyme-linked immunosorbent assay (ELISA). Total cholesterol (Roche Diagnostics), HDL-cholesterol (L-type HDL-cholesterol assay, Wako Diagnostics) and triglycerides (triglycerides glycerol blanked assay, Roche Diagnostics) were measured with commercially available enzymatic kits on a Hitachi 917 analyzer.

Supplement Table 1. Metabolic measurements in *male* C57Bl/6 (control) and apoE -/- mice in normoxia

	Regular Chow (Normoxia)		High Fat Diet (Normoxia)			
Parameter	**Control (CR)**	**ApoE -/- (AR)**	**Control (CF)**	**ApoE -/- (AF)**	**P-value**	**N**
Blood Glucose (mg/dl)	94 ± 5.4	76 ± 2.5	85 ± 7.5	148 ± 7.4***	***AF vs CF; ***AF vs AR	5-10
Plasma Insulin (ng/ml)	0.64 ± 0.12	0.35 ± 0.15	0.50 ± 0.24	1.19 ± 0.21*	*AF vs AR	4-10
Plasma Adiponectin (µg/ml)	4.6 ± 0.57	6.2 ± 0.87	8.5 ± 0.45**	7.1 ± 0.60	**CF vs CR	4-6
Plasma Leptin (mg/dl)	318 ± 101	437 ± 96	15015 ± 4536**	2642 ± 784*	**CF vs CR; *AF vs CF	3-6
Total Cholesterol (mg/dl)	100 ± 4.3	457 ± 32.7***	166 ± 18.6	1198 ± 23.1***	***AR vs CR; ***AF vs AR; ***AF vs CF	4-6
HDL-Cholesterol (mg/dl)	74 ± 3.3	66 ± 9.3	132 ± 15.2**	108 ± 7.2	**CF vs CR	4-6
Non-HDL-Cholesterol (mg/dl)	26 ± 2.7	391 ± 33.0***	34 ± 3.5	1099 ± 20.1***	***AR vs CR; ***AF vs AR; ***AF vs CF	4-6
Triglycerides (mg/dl)	59 ± 5.5	128 ± 17.0**	72 ± 8.8	121 ± 7.4	**AR vs CR	4-6

Supplement Table 1. 15 week-old male mice, on regular chow or high fat diet for 11 weeks, in normoxia. Statistically significant differences between C57Bl/6 (control) and apoE -/- mice on either regular chow or high fat diet, and differences between mice of the same genotype on either diet are indicated. * p<0.05; ** p<0.01; *** p<0.001.

Supplement Table 2. Metabolic measurements in *female* C57Bl/6 (control) and apoE -/- mice in normoxia

	Regular Chow (Normoxia)		High Fat Diet (Normoxia)			
Parameter	**Control (CR)**	**ApoE -/- (AR)**	**Control (CF)**	**ApoE -/- (AF)**	**P-value**	**n**
Blood Glucose (mg/dl)	85 ± 4.1	79 ± 6.9	105 ± 8.9**	77 ± 3.0	** CF vs AF	5-10
Plasma Insulin (ng/ml)	0.26 ± 0.08	0.09 ± 0.04	0.46 ± .10	0.29 ± 0.05		4-11
Plasma Adiponectin (µg/ml)	8.9 ± 0.8	12.5 ± 1.1	19.1 ± 2.5***	11.2 ± 0.43***	***CF vs CR; **AF vs CF	4-9
Plasma Leptin (mg/dl)	2279 ± 540	649 ± 112	13560 ± 6980*	821 ± 184*	*CF vs CR; ; *AF vs CF	4-9
Total Cholesterol (mg/dl)	59 ± 4.8	408 ± 15.4***	129 ± 14.1	1159 ± 27.6***	***AR vs CR; ***AF vs AR; ***AF vs CF	4-7
HDL-Cholesterol (mg/dl)	40 ± 8.0	44 ± 6.1	94 ± 16.1*	70 ± 12.2	*CF vs CR	4-7
Non-HDL-Cholesterol (mg/dl)	19 ± 4.3	364 ± 12.0***	35 ± 4.4	1089 ± 28.9***	***AR vs CR; ***AF vs AR; ***AF vs CF	4-7
Triglycerides (mg/dl)	82 ± 5.5	97 ± 9.3	54 ± 5.6	120 ± 7.0***	***AF vs CF	4-7

Supplement Table 2. 15 week-old female mice, on regular chow or high fat diet for 11 weeks, in normoxia. Statistically significant differences between C57Bl/6 (control) and apoE -/- mice on either regular chow or high fat diet, and differences between mice of the same genotype on either diet are indicated. * p<0.05; ** p<0.01; *** p<0.001.

Supplement Table 3. Metabolic, hemodynamic, echocardiographic, heart weight and hematocrit measurements in *male* C57Bl/6 (control) and apoE -/- mice after 10-week treatment with rosiglitazone

Parameter	Control (C)	Control Rosi (CR)	ApoE -/- (A)	ApoE-/- Rosi (AR)	P-Value	N
Body weight (g)	35.1 ± 3.6	31.2 ± 2.0	47.5 ± 1.4**	48.5 ± 2.4***	**A vs C; ***AR vs CR	8-9
Metabolism						
Blood Glucose (mg/dl)	90 ± 7.4	77 ± 5.3	137 ± 5.7***	98 ± 5.6***	***A vs C; ***AR vs A	8-9
HgA1c (%)	3.81 ± 0.10	3.52 ± 0.13	4.18 ± 0.13	3.85 ± 0.12		5-8
Hemodynamics						
RVSP (mmHg)	22.3 ± 0.2	22.2 ± 0.7	28.3 ± 0.5***	24.4 ± 0.5***	***A vs C; ***AR vs A	5-8
RV dp/dt max (mmHg/s)	1477 ± 76.5	1408 ± 104.7	1601 ± 46.6	1580 ± 94.9		5-8
RV dp/dt min (mmHg/s)	-1262 ± 75.6	-1134 ± 60.0	-1521 ± 64.2	-1383 ± 106.0		5-8
Systolic BP (mmHg) †	103 ± 3.4	95 ± 2.4	108 ± 4.0	100 ± 2.3		7-8
MAP (mmHg) †	85 ± 3.3	78 ± 2.6	90 ± 4.2	81 ± 3.3		7-8
Diastolic BP (mmHg) †	75 ± 3.3	70 ± 2.8	81 ± 4.4	71 ± 3.9		7-8
Echocardiography						
Heart Rate (bpm)	313 ± 11.7	351 ± 15.6	360 ± 11.5	341 ± 11.4		6-8
EF (%)	68.2 ± 1.9	65.1 ± 1.1	68.9 ± 1.0	62.9 ± 0.8*	*AR vs A	6-8
FS (%)	33.0 ± 1.3	30.8 ± 0.8	33.4 ± 0.8	29.3 ± 0.5*	*AR vs A	6-8
CO (ml/min)	38.5 ± 2.3	44.3 ± 2.6	44.4 ± 2.3	50.0 ± 3.4		6-8
LVIDD (mm)	4.20 ± 0.10	4.26 ± 0.06	4.23 ± 0.10	4.58 ± 0.16		6-8
LVISD (mm)	2.81 ± 0.11	2.95 ± 0.05	2.83 ± 0.06	3.23 ± 0.13*	*AR vs A	6-8
LVPWd (mm)	0.69 ± 0.05	0.79 ± 0.07	0.64 ± 0.04	0.60 ± 0.06		6-8
IVSd (mm)	0.89 ± 0.10	0.96 ± 0.07	0.84 ± 0.07	0.87 ± 0.10		6-8
TEI-Index	0.51 ± 0.06	0.60 ± 0.04	0.77 ± 0.14	0.61 ± 0.04		6-8
Heart weight						
RV (mg)	23.5 ± 1.5	26.8 ± 1.5	35.5 ± 1.4***	29.3 ± 1.9	***A vs C	6
RV/LV+S	0.24 ± 0.01	0.25 ± 0.02	0.43 ± 0.02***	0.25 ± 0.02***	***A vs C; ***AR vs A	6
LV+S (mg)	96.2 ± 3.7	110.0 ± 5.7	82.3 ± 3.2	117.0 ± 7.5**	**AR vs A	6
Blood						
HCT (%)	46.3 ± 2.0	40.6 ± 0.9*	48.8 ± 0.5	42.2 ± 1.2*	*CR vs C; *AR vs A	6-8
WBC (x10^3 cells/µL)	5.6 ± 1.1	10.1 ± 2.3	8.0 ± 1.5	6.7 ± 1.2		6-7

Supplement Table 3. 25 week-old male mice on high fat diet for 21 weeks, untreated or treated with rosiglitazone (Rosi) for 10 weeks, in normoxia. Statistically significant differences between C57Bl/6 (control) and apoE -/- mice of either group, and between treated and untreated mice of the same genotype are indicated. * p<0.05; ** p<0.01; *** p<0.001. HgA1c, glucosylated hemoglobin A1c; RVSP, right ventricular systolic pressure; dp/dt max., maximal rate of pressure development (systolic RV function); dp/dt min., max. rate of pressure decay (diastolic RV function); BP, blood pressure; MAP, mean arterial pressure; EF, ejection fraction; FS, fractional shortening; CO, cardiac output; LVIDD, left-ventricular enddiastolic inner diameter; LVISD, left-ventricular endsystolic inner diameter; LVPWd, left-ventricular enddiastolic posterior wall thickness; IVSd, end-diastolic interventricular septum thickness; Tei-Index, parameter of RV dysfunction ([isovolumetric contraction time + isovolumetric relaxation time]/ ejection time); ; RV, right ventricle; LV+S, left ventricle plus septum; HCT, hematocrit; WBC, white blood cell count. † Systemic blood pressure was measured at 24 weeks of age, i.e. after treatment with rosiglitazone for 9 weeks.

Supplementary Figure 1:

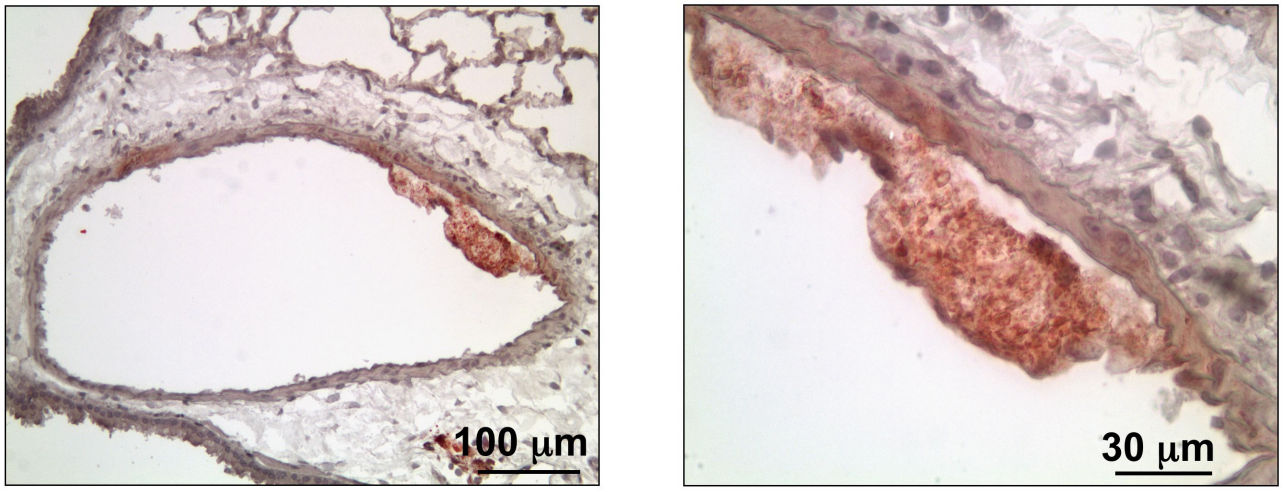

Supplementary Figure 1. Non-occlusive, atherosclerotic lesion in a large intrapulmonary artery of an apoE -/- mouse on high fat diet.

Representative Oil-red-O (fat) photomicrographs of a histological section taken from the lung of a 15-week old apoE-/- mouse on high fat diet for 11 weeks. Atherosclerotic plaques were neither observed in smaller pulmonary arteries (less than 500μm) of apoE -/- mice on high fat diet, nor in apoE -/- on regular chow or in C57/Bl6 mice on either diet.

References

1. Ueshima K, Akihisa-Umeno H, Nagayoshi A, Takakura S, Matsuo M, Mutoh S. A gastrointestinal lipase inhibitor reduces progression of atherosclerosis in mice fed a western-type diet. *Eur J Pharmacol.* 2004;501:137-142.
2. Teichholz LE, Kreulen T, Herman MV, Gorlin R. Problems in echocardiographic volume determinations: echocardiographic-angiographic correlations in the presence of absence of asynergy. *Am J Cardiol.* 1976;37:7-11.
3. Tei C, Ling LH, Hodge DO, Bailey KR, Oh JK, Rodeheffer RJ, Tajik AJ, Seward JB. New index of combined systolic and diastolic myocardial performance: a simple and reproducible measure of cardiac function--a study in normals and dilated cardiomyopathy. *J Cardiol.* 1995;26:357-366.
4. Grignola JC, Gines F, Guzzo D. Comparison of the Tei index with invasive measurements of right ventricular function. *Int J Cardiol.* 2005.
5. Zaidi SH, You XM, Ciura S, Husain M, Rabinovitch M. Overexpression of the serine elastase inhibitor elafin protects transgenic mice from hypoxic pulmonary hypertension. *Circulation.* 2002;105:516-521.
6. Johnson FB. Lipids. In: Prophet EB, Mills B, Arrington J, et al., eds. *Laboratory Methods in Histotechnology.* 2nd ed. Washington, D.C.: American Registry of Pathology; 1994:175-182.
7. Ye CL, Rabinovitch M. Inhibition of elastolysis by SC-37698 reduces development and progression of monocrotaline pulmonary hypertension. *Am J Physiol.* 1991;261:H1255-1267.
8. Pomplun D, Mohlig M, Spranger J, Pfeiffer AF, Ristow M. Elevation of blood glucose following anaesthetic treatment in C57BL/6 mice. *Horm Metab Res.* 2004;36:67-69.

2.3 Insulin Resistance Is Common In Patients With Pulmonary Arterial Hypertension And Associated With Worse 6 Months-Event-Free Survival

In the past two decades we have seen a remarkable increase in the number of children, adolescents[69] and adults[70] with the metabolic syndrome at high risk for *systemic* cardiovascular disease. However, it was not known whether the metabolic syndrome, and especially its key element, insulin resistance (IR), is associated with clinical pulmonary arterial hypertension. The association between IR and PAH in the apoE deficient mouse on high fat diet (see **2.2**)[118] raised the question whether IR-directed pharmacotherapy or pulmonary rehabilitation may play a role in improving the functional status of patients with PAH through the amelioration of insulin resistance.

Based on our clinical observations, suggestive literature, and laboratory results[118] we hypothesized that insulin resistance is (1) more common in PAH patients, and (2) may be associated with severity of disease. In this study[120], we stratified a cohort of PAH patients by insulin resistance profile and compared it to a matched control population using the National Health and Nutrition Examination Surveys (NHANES). Our analysis focused on women since PAH is a female predominant disease. Clinical data and fasting blood samples were evaluated in 81 non-diabetic PAH females and 967 NHANES female controls. Subjects were excluded if they had a known history of diabetes mellitus, a fasting blood glucose of greater than 126 mg/dl, a hemoglobin A_{1C} ($HgbA_{1C}$) of greater than 7.0, or pulmonary capillary wedge pressure of greater than 15 mmHg. Fasting triglyceride to high-density lipoprotein cholesterol ratio (TG/HDL-C) was used as a surrogate of insulin sensitivity. TG/HDL-C has been shown to be as sensitive and specific as fasting insulin in determining insulin resistance in both obese, nondiabetic individuals[121, 122] and in women with polycystic ovarian syndrome[123]. Based upon these studies, we defined an individual as insulin resistant (IR) when TG/HDL-C ratio was greater than 3.0, and insulin sensitive (IS) when TG/HDL-C ratio was less than 2.0. The TG/HDL-C ratio was validated by a direct comparison with the homeostasis model assessment of insulin resistance (HOMA-IR) in the large NHANES control group (see Eur Respir J, epub Dec. 1, 2008; Supplementary Figure S1). We considered subjects with BMI>25 kg/m^2 as overweight and those with BMI>30 kg/m^2 as obese.

While BMI was very similar in PAH and NHANES females (28.7 vs. 28.6 kg/m^2), PAH females were more likely to be insulin resistant (45.7% vs. 21.5%) and less likely to be insulin sensitive (43.2% vs. 57.8%, $p<0.0001$). PAH females mostly had NYHA class II and III symptoms (82.7%). Etiology, NYHA class, 6-minute-walk-distance, and hemodynamics did not differ between IR and IS PAH groups. However, the presence of IR and a higher NYHA class were associated with poorer combined 6-months event-free survival from death, transplantation, or acute hospitalization due to PAH exacerbation or right heart failure (58% vs. 79%, $p<0.05$; hazard ratio 2.57, 95% CI

1.03-6.06, $p<0.05$; adjusted for age and BMI). For a detailed cohort characterization and full results, see original article (Eur Respir J, epub Dec. 1, 2008; attached)[120].

In this study[120], we have shown for the first time that insulin resistance is more prevalent in women with pulmonary arterial hypertension than in the general female population. While the prevalence of insulin resistance in the NHANES control population was influenced by age and degree of obesity, these factors did *not* account for the increased prevalence of IR in the PAH cohort. Although IR is more common in the obese control subjects *and* PAH females, our data suggest that obesity alone *does not* account for the higher prevalence of IR in PAH women.

Surprisingly, we did not find a significant difference in PAH etiology, NYHA functional classification, number of disease specific therapies, or hemodynamics between our IR and IS PAH groups. While insulin resistance is associated with more advanced NYHA class and reduced 6-minute walk distance (6MWD) in patients with congestive heart failure (CHF) [124-126], our PAH cohort did not exhibit this relationship. However, similar to patients with CHF, insulin resistance in our study was associated with poorer survival and a strong predictor of acute hospitalization for right heart failure, transplantation, or death. Indeed, we could show that an advanced NYHA functional class and presence of insulin resistance in our PAH cohort were associated with a worse (age and BMI adjusted) event-free survival. Our findings suggest that insulin resistance is not solely a result of severity of illness in women with PAH, but potentially a new risk factor for disease progression and worse outcomes.

Insulin resistance in PAH may be a disease modifier rather than simply a metabolic epiphenomenon. Such hypothesis is further fuelled by the fact that several conditions strongly associated with PAH (connective tissues diseases, HIV, stimulant use) have also been linked to insulin resistance[127-131]. These associated conditions are linked to insulin resistance by an underlying inflammatory pathology - a common theme in PAH. In accordance with these observations, many pro-inflammatory cytokines, such as IL-6[49, 81]and MCP-1[51] (also known as CCL2[52]), are elevated in insulin resistance and PAH (see introduction, **1.6**). Insulin resistance states may increase the susceptibility for development or accelerated progression of PAH in the presence of detrimental conditions (connective tissue disease, congenital heart disease, environmental exposures) or genetic mutations (e.g., BMP receptor II, serotonin transporter, potassium channels).

Assuming that insulin resistance contributes to the pathophysiology of PAH, it is reasonable to suggest that interventions which enhance insulin sensitivity in patients with PAH could be of clinical benefit. Since both excess adiposity and sedentary behavior adversely affect insulin action, an obvious choice would be weight loss and increased physical activity – interventions that have

been accomplished safely in PAH patients[21]: PAH patients who underwent a 15 week exercise program had a significant improvement in mean 6MWD (91±61 m) when compared with control PAH patients (-15±54 m)[21]. Though many factors could explain the benefits of exercise in these patients, and many mechanisms could be invoked to explain an improved 6MWD, it is plausible that such enhancement is associated with improved insulin and lipid profiles. Interestingly, physical training has also been shown to improve hyperinsulinemia and insulin resistance in patients with congestive heart failure (CHF)[132].

Beyond diet and exercise, current and future pharmacotherapy for PAH may target the pathways directly or indirectly involved in insulin resistance. It has been suggested that endothelin-1 antagonists may exert some of their effects on the pulmonary vasculature via insulin sensitizing pathways[133, 134]. PPARγ agonists of the thiazolidendione (TZD) class are commonly used in the treatment of diabetes, increase insulin sensitivity, lower circulating plasma insulin levels[135, 136], and improve vascular abnormalities[45, 65, 137] in insulin resistant individuals (see **1.4** and **2.4**).

The dyslipidemia seen in insulin resistance (see Stanford cohort above) may in itself represent an important disease modifier of PAH (see also animal study under **2.2**). Most recently, Yuditskaya et al. (epub November 20, 2008)[119] identified altered apolipoprotein patterns in patients with pulmonary hypertension and vasculopathy of sickle cell disease (SCD) using a proteomics approach. As a group, patients with SCD demonstrated significantly lower apoAI levels than African-American control subjects. The PAH cohort was further characterized by high levels of apolipoproteins A-II and B and serum amyloid A. The authors conclude a relationship of apolipoproteins to the development of PAH vasculopathy in sickle cell disease, potentially involving an unexpected mechanistic parallel to atherosclerosis.

In conclusion of our study[120], insulin resistance (determined by TG/HDL-C. ratio) is more prevalent in women with PAH than in the general population and may be a novel risk factor or disease modifier associated with poorer outcome. While the pathobiology of PAH is multifactorial, we suggest that insulin resistance may represent an important risk factor to disease development and/or its progression. If our findings hold true in a substantial proportion of PAH patients, then treatment aimed at improving insulin resistance, via simple measures such as diet and exercise, or new pharmacologic approaches, may benefit a large percentage of patients with pulmonary arterial hypertension. Randomized controlled trials on the link between IR and PAH are warranted.

Cited own reference:

Zamanian RT*, Hansmann G*, Snook S, Lilienfeld D, Rappaport K, Rabinovitch M, Reaven G, Doyle RL (2009). Insulin Resistance and Pulmonary Arterial Hypertension. ***both authors contributed equally to this work**. **European Respiratory Journal** 33: 318-324 *epub December 1, 2008*

2.4 A Role For PPARγ Agonists And Selective PPAR Modulators (SPPARM) In The Treatment Of Pulmonary Hypertension

In the last two decades, tremendous improvements in the treatment of PAH patients have been made. However, none of the current clinical therapies (inhaled nitric oxide, prostanoids, phosphodiesterase inhibitors, endothelin-1 receptor antagonists, calcium channel blockers) have been shown to be universally effective or able to reverse advanced pulmonary vascular disease[17].

The unique potential of PPARγ agonists and selective PPARγ modulators in the treatment of pulmonary vascular disease relates to the fact that many of its downstream targets are positively or negatively associated with the development of PAH. **Some of the mechanisms underlying the potential benefit from PPARγ activation in PAH patients include (see Figure 1, Figure 2):**

1. *Inhibition of cell cycle progression and vascular SMC proliferation* by inhibiting G1→S phase transition[104,103] (**Figure 1B**).

2. *Apoptosis of proliferating vascular cells by blocking important survival pathway*s downstream of activated PDGFR-β, e.g., phosphatidylinositol 3-kinase (PI3K)[45, 105].

3. *Induction of apoE, adiponectin and LDL receptor related protein (LRP) thereby blocking PDGF-BB signaling and pulmonary vascular remodeling.* ApoE and adiponectin, both targets of PPARγ, inhibit PDGF-BB-induced PASMC proliferation, and deficiency of both proteins has been linked to IR and PAH[118] (**Figure 1A**). ApoE internalizes the PDGF receptor beta (PDGFR-β)[94, 95] and adiponectin sequesters the ligand PDGF-BB[114] (**Figure 1B**). Activated PPARγ also blocks PDGF gene expression[101] and induces LRP [102], the receptor necessary for apoE-mediated suppression of PDGF-BB signaling[94, 95] (**Figure 1B**). Thus, decreased levels of PPARγ, apoE and adiponectin can be expected to enhance PDGF-BB-signaling and pulmonary vascular remodeling (**Figure 1**). Adiponectin, that is secreted from visceral, subcutaneous and perivascular adipocytes[86], recently has been identified as antithrombotic factor[138] and as such may also protect against chronic thromboembolic forms of pulmonary hypertension (CTEPH; i.e., category 4 of PH).

4. *Repression of endothelin-1 and ADMA, thus counteracting vasoconstriction.* Yudkin and colleagues[86] proposed that detrimental adipocytokines, such as TNF-α and IL-6, are secreted from perivascular fat cells ("vasocrine signaling"), and inhibit the eNOS-pathway of insulin signaling, leaving unopposed vasoconstriction mediated by ET-1[79]. PPARγ activation would counteract these deleterious effects by impairing the expression of both ET-1[54] and the eNOS inhibitor ADMA[55, 56]. Increased pulmonary ET-1 expression[79] and plasma elevation of ADMA[90] was observed in PAH patients, and heightened ADMA levels negatively correlated with hemodynamic performance and human survival rates[90], underlining the clinical relevance of these findings.

5. *Inhibition of mitogenic matrix metalloproteinases (MMP) which act downstream of elastase.* PPARγ ligands impair MMPs[107] that are activated by elastase. Elastase inhibitors not only prevent but also reverse advanced fatal PAH in rats[109]. Hence, along with elastase inhibitors such as elafin, PPARγ agonists could counterbalance the detrimental effects of heightened elastase and MMP activity that frequently promote PAH.

6. *Inhibition of vascular growth-promotive RhoA/ROCK pathways*[139] that are known to be implicated in the pathogenesis of PAH. The PPARγ ligand pioglitazone inhibits RhoA/ROCK pathways through upregulation of the phosphatase SHP-2[140]. Thus, PPARγ agonists may provide anti-mitogenic ROCK inhibition in vascular cells that has been shown to be beneficial in experimental[141] and clinical PAH[142].

7. *Rescue of BMP-RII dysfunction and amelioration of insulin resistance - both of which is common in PAH patients.* In the work presented, we have demonstrated a novel antiproliferative BMP-2/PPARγ/apoE axis in human pulmonary smooth muscle cells (HPASMC)[68]. Importantly, pharmacological PPARγ activation in HPASMC from a patient with a BMP-RII frame-shift mutation blocked PDGF-BB induced proliferation[68]. Moreover, PPARγ activation completely reversed pulmonary vascular disease (RVSP elevation, RVH, peripheral PA muscularization) in insulin-resistent apoE -/- mice; this was associated with an 8-fold induction of adiponectin (released by adipocytes) and a marked improvement of insulin sensitivity[118]. We then found that insulin resistance is more than double as prevalent in female PAH patients (Stanford cohort; n=81) than in the general population (matched controls, NHANES database; n=967) and associated with poorer 6-months-event-free survival from hospitalization for RV failure, lung transplantation, or death[120]. If the link between insulin resistance and PAH holds true in larger multicenter studies, then the epidemic “metabolic syndrome” - that is more and more evident particularily in the young - will significantly increase the incidence of PAH over the next decades.

Differential Safety Profile of PPARγ Agonists (Thiazolidinediones: Rosiglitazone, Pioglitazone)

The safety profile of rosiglitazone is the subject of an ongoing debate[143-147]. A systematic but limited meta-analysis of 42 trials reported a higher incidence of myocardial infarction (MI) and cardiovascular death in diabetic patients taking rosiglitazone[143], whereas published preliminary data of RECORD, a large randomized controlled trial (RCT) specifically designed to study cardiovascular outcomes in diabetic patients, did not show such an association[144]. A meta-analysis of 4 large RCTs with at least 12 months follow-up did find an association between rosiglitazone use and MI but not with cardiovascular mortality[145]. Given these conflicting results and both the very low overall number of adverse events in this high risk population (<1%) as well as the marginal

absolute difference in MI rates between rosiglitazone and control groups (<0.1%), the meta-analysis by Nissen and Wolski[143] likely overestimated the absolute cardiovascular risk. Moreover, there is no evidence that the other FDA-approved TZD, pioglitazone, is associated with higher MI rates as proposed for rosiglitazone (i.e., no TZD-class effect)[143, 148, 149]: In fact, the PROACTIVE trial (n=5,238)[148, 149] and a recent meta-analysis (n=16,390)[150] revealed that pioglitazone reduces macrovascular events including MI in patients with type 2 diabetes (T2DM), and does not increase the incidence of death from congestive heart failure (CHF). However, in several[148-150] but not all[151] studies, pioglitazone was associated with mild to moderate, non-fatal CHF [150] – a rare adverse event also observed with rosiglitazone (DREAM trial: 14 vs. 2 of 5,269 non-diabetic subjects[152]; ADOPT trial: 22 vs. 9 on glyburide of 2,897 T2DM patients[153]; and a recent meta-analysis[145]). Congestive heart failure in high risk patients given TZDs did not increase mortality and might not carry the risk that is usually associated with CHF, i.e. progressive systolic and diastolic left ventricular (LV) dysfunction[154]. Both fluid retention and heart failure observed with TZDs such as pioglitazone are reversible and do not appear to negate the beneficial effects of the drug on irreversible ischemic and fatal end points[150]. Most importantly, it must be underlined that the absolute cardiovascular risk attributed to PPARγ agonists of the TZD class is probably even lower in PAH patients who generally have preserved LV function and no systemic hypertension. Nevertheless, TZDs should be avoided in patients with significant LV dysfunction or chronic renal insufficiency.

Taken together, there is emerging evidence that multiple key genes involved in the pathobiology of PAH are targets of PPARγ, and that pharmacological PPARγ activation would lead to their beneficial induction/stabilization (eNOS, p27KIP1, adiponectin, apoE, LRP) or repression (PDGF, MAPK, cyclin D1, telomerase, ET-1, ADMA, elastase/MMP, RhoA/ROCK). I suggest that PPARγ agonists might reverse pulmonary vascular remodeling in PAH patients with or without BMP-RII dysfunction, and that insulin resistance may be a novel risk factor or disease modifier. Hence, future treatment of both insulin-resistant and insulin-sensitive PAH patients may include PPARγ agonists, or novel selective PPAR modulators (SPPARM)[43]. Randomized controlled trials on the use of PPARγ activating agents in pulmonary vascular disease are urgently needed.

2.5 Novel Therapeutic Approaches for Pulmonary Hypertension

Table 1 Novel Therapeutic Approaches For Pulmonary Hypertension

Compound	Mechanism of Action	Route	Adverse Effects	References/Trial No.
Imatinib* (STI571)	PDGFR beta (tyrosine kinase) inhibition	PO	cardiotoxicity (?), edema, cytopenia, dermatitis, diarrhea, hypothyroidism (?)	[33, 34, 155] NCT00477269 NCT00583115 NCT00506831
PKI166	EGF receptor (tyrosine kinase) inhibition	PO	hepatotoxicity, diarrhea, skin rash	[32, 156]
Sorafenib	VEGFR, PDGFR beta, c-KIT, Raf (tyrosine kinase/ Raf kinase inhibition)	PO	cardiac ischemia, hypertension, fatigue, skin rash, diarrhea	[157, 158] NCT00452218
Elafin (BR4946)	Neutrophil elastase inhibition	IV	hepatotoxicity	[109]
Fasudil (AT-877)	Rho-kinase inhibition	IV	?, hypotension	[142, 159, 160]
Rituximab*	Anti-CD20 monoclonal antibody	IV	progressive multifocal leukoencephalopathy, fever	ACE: Rituximab for Scleroderma (NIH)
Simvastatin *	HMG-CoA reductase inhibition	PO	hepatotoxicity , myopathy	[161, 162] NCT00180713 NCT00384865 NCT00538044
Escitalopram*, Fluoxetine	SERT (5-HTT) inhibition	PO	nausea, diarrhea, constipation, loss of appetite, stomach pain	[163, 164] NCT00190333
Pioglitazone, Rosiglitazone	PPARgamma activation	PO	fluid retention, non-fatal, reversible heart failure [#]	[68, 118, 165, 166]
Dichloroacetate (DCA)	Mitochondrial PDK inhibition, NFAT-mediated upregulation of Kv channels, opening the mitochondrial transition pore	PO	neuropathy/neurotoxicity ? sedation, gait disturbances, numbness	[167-170]
Stem Cell Tx *	Endothelial reconstitution ± eNOS transfection	IV	?	[171, 172] NCT00257413 NCT00469027

eNOS, endothelial nitric oxide synthase; HMG-CoA; 3-hydroxy-3-methyl-glutaryl-CoA;PDGFR beta, platelet-derived growth factor receptor beta; PPARgamma, PDK, pyruvate dehydrogenase kinase; peroxisome proliferator-activated receptor gamma; Tx, transplantation; SERT (=5-HTT), serotonin transporter; Tx, transplantation. Tyrosine kinase inhibitors (in parentheses: kinase preferably blocked): Imatinib (PDGFR beta, ABL, Bcr-Abl, c-KIT), PKI166 (EGF receptor, erbB2 receptor=HER2/neu), Sorafenib (VEGFR, PDGFR beta, Flt-3, c-kit, RET receptor; also Raf kinase).
Additional adverse effects not listed in this table may occur with each of the compounds.
* Compounds or procedures currently studied for the treatment of patients with pulmonary hypertension (NCT trial no.)
[#] For differential safety profile of thiazolidinediones (pioglitatazone, rosiglitazone) see main text.
Clinical trial identifier no. start with NCT and can be found online under http://clinicaltrials.gov

The most promising novel drugs with the potential to reverse pulmonary arterial hypertension are platelet-derived growth factor beta receptor (PDGFR-β)[30, 33] and epidermal growth factor receptor (EGFR) blockers[32], elastase[109] and Rho-Kinase (ROCK) inhibitors[141, 142], mitochondrial metabolic modulators (e.g., dichloroacetate)[167-170], nucleoside and nucleotide analoga[173-185], receptor for activated C-Kinase 1 (RACK1) activators[186], and – as I suggest here – peroxisome proliferator-activated receptor gamma (PPARγ) agonists[68, 118] and selective PPAR modulators (SPPARM)[43] (**Table 1).**

Moreover, there is recent evidence that activation of PPARs, not only PPARγ, but also PPARα and PPARβ/δ, may be beneficial in the treatment of several lung diseases[187] such as asthma, COPD, pulmonary fibrosis (PPARβ/δ[188]), acute lung injury (PPARα[189]) and PAH (PPARγ[68, 118, 165, 166]). The endogenous prostanoid 15-deoxyΔ12,14-prostaglandin J2 (15-d-PGJ2) is a known ligand of PPARγ[187, 190], and both PPARβ/δ[188] and PPARγ have been suggested to be drug targets of prostanoids used for the treatment of advanced PAH (e.g., PGI_2). The actions of PPARα and PPARγ are thought to be due to their ability to down-regulate growth-promotive and proinflammatory gene expression and inflammatory cell functions [45, 65, 187] (see introduction **1.4**, and **2.5**), and as such makes them an attractive target for pharmacotherapy. PPARβ/δ has been shown to be involved in wound healing, and its activation may enhance the effects of PPARγ agonists[187].

3. Summary

Loss-of-function mutations of the bone morphogenetic protein receptor II (BMP-RII) gene are linked to pulmonary arterial hypertension (PAH). The ligand, BMP-2, is a negative regulator of smooth muscle cell (SMC) growth induced by mitogens such as platelet-derived growth factor B (PDGF-BB homodimer) and epidermal growth factor (EGF). We report on a novel downstream mechanism that requires activation of peroxisome proliferator-activated receptor gamma (PPARγ) and its transcriptional target apolipoprotein E (apoE). BMP-2/BMP-RII signaling prevented PDGF-BB-induced proliferation of human and murine pulmonary artery SMC (PASMC), by decreasing nuclear phosphoERK and inducing DNA-binding of PPARγ that is independent of Smad1/5/8 phosphorylation. Both BMP-2 and a PPARγ agonist stimulated production and secretion of apoE in SMC. Using small hairpin RNAi in human PASMC, PASMC from a PAH patient with a known BMP-RII mutation, a PPARγ antagonist, and PASMC isolated from PPARγ and apoE deficient mice, we demonstrated that the antiproliferative effect of BMP-2 is BMP-RII-, PPARγ- and apoE-dependent. Furthermore this work shows for the first time that mice with targeted deletion of PPARγ in SMC spontaneously develop PAH, as indicated by elevated RV systolic pressure, RV hypertrophy and increased muscularization of distal pulmonary arteries. Thus, PPARγ-mediated events protect against PAH, and PPARγ agonists such as pioglitazone or rosiglitazone may reverse PAH in patients with or without BMP-RII dysfunction.

Patients with PAH have reduced expression of apoE and PPARγ in lung tissues, and deficiency of both has been linked to insulin resistance. ApoE deficiency leads to enhanced PDGF signaling that is important in the pathobiology of PAH. We therefore hypothesized that insulin resistant apoE deficient mice (apoE -/-) would develop PAH that could be reversed by a PPARγ agonist, i.e., rosiglitazone. We report that apoE -/- mice on a high fat (HF) diet develop PAH as indicated by elevated right ventricular systolic pressure (RVSP). When compared to females of the same genotype, male apoE -/- were insulin-resistant, had lower plasma adiponectin, and more elevated RVSP, associated with right ventricular hypertrophy (RVH) and increased peripheral PA muscularization. Since male apoE -/- were insulin-resistant and had more severe PAH than female apoE -/-, we treated the former with rosiglitazone PO for 4 and 10 weeks. This resulted in markedly higher plasma adiponectin concentrations, improved insulin sensitivity, and complete regression of PAH, RVH and abnormal PA muscularization in male apoE -/- mice. We further show that recombinant apoE and adiponectin suppress PDGF-BB-mediated proliferation of pulmonary artery SMC harvested from apoE -/- or C57Bl/6 control mice. We conclude that insulin resistance, low plasma adiponectin levels, and deficiency of apoE may be risk factors for PAH, and

that PPARγ activation can reverse PAH in an animal model. Hence, PPARγ agonists could be considered for the treatment of PAH patients, particularly those with documented insulin resistance.

Although obesity, dyslipidemia, and insulin resistance (IR) are well known risk factors for *systemic* cardiovascular disease, their impact on pulmonary arterial hypertension (PAH) was unknown. Our previous experimental studies (see above) indicated that insulin resistance may be a risk factor for PAH. We therefore investigated the prevalence of insulin resistance in PAH and explored its relationship to disease severity. Clinical data and fasting blood samples were evaluated in 81 non-diabetic women with PAH. National Health and Nutrition Examination Surveys (NHANES) females (n=967) served as controls. Fasting triglyceride to high-density lipoprotein cholesterol ratio (TG/HDL-C) was used as a surrogate of insulin sensitivity. While body-mass-index (BMI) was similar in PAH and NHANES females (28.7 vs. 28.6 kg/m^2), PAH females were more likely to be insulin resistant (45.7% vs. 21.5%) and less likely to be insulin sensitive (43.2% vs. 57.8%, $p<0.0001$). PAH females mostly had NYHA class II and III symptoms (82.7%). Etiology, NYHA class, 6-minute walk distance, and hemodynamics did not differ between IR and IS PAH groups. However, the presence of insulin resistance and a higher NYHA class were associated with poorer combined 6-months event-free survival from death, transplantation, or acute hospitalization due to PAH exacerbation or right heart failure (58% vs. 79%, $p<0.05$; hazard ratio 2.57, 95% CI 1.03-6.06, $p<0.05$; adjusted for age and BMI). In conclusion, insulin resistance appears to be more common in PAH females than in the general population, and may be a novel risk factor or disease modifier which might impact survival.

3. Zusammenfassung

Mutationen, die zu einem Funktionsverlust des bone morphogenetic protein receptor II (BMP-RII) Gens führen, sind mit pulmonalarterieller Hypertonie (PAH) assoziiert. Der Ligand des Rezeptors, BMP-2, ist ein negativer Regulator der durch Wachstumsfaktoren wie platelet-derived growth factor B (PDGF-BB-Homodimer) und epidermal growth factor (EGF) induzierte Proliferation von glatten Muskelzellen (SMC). Wir weisen hier einen neuen Signalweg (downstream von BMP-2) nach, der die Aktivierung des Transkriptionsfaktors peroxisome proliferator-activated receptor gamma (PPARγ) und seines transkriptionellen Zielgens Apolipoprotein E (APOE) erfordert. Der aktivierte BMP-2/BMP-RII Signalweg verhindert die PDGF-BB-induzierte Proliferation von humanen und murinen, pulmonarteriellen glatten Muskelzellen (PASMC), indem er phosphoERK im Zellkern erniedrigt und die DNA-Bindung von PPARγ, die unabhängig von einer Smad1/5/8 Phosphorylierung abläuft, induziert. Sowohl BMP-2 als auch ein PPARγ agonist stimuliert die Expression und Sekretion von apoE-Protein in PASMC. Unter Zuhilfenahme von small hairpin RNAi in humanen PASMC, PASMC eines PAH Patienten mit bekannter BMP-RII Mutation, einem PPARγ Antagonisten, und PASMC von PPARγ- bzw. ApoE-defizienten Mäusen, konnten wir zeigen, dass der antiproliferative Effekt von BMP-2 abhängig ist von BMP-RII, PPARγ and apoE. Darüberhinaus zeigt diese Arbeit zum ersten Mal, dass Mäuse mit gezielter Ausschaltung von PPARγ in arteriellen glatten Muskelzellen spontan PAH entwickeln. Dies wird belegt durch einen erhöhten rechtsventrikulären Druck (RVSP), rechtsventrikuläre Hypertrophie (RVH), und eine verstärkte Muskularisierung der kleinen, peripheren Pulmonalarterien. Demzufolge schützten PPARγ-vermittelte Ereignisse gegen PAH, und PPARγ-Agonisten (Pioglitazon, Rosiglitazon) haben das Potential, eine Regression der Pulmonalvaskulären Erkrankung bei PAH Patienten mit oder ohne BMP-RII-Dysfunktion herbeizuführen (s.u.).

Patienten mit PAH zeigen eine verminderte pulmonale Expression von ApoE und PPARγ, und der Mangel an diesen beiden Faktoren ist mit Insulinresistenz (IR) in Verbindung gebracht worden. ApoE-Mangel führt zur Verstärkung des PDGF Signalwegs, der bei Pathophysiologie der PAH ein grosse Rolle spielt. Wir stellten daher die Hypothese auf, dass insulinresistente ApoE knock out Mäuse (ApoE -/-) eine PAH entwickeln, die dann durch einen PPARγ Agonisten wie Rosiglitazon rückgängig gemacht werden könnte. ApoE -/- Mäuse, die auf fettreiche Diät gesetzt wurden, entwickelten erhöhte rechtsventrikuläre Drücke (RVSP) als Zeichen einer PAH. Im Vergleich mit den Weibchen waren die männlichen ApoE -/- Mäuse insulinresistent, hatten niedrigere Plasma-Adiponektinspiegel, und eine stärkere RVSP-Erhöhung, sowie eine rechtsventrikuläre Hypertrophie und eine verstärkte Muskularisierung der peripheren Pulmonalarterien.. Da männliche ApoE -/-

Mäuse insulinresistent waren und einen stärkeren PAH-Phenotyp als die Weibchen hatten, behandelten wir erstere mit Rosiglitazon für 4 und 10 Wochen per os. Dies resultierte in einer deutlich erhöhten Plasma-Adiponektinkonzentration, einer verbesserten Insulinsensitivität, und einer vollständigen Regression von PAH, RVH und abnormaler pulmonalarterieller Muskularizierung in männlichen ApoE -/- Mäusen. Wir konnten zudem demonstrieren, dass rekombinantes Apolipoprotein E und Adiponektin die PDGF-BB-vermittelte Proliferation von apoE-defizienten und Kontroll-PASMC supprimieren. Wir schlussfolgern daher, dass niedrige Plasma-Adiponektinspiegel und ApoE-Mangel neue Risikofaktoren für PAH sein könnten. Wir zeigen ferner, dass die pharmakologische Aktivierung von PPARγ zur Regression der PAH in einem Tiermodell führt. Daher sollten PPARγ-Agonisten für die Behandlung von Patienten mit PAH in Erwägung gezogen werden - vor allem bei solchen mit nachgewiesener Insulinresistenz.

Adipositas, Dyslipidämie und Insulinresistenz (IR) sind bekannte Risikofaktoren für kardiovaskuläre Erkrankungen im systemischen Kreislauf, jedoch war ihr Einfluss auf die Enstehung oder Progression einer Pulmonalarterielle Hypertonie (PAH) bislang unbekannt. Unsere bisherigen Arbeiten (siehe oben) deuteten jedoch daraufhin, dass Insulinresistenz eine Risikofaktor für PAH sein könnte. Wir untersuchten daher die Prävalenz einer Insulinresistenz bei klinischer PAH und ihre Rolle hinsichtlich der Erkrankungschwere. Klinische Daten und Nüchtern-Blutzuckerproben wurden von 81 nicht-diabetischen Frauen mit PAH entnommen. Eine Kohorte von Frauen, deren Daten über eine grosse US-amerikanischen Datenbank (National Health and Nutrition Examination Surveys, NHANES; n=967) zugänglich waren, diente als Kontrolle. Das Verhältnis Nüchtern-Triglyzerid-zu-HDL-Cholesterol (TG/HDL-C-Ratio) wurde als Indikator der Insulinsensitivität bestimmt. Obwohl der body-mass-index (BMI) bei PAH- und NHANES-Frauen ähnlich war (28.7 vs. 28.6 kg/m^2), waren die PAH Frauen häufiger insulin-resistent (45.7% vs. 21.5%) und seltener insulinsensitiv (43.2% vs. 57.8%, $p<0.0001$). PAH-Frauen hatten überwiegend Symptome der NYHA-Kllasse II und III (82.7%). Ätiologie, NYHA-Klasse, 6-Minuten-Gehstrecke, und Hämodynamik unterschieden sich nicht zwischen den insulinresistenten und insulinsensitiven PAH-Patientinnen. Allerdings war das Vorliegen einer Insulinresistenz und eine höhere (d.h. funktionell schlechtere) NYHA-Klasse mit einer schlechteren Prognose hinsichtlich des 6-Monats-Überlebensrate ohne Tod, Transplantation oder akute stationärer Krankenhausaufnahme wegen PAH-Exazerbation oder Rechstherzversagen assoziiert (58% vs. 79%, $p<0.05$; hazard ratio 2.57, 95% CI 1.03-6.06, $p<0.05$; adjustiert nach Alter und BMI). Zusammengefasst ist eine Insulinresistenz bei Patientinnen mit PAH häufger als in der Normalbevölkerung und stellt wahrscheinlich einen neuen Riskofaktor oder Krankheitsmodulator dar, welcher Einfluss auf die Überlebensrate bei PAH haben könnte.

4. References

1. McLaughlin VV, Presberg KW, Doyle RL, Abman SH, McCrory DC, Fortin T, Ahearn G. Prognosis of pulmonary arterial hypertension: ACCP evidence-based clinical practice guidelines. *Chest.* 2004;126:78S-92S.
2. Hyduk A, Croft JB, Ayala C, Zheng K, Zheng ZJ, Mensah GA. Pulmonary hypertension surveillance--United States, 1980-2002. *MMWR Surveill Summ.* 2005;54:1-28.
3. Peacock AJ. Treatment of pulmonary hypertension. *Bmj.* 2003;326:835-836.
4. Sitbon O, Lascoux-Combe C, Delfraissy JF, Yeni PG, Raffi F, De Zuttere D, Gressin V, Clerson P, Sereni D, Simonneau G. Prevalence of HIV-related pulmonary arterial hypertension in the current antiretroviral therapy era. *Am J Respir Crit Care Med.* 2008;177:108-113.
5. McGoon M, Gutterman D, Steen V, Barst R, McCrory DC, Fortin TA, Loyd JE. Screening, early detection, and diagnosis of pulmonary arterial hypertension: ACCP evidence-based clinical practice guidelines. *Chest.* 2004;126:14S-34S.
6. Lin EE, Rodgers GP, Gladwin MT. Hemolytic anemia-associated pulmonary hypertension in sickle cell disease. *Curr Hematol Rep.* 2005;4:117-125.
7. Gladwin MT, Vichinsky E. Pulmonary complications of sickle cell disease. *N Engl J Med.* 2008;359:2254-2265.
8. Simonneau G, Galie N, Rubin LJ, Langleben D, Seeger W, Domenighetti G, Gibbs S, Lebrec D, Speich R, Beghetti M, Rich S, Fishman A. Clinical classification of pulmonary hypertension. *J Am Coll Cardiol.* 2004;43:5S-12S.
9. Rubin LJ. Diagnosis and management of pulmonary arterial hypertension: ACCP evidence-based clinical practice guidelines. *Chest.* 2004;126:7S-10S.
10. Hoeper MM, Ghofrani HA, Grimminger F, Rosenkranz S. [Dana Point: what is new in the treatment of pulmonary hypertension?]. *Dtsch Med Wochenschr.* 2008;133 Suppl 6:S191-195.
11. Gaine SP, Rubin LJ. Primary pulmonary hypertension. *Lancet.* 1998;352:719-725.
12. Haddad F, Hunt SA, Rosenthal DN, Murphy DJ. Right ventricular function in cardiovascular disease, part I: Anatomy, physiology, aging, and functional assessment of the right ventricle. *Circulation.* 2008;117:1436-1448.
13. Benza R, Biederman R, Murali S, Gupta H. Role of cardiac magnetic resonance imaging in the management of patients with pulmonary arterial hypertension. *J Am Coll Cardiol.* 2008;52:1683-1692.
14. Kuehne T, Yilmaz S, Schulze-Neick I, Wellnhofer E, Ewert P, Nagel E, Lange P. Magnetic resonance imaging guided catheterisation for assessment of pulmonary vascular resistance: in vivo validation and clinical application in patients with pulmonary hypertension. *Heart.* 2005;91:1064-1069.
15. Kuehne T, Yilmaz S, Steendijk P, Moore P, Groenink M, Saaed M, Weber O, Higgins CB, Ewert P, Fleck E, Nagel E, Schulze-Neick I, Lange P. Magnetic resonance imaging analysis of right ventricular pressure-volume loops: in vivo validation and clinical application in patients with pulmonary hypertension. *Circulation.* 2004;110:2010-2016.
16. Oikawa M, Kagaya Y, Otani H, Sakuma M, Demachi J, Suzuki J, Takahashi T, Nawata J, Ido T, Watanabe J, Shirato K. Increased [18F]fluorodeoxyglucose accumulation in right ventricular free wall in patients with pulmonary hypertension and the effect of epoprostenol. *J Am Coll Cardiol.* 2005;45:1849-1855.
17. Humbert M, Sitbon O, Simonneau G. Treatment of pulmonary arterial hypertension. *N Engl J Med.* 2004;351:1425-1436.
18. Badesch DB, Abman SH, Ahearn GS, Barst RJ, McCrory DC, Simonneau G, McLaughlin VV. Medical therapy for pulmonary arterial hypertension: ACCP evidence-based clinical practice guidelines. *Chest.* 2004;126:35S-62S.
19. Ghofrani HA, Wilkins MW, Rich S. Uncertainties in the diagnosis and treatment of pulmonary arterial hypertension. *Circulation.* 2008;118:1195-1201.
20. Redelmeier DA, Bayoumi AM, Goldstein RS, Guyatt GH. Interpreting small differences in functional status: the Six Minute Walk test in chronic lung disease patients. *Am J Respir Crit Care Med.* 1997;155:1278-1282.
21. Mereles D, Ehlken N, Kreuscher S, Ghofrani S, Hoeper MM, Halank M, Meyer FJ, Karger G, Buss J, Juenger J, Holzapfel N, Opitz C, Winkler J, Herth FF, Wilkens H, Katus HA, Olschewski H, Grunig E. Exercise and respiratory training improve exercise capacity and quality of life in patients with severe chronic pulmonary hypertension. *Circulation.* 2006;114:1482-1489.
22. Rosenzweig EB, Barst RJ. Pulmonary arterial hypertension in children: a medical update. *Curr Opin Pediatr.* 2008;20:288-293.
23. Badesch DB, Abman SH, Simonneau G, Rubin LJ, McLaughlin VV. Medical therapy for pulmonary arterial hypertension: updated ACCP evidence-based clinical practice guidelines. *Chest.* 2007;131:1917-1928.
24. Rich S, Rabinovitch M. Diagnosis and treatment of secondary (non-category 1) pulmonary hypertension. *Circulation.* 2008;118:2190-2199.

25. Newman JH, Fanburg BL, Archer SL, Badesch DB, Barst RJ, Garcia JG, Kao PN, Knowles JA, Loyd JE, McGoon MD, Morse JH, Nichols WC, Rabinovitch M, Rodman DM, Stevens T, Tuder RM, Voelkel NF, Gail DB. Pulmonary arterial hypertension: future directions: report of a National Heart, Lung and Blood Institute/Office of Rare Diseases workshop. *Circulation.* 2004;109:2947-2952.
26. Humbert M, Morrell NW, Archer SL, Stenmark KR, MacLean MR, Lang IM, Christman BW, Weir EK, Eickelberg O, Voelkel NF, Rabinovitch M. Cellular and molecular pathobiology of pulmonary arterial hypertension. *J Am Coll Cardiol.* 2004;43:13S-24S.
27. Farber HWHW, Loscalzo JJ. Pulmonary arterial hypertension. *N Engl J Med.* 2004;351:1655-1665.
28. Michelakis ED, Wilkins MR, Rabinovitch M. Emerging concepts and translational priorities in pulmonary arterial hypertension. *Circulation.* 2008;118:1486-1495.
29. Rabinovitch M. Molecular pathogenesis of pulmonary arterial hypertension. *J Clin Invest.* 2008;118:2372-2379.
30. Schermuly RT, Dony EE, Ghofrani HA, Pullamsetti S, Savai R, Roth M, Sydykov A, Lai YJ, Weissmann N, Seeger W, Grimminger F. Reversal of experimental pulmonary hypertension by PDGF inhibition. *J Clin Invest.* 2005;115:2811-2821.
31. Jones PL, Cowan KN, Rabinovitch M. Tenascin-C, proliferation and subendothelial fibronectin in progressive pulmonary vascular disease. *Am J Pathol.* 1997;150:1349-1360.
32. Merklinger SL, Jones PL, Martinez EC, Rabinovitch M. Epidermal growth factor receptor blockade mediates smooth muscle cell apoptosis and improves survival in rats with pulmonary hypertension. *Circulation.* 2005;112:423-431.
33. Ghofrani HA, Seeger W, Grimminger F. Imatinib for the treatment of pulmonary arterial hypertension. *N Engl J Med.* 2005;353:1412-1413.
34. Patterson KC, Weissmann A, Ahmadi T, Farber HW. Imatinib mesylate in the treatment of refractory idiopathic pulmonary arterial hypertension. *Ann Intern Med.* 2006;145:152-153.
35. Lane KB, Machado RD, Pauciulo MW, Thomson JR, Phillips JA, 3rd, Loyd JE, Nichols WC, Trembath RC. Heterozygous germline mutations in BMPR2, encoding a TGF-beta receptor, cause familial primary pulmonary hypertension. The International PPH Consortium. *Nat Genet.* 2000;26:81-84.
36. Deng Z, Morse JH, Slager SL, Cuervo N, Moore KJ, Venetos G, Kalachikov S, Cayanis E, Fischer SG, Barst RJ, Hodge SE, Knowles JA. Familial primary pulmonary hypertension (gene PPH1) is caused by mutations in the bone morphogenetic protein receptor-II gene. *Am J Hum Genet.* 2000;67:737-744.
37. Newman JH, Trembath RC, Morse JA, Grunig E, Loyd JE, Adnot S, Coccolo F, Ventura C, Phillips JA, 3rd, Knowles JA, Janssen B, Eickelberg O, Eddahibi S, Herve P, Nichols WC, Elliott G. Genetic basis of pulmonary arterial hypertension: current understanding and future directions. *J Am Coll Cardiol.* 2004;43:33S-39S.
38. Humbert M, Deng Z, Simonneau G, Barst RJ, Sitbon O, Wolf M, Cuervo N, Moore KJ, Hodge SE, Knowles JA, Morse JH. BMPR2 germline mutations in pulmonary hypertension associated with fenfluramine derivatives. *Eur Respir J.* 2002;20:518-523.
39. Roberts KE, McElroy JJ, Wong WP, Yen E, Widlitz A, Barst RJ, Knowles JA, Morse JH. BMPR2 mutations in pulmonary arterial hypertension with congenital heart disease. *Eur Respir J.* 2004;24:371-374.
40. Atkinson C, Stewart S, Upton PD, Machado R, Thomson JR, Trembath RC, Morrell NW. Primary pulmonary hypertension is associated with reduced pulmonary vascular expression of type II bone morphogenetic protein receptor. *Circulation.* 2002;105:1672-1678.
41. Yuan JX, Rubin LJ. Pathogenesis of pulmonary arterial hypertension: the need for multiple hits. *Circulation.* 2005;111:534-538.
42. He W, Barak Y, Hevener A, Olson P, Liao D, Le J, Nelson M, Ong E, Olefsky JM, Evans RM. Adipose-specific peroxisome proliferator-activated receptor gamma knockout causes insulin resistance in fat and liver but not in muscle. *Proc Natl Acad Sci U S A.* 2003;100:15712-15717.
43. Lehrke M, Lazar MA. The many faces of PPARgamma. *Cell.* 2005;123:993-999.
44. Hevener AL, He W, Barak Y, Le J, Bandyopadhyay G, Olson P, Wilkes J, Evans RM, Olefsky J. Muscle-specific Pparg deletion causes insulin resistance. *Nat Med.* 2003;9:1491-1497.
45. Marx N, Duez H, Fruchart JC, Staels B. Peroxisome proliferator-activated receptors and atherogenesis: regulators of gene expression in vascular cells. *Circ Res.* 2004;94:1168-1178.
46. Gilde AJ, Fruchart JC, Staels B. Peroxisome proliferator-activated receptors at the crossroads of obesity, diabetes, and cardiovascular disease. *J Am Coll Cardiol.* 2006;48:A24-32.
47. Armoni M, Kritz N, Harel C, Bar-Yoseph F, Chen H, Quon MJ, Karnieli E. Peroxisome proliferator-activated receptor-gamma represses GLUT4 promoter activity in primary adipocytes, and rosiglitazone alleviates this effect. *J Biol Chem.* 2003;278:30614-30623.
48. Kintscher U, Law RE. PPARgamma-mediated insulin sensitization: the importance of fat versus muscle. *Am J Physiol Endocrinol Metab.* 2005;288:E287-E291.
49. Combs CK, Johnson DE, Karlo JC, Cannady SB, Landreth GE. Inflammatory mechanisms in Alzheimer's disease: inhibition of beta-amyloid-stimulated proinflammatory responses and neurotoxicity by PPARgamma agonists. *J Neuroscience.* 2000;20:558-567.

50. Pfützner A, Marx N, Lübben G, Langenfeld M, Walcher D, Konrad T, Forst T. Improvement of cardiovascular risk markers by pioglitazone is independent from glycemic control: results from the pioneer study. *Journal of the American College of Cardiology.* 2005;45:1925-1931.
51. Ikeda Y, Yonemitsu Y, Kataoka C, Kitamoto S, Yamaoka T, Nishida K, Takeshita A, Egashira K, Sueishi K. Anti-monocyte chemoattractant protein-1 gene therapy attenuates pulmonary hypertension in rats. *Am J Physiol Heart Circ Physiol.* 2002;283:H2021-2028.
52. Sanchez O, Marcos E, Perros F, Fadel E, Tu L, Humbert M, Dartevelle P, Simonneau G, Adnot S, Eddahibi S. Role of endothelium-derived CC chemokine ligand 2 in idiopathic pulmonary arterial hypertension. *Am J Respir Crit Care Med.* 2007;176:1041-1047.
53. Martin-Nizard F, Furman C, Delerive P, Kandoussi A, Fruchart JC, Staels B, Duriez P. Peroxisome proliferator-activated receptor activators inhibit oxidized low-density lipoprotein-induced endothelin-1 secretion in endothelial cells. *J Cardiovasc Pharmacol.* 2002;40:822-831.
54. Delerive P, Martin-Nizard F, Chinetti G, Trottein F, Fruchart JC, Najib J, Duriez P, Staels B. Peroxisome proliferator-activated receptor activators inhibit thrombin-induced endothelin-1 production in human vascular endothelial cells by inhibiting the activator protein-1 signaling pathway. *Circ Res.* 1999;85:394-402.
55. Wakino S, Hayashi K, Tatematsu S, Hasegawa K, Takamatsu I, Kanda T, Homma K, Yoshioka K, Sugano N, Saruta T. Pioglitazone lowers systemic asymmetric dimethylarginine by inducing dimethylarginine dimethylaminohydrolase in rats. *Hypertens Res.* 2005;28:255-262.
56. Stühlinger MC, Abbasi F, Chu JW, Lamendola C, McLaughlin TL, Cooke JP, Reaven GM, Tsao PS. Relationship between insulin resistance and an endogenous nitric oxide synthase inhibitor. *JAMA.* 2002;287:1420-1426.
57. Benkirane K, Amiri F, Diep QN, El Mabrouk M, Schiffrin EL. PPAR-gamma inhibits ANG II-induced cell growth via SHIP2 and 4E-BP1. *Am J Physiol Heart Circ Physiol.* 2006;290:H390-H397.
58. Wakino S, Kintscher U, Liu Z, Kim S, Yin F, Ohba M, Kuroki T, Schonthal AH, Hsueh WA, Law RE. Peroxisome proliferator-activated receptor gamma ligands inhibit mitogenic induction of p21(Cip1) by modulating the protein kinase Cdelta pathway in vascular smooth muscle cells. *J Biol Chem.* 2001;276:47650-47657.
59. Law RE, Goetze S, Xi XP, Jackson S, Kawano Y, Demer L, Fishbein MC, Meehan WP, Hsueh WA. Expression and function of PPARgamma in rat and human vascular smooth muscle cells. *Circulation.* 2000;101:1311-1318.
60. Kosuge H, Haraguchi G, Koga N, Maejima Y, Suzuki J, Isobe M. Pioglitazone prevents acute and chronic cardiac allograft rejection. *Circulation.* 2006;113:2613-2622.
61. Sottile V, Seuwen K. Bone morphogenetic protein-2 stimulates adipogenic differentiation of mesenchymal precursor cells in synergy with BRL 49653 (rosiglitazone). *FEBS Lett.* 2000;475:201-204.
62. Bachner D, Ahrens M, Schroder D, Hoffmann A, Lauber J, Betat N, Steinert P, Flohe L, Gross G. BMP-2 downstream targets in mesenchymal development identified by subtractive cloning from recombinant mesenchymal progenitors (C3H10T1/2). *Dev Dyn.* 1998;213:398-411.
63. Akiyama TE, Sakai S, Lambert G, Nicol CJ, Matsusue K, Pimprale S, Lee YH, Ricote M, Glass CK, Brewer HB, Jr., Gonzalez FJ. Conditional disruption of the peroxisome proliferator-activated receptor gamma gene in mice results in lowered expression of ABCA1, ABCG1, and apoE in macrophages and reduced cholesterol efflux. *Mol Cell Biol.* 2002;22:2607-2619.
64. Yue L, Rasouli N, Ranganathan G, Kern PA, Mazzone T. Divergent effects of peroxisome proliferator-activated receptor gamma agonists and tumor necrosis factor alpha on adipocyte ApoE expression. *J Biol Chem.* 2004;279:47626-47632.
65. Duan SZ, Usher MG, Mortensen RM. Peroxisome proliferator-activated receptor-gamma-mediated effects in the vasculature. *Circ Res.* 2008;102:283-294.
66. Ameshima S, Golpon H, Cool CD, Chan D, Vandivier RW, Gardai SJ, Wick M, Nemenoff RA, Geraci MW, Voelkel NF. Peroxisome proliferator-activated receptor gamma (PPARgamma) expression is decreased in pulmonary hypertension and affects endothelial cell growth. *Circ Res.* 2003;92:1162-1169.
67. Geraci MW, Moore M, Gesell T, Yeager ME, Alger L, Golpon H, Gao B, Loyd JE, Tuder RM, Voelkel NF. Gene expression patterns in the lungs of patients with primary pulmonary hypertension: a gene microarray analysis. *Circ Res.* 2001;88:555-562.
68. Hansmann G, de Jesus Perez VA, Alastalo TP, Alvira CM, Guignabert C, Bekker JM, Schellong S, Urashima T, Wang L, Morrell NW, Rabinovitch M. An antiproliferative BMP-2/PPARgamma/apoE axis in human and murine SMCs and its role in pulmonary hypertension. *J Clin Invest.* 2008;118:1846-1857.
69. Weiss R, Dziura J, Burgert TS, Tamborlane WV, Taksali SE, Yeckel CW, Allen K, Lopes M, Savoye M, Morrison J, Sherwin RS, Caprio S. Obesity and the metabolic syndrome in children and adolescents. *N Engl J Med.* 2004;350:2362-2374.
70. Eckel RH, Grundy SM, Zimmet PZ. The metabolic syndrome. *Lancet.* 2005;365:1415-1428.
71. Opie LH. Metabolic syndrome. *Circulation.* 2007;115:e32-35.

72. DeFronzo RA, Ferrannini E. Insulin resistance. A multifaceted syndrome responsible for NIDDM, obesity, hypertension, dyslipidemia, and atherosclerotic cardiovascular disease. *Diabetes Care.* 1991;14:173-194.
73. Kaplan NM. The deadly quartet. Upper-body obesity, glucose intolerance, hypertriglyceridemia, and hypertension. *Arch Intern Med.* 1989;149:1514-1520.
74. Alberti KG, Zimmet PZ. Definition, diagnosis and classification of diabetes mellitus and its complications. Part 1: diagnosis and classification of diabetes mellitus provisional report of a WHO consultation. *Diabet Med.* 1998;15:539-553.
75. Executive Summary of The Third Report of The National Cholesterol Education Program (NCEP) Expert Panel on Detection, Evaluation, And Treatment of High Blood Cholesterol In Adults (Adult Treatment Panel III). *Jama.* 2001;285:2486-2497.
76. Alberti KG, Zimmet P, Shaw J. Metabolic syndrome--a new world-wide definition. A Consensus Statement from the International Diabetes Federation. *Diabet Med.* 2006;23:469-480.
77. Hanley AJ, Karter AJ, Williams K, Festa A, D'Agostino RB, Jr., Wagenknecht LE, Haffner SM. Prediction of type 2 diabetes mellitus with alternative definitions of the metabolic syndrome: the Insulin Resistance Atherosclerosis Study. *Circulation.* 2005;112:3713-3721.
78. Greenow K, Pearce NJ, Ramji DP. The key role of apolipoprotein E in atherosclerosis. *J Mol Med.* 2005;83:329-342.
79. Giaid A, Yanagisawa M, Langleben D, Michel RP, Levy R, Shennib H, Kimura S, Masaki T, Duguid WP, Stewart DJ. Expression of endothelin-1 in the lungs of patients with pulmonary hypertension. *N Engl J Med.* 1993;328:1732-1739.
80. Wang TD, Chen WJ, Cheng WC, Lin JW, Chen MF, Lee YT. Relation of improvement in endothelium-dependent flow-mediated vasodilation after rosiglitazone to changes in asymmetric dimethylarginine, endothelin-1, and C-reactive protein in nondiabetic patients with the metabolic syndrome. *Am J Cardiol.* 2006;98:1057-1062.
81. Humbert M, Monti G, Brenot F, Sitbon O, Portier A, Grangeot-Keros L, Duroux P, Galanaud P, Simonneau G, Emilie D. Increased interleukin-1 and interleukin-6 serum concentrations in severe primary pulmonary hypertension. *Am J Respir Crit Care Med.* 1995;151:1628-1631.
82. Lazar MA. The humoral side of insulin resistance. *Nat Med.* 2006;12:43-44.
83. Yamauchi T, Kamon J, Waki H, Terauchi Y, Kubota N, Hara K, Mori Y, Ide T, Murakami K, Tsuboyama-Kasaoka N, Ezaki O, Akanuma Y, Gavrilova O, Vinson C, Reitman ML, Kagechika H, Shudo K, Yoda M, Nakano Y, Tobe K, Nagai R, Kimura S, Tomita M, Froguel P, Kadowaki T. The fat-derived hormone adiponectin reverses insulin resistance associated with both lipoatrophy and obesity. *Nat Med.* 2001;7:941-946.
84. Spranger J, Kroke A, Möhlig M, Bergmann MM, Ristow M, Boeing H, Pfeiffer AF. Adiponectin and protection against type 2 diabetes mellitus. *Lancet.* 2003;361:226-228.
85. Winer JC, Zern TL, Taksali SE, Dziura J, Cali AM, Wollschlager M, Seyal AA, Weiss R, Burgert TS, Caprio S. Adiponectin in Childhood and Adolescent Obesity and Its Association with Inflammatory Markers and Components of the Metabolic Syndrome. *J Clin Endocrinol Metab.* 2006.
86. Yudkin JS, Eringa E, Stehouwer CD. "Vasocrine" signalling from perivascular fat: a mechanism linking insulin resistance to vascular disease. *Lancet.* 2005;365:1817-1820.
87. Bedi D, Clarke KJ, Dennis JC, Zhong Q, Brunson BL, Morrison EE, Judd RL. Endothelin-1 inhibits adiponectin secretion through a phosphatidylinositol 4,5-bisphosphate/actin-dependent mechanism. *Biochem Biophys Res Commun.* 2006;345:332-339.
88. Ottosson-Seeberger A, Lundberg JM, Alvestrand A, Ahlborg G. Exogenous endothelin-1 causes peripheral insulin resistance in healthy humans. *Acta Physiol Scand.* 1997;161:211-220.
89. Verma S, Arikawa E, Lee S, Dumont AS, Yao L, McNeill JH. Exaggerated coronary reactivity to endothelin-1 in diabetes: reversal with bosentan. *Can J Physiol Pharmacol.* 2002;80:980-986.
90. Kielstein JT, Bode-Böger SM, Hesse G, Martens-Lobenhoffer J, Takacs A, Fliser D, Hoeper MM. Asymmetrical dimethylarginine in idiopathic pulmonary arterial hypertension. *Arterioscler Thromb Vasc Biol.* 2005;25:1414-1418.
91. Galetto R, Albajar M, Polanco JI, Zakin MM, Rodriguez-Rey JC. Identification of a peroxisome-proliferator-activated-receptor response element in the apolipoprotein E gene control region. *Biochem J.* 2001;357:521-527.
92. Zeleny M, Swertfeger DK, Weisgraber KH, Hui DY. Distinct apolipoprotein E isoform preference for inhibition of smooth muscle cell migration and proliferation. *Biochemistry.* 2002;41:11820-11823.
93. Ishigami M, Swertfeger DK, Granholm NA, Hui DY. Apolipoprotein E inhibits platelet-derived growth factor-induced vascular smooth muscle cell migration and proliferation by suppressing signal transduction and preventing cell entry to G1 phase. *J Biol Chem.* 1998;273:20156-20161.
94. Boucher P, Gotthardt M, Li WP, Anderson RG, Herz J. LRP: role in vascular wall integrity and protection from atherosclerosis. *Science.* 2003;300:329-332.

95. Newton CS, Loukinova E, Mikhailenko I, Ranganathan S, Gao Y, Haudenschild C, Strickland DK. Platelet-derived growth factor receptor-beta (PDGFR-beta) activation promotes its association with the low density lipoprotein receptor-related protein (LRP). Evidence for co-receptor function. *J Biol Chem.* 2005;280:27872-27878.
96. Lassila M, Allen TJ, Cao Z, Thallas V, Jandeleit-Dahm KA, Candido R, Cooper ME. Imatinib attenuates diabetes-associated atherosclerosis. *Arterioscler Thromb Vasc Biol.* 2004;24:935-942.
97. Humbert M, Monti G, Fartoukh M, Magnan A, Brenot F, Rain B, Capron F, Galanaud P, Duroux P, Simonneau G, Emilie D. Platelet-derived growth factor expression in primary pulmonary hypertension: comparison of HIV seropositive and HIV seronegative patients. *Eur Respir J.* 1998;11:554-559.
98. Ghosh SS, Gehr TWB, Ghosh S, Fakhry I, Sica DA, Lyall V, Schoolwerth AC. PPARgamma ligand attenuates PDGF-induced mesangial cell proliferation: role of MAP kinase. *Kidney Int.* 2003;64:52-62.
99. Goetze S, Kintscher U, Kim S, Meehan WP, Kaneshiro K, Collins AR, Fleck E, Hsueh WA, Law RE. Peroxisome proliferator-activated receptor-gamma ligands inhibit nuclear but not cytosolic extracellular signal-regulated kinase/mitogen-activated protein kinase-regulated steps in vascular smooth muscle cell migration. *J Cardiovasc Pharmacol.* 2001;38:909-921.
100. Hu E, Kim JB, Sarraf P, Spiegelman BM. Inhibition of adipogenesis through MAP kinase-mediated phosphorylation of PPARgamma. *Science.* 1996;274:2100-2103.
101. Zhang J, Fu M, Zhao L, Chen YE. 15-Deoxy-prostaglandin J(2) inhibits PDGF-A and -B chain expression in human vascular endothelial cells independent of PPAR gamma. *Biochemical and biophysical research communications.* 2002;298:128-132.
102. Gauthier A, Vassiliou G, Benoist F, McPherson R. Adipocyte low density lipoprotein receptor-related protein gene expression and function is regulated by peroxisome proliferator-activated receptor gamma. *J Biol Chem.* 2003;278:11945-11953.
103. Wakino S, Kintscher U, Kim S, Yin F, Hsueh WA, Law RE. Peroxisome proliferator-activated receptor gamma ligands inhibit retinoblastoma phosphorylation and G1--> S transition in vascular smooth muscle cells. *J Biol Chem.* 2000;275:22435-22441.
104. Ogawa D, Nomiyama T, Nakamachi T, Heywood EB, Stone JF, Berger JP, Law RE, Bruemmer D. Activation of peroxisome proliferator-activated receptor gamma suppresses telomerase activity in vascular smooth muscle cells. *Circ Res.* 2006;98:e50-59.
105. Vantler M, Caglayan E, Zimmermann WH, Baumer AT, Rosenkranz S. Systematic evaluation of anti-apoptotic growth factor signaling in vascular smooth muscle cells. Only phosphatidylinositol 3'-kinase is important. *J Biol Chem.* 2005;280:14168-14176.
106. Bruemmer D, Yin F, Liu J, Berger JP, Sakai T, Blaschke F, Fleck E, Van Herle AJ, Forman BM, Law RE. Regulation of the growth arrest and DNA damage-inducible gene 45 (GADD45) by peroxisome proliferator-activated receptor gamma in vascular smooth muscle cells. *Circ Res.* 2003;93:e38-e47.
107. Worley JR, Baugh MD, Hughes DA, Edwards DR, Hogan A, Sampson MJ, Gavrilovic J. Metalloproteinase expression in PMA-stimulated THP-1 cells. Effects of peroxisome proliferator-activated receptor-gamma (PPAR gamma) agonists and 9-cis-retinoic acid. *J Biol Chem.* 2003;278:51340-51346.
108. Nagase H, Enghild JJ, Suzuki K, Salvesen G. Stepwise activation mechanisms of the precursor of matrix metalloproteinase 3 (stromelysin) by proteinases and (4-aminophenyl)mercuric acetate. *Biochemistry.* 1990;29:5783-5789.
109. Cowan KN, Heilbut A, Humpl T, Lam C, Ito S, Rabinovitch M. Complete reversal of fatal pulmonary hypertension in rats by a serine elastase inhibitor. *Nat Med.* 2000;6:698-702.
110. Nakaoka T, Gonda K, Ogita T, Otawara-Hamamoto Y, Okabe F, Kira Y, Harii K, Miyazono K, Takuwa Y, Fujita T. Inhibition of rat vascular smooth muscle proliferation in vitro and in vivo by bone morphogenetic protein-2. *J Clin Invest.* 1997;100:2824-2832.
111. Risner ME, Saunders AM, Altman JF, Ormandy GC, Craft S, Foley IM, Zvartau-Hind ME, Hosford DA, Roses AD. Efficacy of rosiglitazone in a genetically defined population with mild-to-moderate Alzheimer's disease. *Pharmacogenomics J.* 2006;6:246-254.
112. Arita Y, Kihara S, Ouchi N, Maeda K, Kuriyama H, Okamoto Y, Kumada M, Hotta K, Nishida M, Takahashi M, Nakamura T, Shimomura I, Muraguchi M, Ohmoto Y, Funahashi T, Matsuzawa Y. Adipocyte-derived plasma protein adiponectin acts as a platelet-derived growth factor-BB-binding protein and regulates growth factor-induced common postreceptor signal in vascular smooth muscle cell. *Circulation.* 2002;105:2893-2898.
113. Boucher P, Gotthardt M. LRP and PDGF signaling: a pathway to atherosclerosis. *Trends Cardiovasc Med.* 2004;14:55-60.
114. Wang Y, Lam KS, Xu JY, Lu G, Xu LY, Cooper GJ, Xu A. Adiponectin inhibits cell proliferation by interacting with several growth factors in an oligomerization-dependent manner. *J Biol Chem.* 2005;280:18341-18347.
115. Wagenvoort CA. Pulmonary Atherosclerosis. In: Wagenvoort CA, Heath D, Edwards JE, eds. *The Pathology of the Pulmonary Vasuclature.* Springfield, IL: Charles C Thomas; 1964:58-59.

116. Xu A, Chan KW, Hoo RL, Wang Y, Tan KC, Zhang J, Chen B, Lam M, Tse C, Cooper GJ, Lam KS. Testosterone selectively reduces the high molecular weight form of adiponectin by inhibiting its secretion from adipocytes. *J Biol Chem.* 2005;280:18073-18080.
117. Phillips JW, Barringhaus KG, Sanders JM, Yang Z, Chen M, Hesselbacher SS, Czarnik AC, Ley K, Nadler J, Sarembock IJ. Rosiglitazone reduces the accelerated neointima formation after arterial injury in a mouse injury model of type 2 diabetes. *Circulation.* 2003;108:1994-1999.
118. Hansmann G, Wagner RA, Schellong S, Perez VA, Urashima T, Wang L, Sheikh AY, Suen RS, Stewart DJ, Rabinovitch M. Pulmonary arterial hypertension is linked to insulin resistance and reversed by peroxisome proliferator-activated receptor-gamma activation. *Circulation.* 2007;115:1275-1284.
119. Yuditskaya S, Tumblin A, Hoehn GT, Wang G, Drake SK, Xu X, Ying S, Chi AH, Remaley AT, Shen RF, Munson PJ, Suffredini AF, Kato GJ. Proteomic identification of altered apolipoprotein patterns in pulmonary hypertension and vasculopathy of sickle cell disease. *Blood.* 2008.
120. Zamanian RT, Hansmann G, Snook S, Lilienfeld D, Rappaport KM, Reaven GM, Rabinovitch M, Doyle RL. Insulin resistance in pulmonary arterial hypertension. *Eur Respir J.* 2008.
121. Brehm A, Pfeiler G, Pacini G, Vierhapper H, Roden M. Relationship between serum lipoprotein ratios and insulin resistance in obesity. *Clin Chem.* 2004;50:2316-2322.
122. McLaughlin T, Abbasi F, Cheal K, Chu J, Lamendola C, Reaven G. Use of metabolic markers to identify overweight individuals who are insulin resistant. *Ann Intern Med.* 2003;139:802-809.
123. Dokras A, Bochner M, Hollinrake E, Markham S, Vanvoorhis B, Jagasia DH. Screening women with polycystic ovary syndrome for metabolic syndrome. *Obstet Gynecol.* 2005;106:131-137.
124. Doehner W, Rauchhaus M, Ponikowski P, Godsland IF, von Haehling S, Okonko DO, Leyva F, Proudler AJ, Coats AJ, Anker SD. Impaired insulin sensitivity as an independent risk factor for mortality in patients with stable chronic heart failure. *J Am Coll Cardiol.* 2005;46:1019-1026.
125. Suskin N, McKelvie RS, Burns RJ, Latini R, Pericak D, Probstfield J, Rouleau JL, Sigouin C, Solymoss CB, Tsuyuki R, White M, Yusuf S. Glucose and insulin abnormalities relate to functional capacity in patients with congestive heart failure. *Eur Heart J.* 2000;21:1368-1375.
126. Swan JW, Anker SD, Walton C, Godsland IF, Clark AL, Leyva F, Stevenson JC, Coats AJ. Insulin resistance in chronic heart failure: relation to severity and etiology of heart failure. *J Am Coll Cardiol.* 1997;30:527-532.
127. Dessein PH, Joffe BI. Insulin resistance and impaired beta cell function in rheumatoid arthritis. *Arthritis Rheum.* 2006;54:2765-2775.
128. Engelson ES, Agin D, Kenya S, Werber-Zion G, Luty B, Albu JB, Kotler DP. Body composition and metabolic effects of a diet and exercise weight loss regimen on obese, HIV-infected women. *Metabolism.* 2006;55:1327-1336.
129. Escarcega RO, Garcia-Carrasco M, Fuentes-Alexandro S, Jara LJ, Rojas-Rodriguez J, Escobar-Linares LE, Cervera R. Insulin resistance, chronic inflammatory state and the link with systemic lupus erythematosus-related coronary disease. *Autoimmun Rev.* 2006;6:48-53.
130. Lee WC, Chen JJ, Hunt DD, Hou CW, Lai YC, Lin FC, Chen CY, Lin CH, Liao YH, Kuo CH. Effects of hiking at altitude on body composition and insulin sensitivity in recovering drug addicts. *Prev Med.* 2004;39:681-688.
131. Paolisso G, Valentini G, Giugliano D, Marrazzo G, Tirri R, Gallo M, Tirri G, Varricchio M, D'Onofrio F. Evidence for peripheral impaired glucose handling in patients with connective tissue diseases. *Metabolism.* 1991;40:902-907.
132. Nishiyama Y, Minohara M, Ohe M, Hirai Y, Katoh A, Miyamoto T, Iwami G, Nakata M, Koga Y. Effect of physical training on insulin resistance in patients with chronic heart failure. *Circ J.* 2006;70:864-867.
133. Said SA, Ammar el SM, Suddek GM. Effect of bosentan (ETA/ETB receptor antagonist) on metabolic changes during stress and diabetes. *Pharmacol Res.* 2005;51:107-115.
134. Verma S, Arikawa E, McNeill JH. Long-term endothelin receptor blockade improves cardiovascular function in diabetes. *Am J Hypertens.* 2001;14:679-687.
135. Haffner SM, Greenberg AS, Weston WM, Chen H, Williams K, Freed MI. Effect of rosiglitazone treatment on nontraditional markers of cardiovascular disease in patients with type 2 diabetes mellitus. *Circulation.* 2002;106:679-684.
136. Wang TD, Chen WJ, Lin JW, Chen MF, Lee YT. Effects of rosiglitazone on endothelial function, C-reactive protein, and components of the metabolic syndrome in nondiabetic patients with the metabolic syndrome. *Am J Cardiol.* 2004;93:362-365.
137. Chu JW, Abbasi F, Lamendola C, McLaughlin T, Reaven GM, Tsao PS. Effect of rosiglitazone treatment on circulating vascular and inflammatory markers in insulin-resistant subjects. *Diab Vasc Dis Res.* 2005;2:37-41.
138. Kato H, Kashiwagi H, Shiraga M, Tadokoro S, Kamae T, Ujiie H, Honda S, Miyata S, Ijiri Y, Yamamoto J, Maeda N, Funahashi T, Kurata Y, Shimomura I, Tomiyama Y, Kanakura Y. Adiponectin acts as an endogenous antithrombotic factor. *Arterioscler Thromb Vasc Biol.* 2006;26:224-230.
139. Loirand G, Guerin P, Pacaud P. Rho kinases in cardiovascular physiology and pathophysiology. *Circ Res.* 2006;98:322-334.

140. Wakino S, Hayashi K, Kanda T, Tatematsu S, Homma K, Yoshioka K, Takamatsu I, Saruta T. Peroxisome proliferator-activated receptor gamma ligands inhibit Rho/Rho kinase pathway by inducing protein tyrosine phosphatase SHP-2. *Circ Res.* 2004;95:e45-55.
141. Abe K, Shimokawa H, Morikawa K, Uwatoku T, Oi K, Matsumoto Y, Hattori T, Nakashima Y, Kaibuchi K, Sueishi K, Takeshit A. Long-term treatment with a Rho-kinase inhibitor improves monocrotaline-induced fatal pulmonary hypertension in rats. *Circ Res.* 2004;94:385-393.
142. Fukumoto Y, Matoba T, Ito A, Tanaka H, Kishi T, Hayashidani S, Abe K, Takeshita A, Shimokawa H. Acute vasodilator effects of a Rho-kinase inhibitor, fasudil, in patients with severe pulmonary hypertension. *Heart.* 2005;91:391-392.
143. Nissen SE, Wolski K. Effect of rosiglitazone on the risk of myocardial infarction and death from cardiovascular causes. *N Engl J Med.* 2007;356:2457-2471.
144. Home PD, Pocock SJ, Beck-Nielsen H, Gomis R, Hanefeld M, Jones NP, Komajda M, McMurray JJ. Rosiglitazone evaluated for cardiovascular outcomes--an interim analysis. *N Engl J Med.* 2007;357:28-38.
145. Singh S, Loke YK, Furberg CD. Long-term risk of cardiovascular events with rosiglitazone: a meta-analysis. *JAMA.* 2007;298:1189-1195.
146. Dargie HJ, Hildebrandt PR, Riegger GA, McMurray JJ, McMorn SO, Roberts JN, Zambanini A, Wilding JP. A randomized, placebo-controlled trial assessing the effects of rosiglitazone on echocardiographic function and cardiac status in type 2 diabetic patients with New York Heart Association Functional Class I or II Heart Failure. *J Am Coll Cardiol.* 2007;49:1696-1704.
147. Cleland JG, Atkin SL. Thiazolidinediones, deadly sins, surrogates, and elephants. *Lancet.* 2007;370:1103-1104.
148. Dormandy JA, Charbonnel B, Eckland DJ, Erdmann E, Massi-Benedetti M, Moules IK, Skene AM, Tan MH, Lefèbvre PJ, Murray GD, Standl E, Wilcox RG, Wilhelmsen L, Betteridge J, Birkeland K, Golay A, Heine RJ, Korányi L, Laakso M, Mokán M, Norkus A, Pirags V, Podar T, Scheen A, Scherbaum W, Schernthaner G, Schmitz O, Skrha J, Smith U, Taton J. Secondary prevention of macrovascular events in patients with type 2 diabetes in the PROactive Study (PROspective pioglitAzone Clinical Trial In macroVascular Events): a randomised controlled trial. *Lancet.* 2005;366:1279-1289.
149. Erdmann E, Dormandy JA, Charbonnel B, Massi-Benedetti M, Moules IK, Skene AM. The effect of pioglitazone on recurrent myocardial infarction in 2,445 patients with type 2 diabetes and previous myocardial infarction: results from the PROactive (PROactive 05) Study. *J Am Coll Cardiol.* 2007;49:1772-1780.
150. Lincoff AM, Wolski K, Nicholls SJ, Nissen SE. Pioglitazone and risk of cardiovascular events in patients with type 2 diabetes mellitus: a meta-analysis of randomized trials. *JAMA.* 2007;298:1180-1188.
151. Karter AJ, Ahmed AT, Liu J, Moffet HH, Parker MM. Pioglitazone initiation and subsequent hospitalization for congestive heart failure. *Diabet Med.* 2005;22:986-993.
152. Gerstein HC, Yusuf S, Bosch J, Pogue J, Sheridan P, Dinccag N, Hanefeld M, Hoogwerf B, Laakso M, Mohan V, Shaw J, Zinman B, Holman RR. Effect of rosiglitazone on the frequency of diabetes in patients with impaired glucose tolerance or impaired fasting glucose: a randomised controlled trial. *Lancet.* 2006;368:1096-1105.
153. Kahn SE, Haffner SM, Heise MA, Herman WH, Holman RR, Jones NP, Kravitz BG, Lachin JM, O'Neill MC, Zinman B, Viberti G. Glycemic durability of rosiglitazone, metformin, or glyburide monotherapy. *N Engl J Med.* 2006;355:2427-2443.
154. Lago RM, Singh PP, Nesto RW. Congestive heart failure and cardiovascular death in patients with prediabetes and type 2 diabetes given thiazolidinediones: a meta-analysis of randomised clinical trials. *Lancet.* 2007;370:1129-1136.
155. Schermuly R, Yilmaz H, Ghofrani H, Woyda K, Pullamsetti S, Schulz A, Gessler T, Dumitrascu R, Weissmann N, Grimminger, Seeger W. Inhaled iloprost reverses vascular remodeling in chronic experimental pulmonary hypertension. *American journal of respiratory and critical care medicine.* 2005;172:358-363.
156. Hoekstra R, Dumez H, Eskens FA, van der Gaast A, Planting AS, de Heus G, Sizer KC, Ravera C, Vaidyanathan S, Bucana C, Fidler IJ, van Oosterom AT, Verweij J. Phase I and pharmacologic study of PKI166, an epidermal growth factor receptor tyrosine kinase inhibitor, in patients with advanced solid malignancies. *Clin Cancer Res.* 2005;11:6908-6915.
157. Klein M, Schermuly RT, Ellinghaus P, Milting H, Riedl B, Nikolova S, Pullamsetti SS, Weissmann N, Dony E, Savai R, Ghofrani HA, Grimminger F, Busch AE, Schafer S. Combined tyrosine and serine/threonine kinase inhibition by sorafenib prevents progression of experimental pulmonary hypertension and myocardial remodeling. *Circulation.* 2008;118:2081-2090.
158. Escudier B, Eisen T, Stadler WM, Szczylik C, Oudard S, Siebels M, Negrier S, Chevreau C, Solska E, Desai AA, Rolland F, Demkow T, Hutson TE, Gore M, Freeman S, Schwartz B, Shan M, Simantov R, Bukowski RM. Sorafenib in advanced clear-cell renal-cell carcinoma. *N Engl J Med.* 2007;356:125-134.
159. Ishikura K, Yamada N, Ito M, Ota S, Nakamura M, Isaka N, Nakano T. Beneficial acute effects of rho-kinase inhibitor in patients with pulmonary arterial hypertension. *Circ J.* 2006;70:174-178.

160. Oka M, Homma N, Taraseviciene-Stewart L, Morris KG, Kraskauskas D, Burns N, Voelkel NF, McMurtry IF. Rho kinase-mediated vasoconstriction is important in severe occlusive pulmonary arterial hypertension in rats. *Circ Res.* 2007;100:923-929.
161. Nishimura T, Vaszar LT, Faul JL, Zhao G, Berry GJ, Shi L, Qiu D, Benson G, Pearl RG, Kao PN. Simvastatin rescues rats from fatal pulmonary hypertension by inducing apoptosis of neointimal smooth muscle cells. *Circulation.* 2003;108:1640-1645.
162. Kao PN. Simvastatin treatment of pulmonary hypertension: an observational case series. *Chest.* 2005;127:1446-1452.
163. Guignabert C, Raffestin B, Benferhat R, Raoul W, Zadigue P, Rideau D, Hamon M, Adnot S, Eddahibi S. Serotonin transporter inhibition prevents and reverses monocrotaline-induced pulmonary hypertension in rats. *Circulation.* 2005;111:2812-2819.
164. Guignabert C, Izikki M, Tu LI, Li Z, Zadigue P, Barlier-Mur AM, Hanoun N, Rodman D, Hamon M, Adnot S, Eddahibi S. Transgenic mice overexpressing the 5-hydroxytryptamine transporter gene in smooth muscle develop pulmonary hypertension. *Circ Res.* 2006;98:1323-1330.
165. Matsuda Y, Hoshikawa Y, Ameshima S, Suzuki S, Okada Y, Tabata T, Sugawara T, Matsumura Y, Kondo T. [Effects of peroxisome proliferator-activated receptor gamma ligands on monocrotaline-induced pulmonary hypertension in rats]. *Nihon Kokyuki Gakkai Zasshi.* 2005;43:283-288.
166. Crossno JT, Jr., Garat CV, Reusch JE, Morris KG, Dempsey EC, McMurtry IF, Stenmark KR, Klemm DJ. Rosiglitazone attenuates hypoxia-induced pulmonary arterial remodeling. *Am J Physiol Lung Cell Mol Physiol.* 2007;292:L885-897.
167. Michelakis ED, McMurtry MS, Wu XC, Dyck JR, Moudgil R, Hopkins TA, Lopaschuk GD, Puttagunta L, Waite R, Archer SL. Dichloroacetate, a metabolic modulator, prevents and reverses chronic hypoxic pulmonary hypertension in rats: role of increased expression and activity of voltage-gated potassium channels. *Circulation.* 2002;105:244-250.
168. McMurtry MS, Bonnet S, Wu X, Dyck JR, Haromy A, Hashimoto K, Michelakis ED. Dichloroacetate prevents and reverses pulmonary hypertension by inducing pulmonary artery smooth muscle cell apoptosis. *Circ Res.* 2004;95:830-840.
169. Bonnet S, Archer SL, Allalunis-Turner J, Haromy A, Beaulieu C, Thompson R, Lee CT, Lopaschuk GD, Puttagunta L, Bonnet S, Harry G, Hashimoto K, Porter CJ, Andrade MA, Thebaud B, Michelakis ED. A mitochondria-K+ channel axis is suppressed in cancer and its normalization promotes apoptosis and inhibits cancer growth. *Cancer Cell.* 2007;11:37-51.
170. Bonnet S, Rochefort G, Sutendra G, Archer SL, Haromy A, Webster L, Hashimoto K, Bonnet SN, Michelakis ED. The nuclear factor of activated T cells in pulmonary arterial hypertension can be therapeutically targeted. *Proc Natl Acad Sci U S A.* 2007;104:11418-11423.
171. Zhao YD, Courtman DW, Deng Y, Kugathasan L, Zhang Q, Stewart DJ. Rescue of monocrotaline-induced pulmonary arterial hypertension using bone marrow-derived endothelial-like progenitor cells: efficacy of combined cell and eNOS gene therapy in established disease. *Circ Res.* 2005;96:442-450.
172. Wang XX, Zhang FR, Shang YP, Zhu JH, Xie XD, Tao QM, Zhu JH, Chen JZ. Transplantation of autologous endothelial progenitor cells may be beneficial in patients with idiopathic pulmonary arterial hypertension: a pilot randomized controlled trial. *J Am Coll Cardiol.* 2007;49:1566-1571.
173. Brook MM, Fineman JR, Bolinger AM, Wong AF, Heymann MA, Soifer SJ. Use of ATP-MgCl2 in the evaluation and treatment of children with pulmonary hypertension secondary to congenital heart defects. *Circulation.* 1994;90:1287-1293.
174. Bultmann R, Hansmann G, Tuluc F, Starke K. Vasoconstrictor and vasodilator effects of guanine nucleotides in the rat aorta. *Naunyn Schmiedebergs Arch Pharmacol.* 1997;356:653-661.
175. Hansmann G, Bultmann R, Tuluc F, Starke K. Characterization by antagonists of P2-receptors mediating endothelium-dependent relaxation in the rat aorta. *Naunyn Schmiedebergs Arch Pharmacol.* 1997;356:641-652.
176. McMillan MR, Burnstock G, Haworth SG. Vasoconstriction of intrapulmonary arteries to P2-receptor nucleotides in normal and pulmonary hypertensive newborn piglets. *Br J Pharmacol.* 1999;128:549-555.
177. McMillan MR, Burnstock G, Haworth SG. Vasodilatation of intrapulmonary arteries to P2-receptor nucleotides in normal and pulmonary hypertensive newborn piglets. *Br J Pharmacol.* 1999;128:543-548.
178. Hansmann G, Ihling C, Pieske B, Bültmann R. Nucleotide-evoked relaxation of human coronary artery. *Eur J Pharmacol.* 1998;359:59-67.
179. Burnstock G. Vessel tone and remodeling. *Nat Med.* 2006;12:16-17.
180. Davie NJ, Gerasimovskaya EV, Hofmeister SE, Richman AP, Jones PL, Reeves JT, Stenmark KR. Pulmonary artery adventitial fibroblasts cooperate with vasa vasorum endothelial cells to regulate vasa vasorum neovascularization: a process mediated by hypoxia and endothelin-1. *Am J Pathol.* 2006;168:1793-1807.
181. Gerasimovskaya EV, Ahmad S, White CW, Jones PL, Carpenter TC, Stenmark KR. Extracellular ATP is an autocrine/paracrine regulator of hypoxia-induced adventitial fibroblast growth. Signaling through extracellular signal-regulated kinase-1/2 and the Egr-1 transcription factor. *J Biol Chem.* 2002;277:44638-44650.

182. Gerasimovskaya EV, Davie NJ, Ahmad S, Tucker DA, White CW, Stenmark KR. Extracellular adenosine triphosphate: a potential regulator of vasa vasorum neovascularization in hypoxia-induced pulmonary vascular remodeling. *Chest.* 2005;128:608S-610S.
183. Gerasimovskaya EV, Tucker DA, Weiser-Evans M, Wenzlau JM, Klemm DJ, Banks M, Stenmark KR. Extracellular ATP-induced proliferation of adventitial fibroblasts requires phosphoinositide 3-kinase, Akt, mammalian target of rapamycin, and p70 S6 kinase signaling pathways. *J Biol Chem.* 2005;280:1838-1848.
184. Gerasimovskaya EV, Woodward HN, Tucker DA, Stenmark KR. Extracellular ATP is a pro-angiogenic factor for pulmonary artery vasa vasorum endothelial cells. *Angiogenesis.* 2008;11:169-182.
185. Stenmark KR, Davie N, Frid M, Gerasimovskaya E, Das M. Role of the adventitia in pulmonary vascular remodeling. *Physiology (Bethesda).* 2006;21:134-145.
186. Zakrzewicz A, Hecker M, Marsh LM, Kwapiszewska G, Nejman B, Long L, Seeger W, Schermuly RT, Morrell NW, Morty RE, Eickelberg O. Receptor for activated C-kinase 1, a novel interaction partner of type II bone morphogenetic protein receptor, regulates smooth muscle cell proliferation in pulmonary arterial hypertension. *Circulation.* 2007;115:2957-2968.
187. Belvisi MG, Hele DJ. Peroxisome proliferator-activated receptors as novel targets in lung disease. *Chest.* 2008;134:152-157.
188. Ali FY, Egan K, FitzGerald GA, Desvergne B, Wahli W, Bishop-Bailey D, Warner TD, Mitchell JA. Role of prostacyclin versus peroxisome proliferator-activated receptor beta receptors in prostacyclin sensing by lung fibroblasts. *Am J Respir Cell Mol Biol.* 2006;34:242-246.
189. Schaefer MB, Pose A, Ott J, Hecker M, Behnk A, Schulz R, Weissmann N, Gunther A, Seeger W, Mayer K. Peroxisome proliferator-activated receptor-alpha reduces inflammation and vascular leakage in a murine model of acute lung injury. *Eur Respir J.* 2008;32:1344-1353.
190. Hihi AK, Michalik L, Wahli W. PPARs: transcriptional effectors of fatty acids and their derivatives. *Cell Mol Life Sci.* 2002;59:790-798.

5. Acknowledgements

This manuscript would not be complete without acknowledging the people who made this work possible. I like to thank Dr. Marlene Rabinovitch, Stanford University, for the years of mentorship that guided me through the postdoctoral research fellowship and beyond. I learned a lot from Marlene both as a scientist and group leader. Already nine months into the fellowship, I showed her pilot data and outlined a new hypothesis not related to the initial project, and she allowed me to persue the novel but risky PPARγ projects with full force. I was supported by a joint postdoctoral research grant from the Pulmonary Hypertension Association and the American Heart Association.

Secondly, I want to thank my former attending, Professor Dr. Christoph Bührer, Charité University Medical Center, Berlin, not only for being a true role model as a physician, but also for his mentorship and support of my interests in critical care and cardiovascular research.

Moreover, I am indebted to my colleagues and friends in the laboratory at Stanford: When I joined the group it was Dr. Gordon Cann who was invaluable in overcoming the initial hurdles and settling in. Moreover, I like to thank Dr. Eliana C. Martinez (now Singapore) for being all, a wonderful colleague, stellar friend, and outstanding scientist who shared many long hours and a series of negative results. Exemplary for the many colleagues who collaborated on the projects, I particularily thank my dear friends Dr. Roham T. Zamanian, who persued the clinical study on insulin resistance in PAH patients with me, as well as Drs. Cristina M. Alvira and Roger A. Wagner, all at Stanford University. The laboratories of Dr. Duncan J. Stewart (Toronto/Ottawa, Canada) and Dr. Nicholas W. Morrell (Cambridge, UK) kindly provided an ELISA (ET-1, ADMA) and BMP-RII mutant human pulmonary artery smooth muscle cells, respectively.

My mentors at UC San Francisco have been Drs. Ian Adatia and Jeffrey R. Fineman who continue to fuel my enthusiasm on PAH. I also acknowledge my mentor at Harvard, Dr. Peter Laussen, for leading the way through my pediatric cardiology fellowship at Children's Hospital Boston. My friends Danielle Wenemoser, Dr. Alexander von Gise and Dr. Mark Dzietko were of great help getting started in Boston and keeping in touch with Berlin – thanks so much. I thank PD Dr. Peter Rosenberger not only for understanding the challenges and sacrifices of combining clinical training with basic research and personal life, but also for being a good friend for more than a decade.

Above all, I like to thank my parents Klaus and Dietlind (Kiki) who allowed me to choose my career, sometimes wondering about the path. I thank them for their efforts, personnel guidance and support that made my academic career possible. I do not want to forget my brothers, Stephan and Martin, and their lovely families, as well as Ines Hoepffner, for inviting me anytime the "Californian" made it to Europe, ….the world would not be the same without you.

Declaration in lieu of oath

Erklärung

§ 4 Abs. 3 (k) der HabOMed der Charité

Hiermit erkläre ich, daß

- weder früher noch gleichzeitig ein Habilitationsverfahren durchgeführt oder angemeldet wurde.
- die vorgelegte Habilitationsschrift ohne fremde Hilfe verfasst, die beschriebenen Ergebnisse selbst gewonnen sowie die verwendeten Hilfsmittel, die Zusammenarbeit mit anderen Wissenschaftlern/Wissenschaftlerinnen und mit technischen Hilfskräften sowie die Literatur vollständig angegeben wurden.
- mir die geltende Habilitationsordnung der Charité bekannt ist.

_____ _____

Datum Unterschrift